Alma Mater Studiorum – Università di Bologna

DOTTORATO DI RICERCA IN

ONCOLOGIA, EMATOLOGIA E PATOLOGIA

Ciclo 35

Settore Concorsuale: 06/A2 – PATOLOGIA GENERALE E PATOLOGIA CLINICA

Settore Scientifico Disciplinare: MED/04- PATOLOGIA GENERALE

ROLE OF SHIGA TOXINS IN THE PATHOGENESIS OF HEMOLYTIC UREMIC SYNDROME

Presentata da: Elisa Varrone

Coordinatore Dottorato Manuela Ferracin

Supervisore Maurizio Brigotti

Esame finale anno 2023

Index

Abstract

Hemolytic uremic syndrome (HUS) is a thrombotic microangiopathy, presenting with hemolytic anemia, thrombocytopenia and acute renal failure, which occurs as a severe sequela of Shiga toxin (Stx)-producing *Escherichia coli* (STEC) gastrointestinal infections. During the pathogenesis of HUS, before the toxins act on the target endothelial cells of the kidney and brain, several Stx forms are transported in the bloodstream: (i) free Stx; (ii) Stx bound to circulating cells (neutrophils, monocytes and erythrocytes) and platelets through the receptors globotriaosylceramide (Gb3Cer) and (Toll-like receptor 4) TLR4, hence inducing the formation of aggregates and extracellular vesicles; and (iii) Stx associated to blood cell-derived microvesicles. The latter toxin form is considered the main pathogenic factor responsible for the transition from bloody diarrhea to life-threatening HUS in approximately 15% of STEC-infected patients, especially children under 3 years. Stx consist of a pentamer of B subunits non-covalently bound to a single A subunit (uncleaved Stx) which can be cleaved by proteases originating two fragments (A1 and A2) held by a disulphide bond (cleaved Stx). Under reducing conditions, the enzymatically active A1 fragment responsible for toxicity is released. Cleaved and uncleaved Stx are biologically active but functionally different in their binding properties for circulating cells and host serum components, as well as in the formation of aggregates. Currently, there are no effective therapies for the treatment of patients with STEC infection and the gold standard strategies available for the diagnosis (microbiological and serological diagnostic methods) are very expensive, time-consuming and require specialized reference laboratories.

In this thesis, by exploiting the resolving power of SERS technology (Amplified Raman Spectroscopy on Surfaces), a plasmonic biosensor was developed as effective diagnostic tool for early detection of Stx in patients' sera. Purified Stx2a samples were directly adsorbed or were captured by an anti-Stx2 antibody previously adsorbed on the nanostructure, returning a characteristic fingerprinting of the toxin where each peak of the spectra was associated to a specific functional group.

The presence of the uncleaved and/or cleaved form of the toxin in the blood of patients could affect the outcome of STEC infections and the consequent onset of HUS. A method for detecting the cleaved form of Stx2a in human serum was developed using an acellular protein synthesis system. The different forms of Stx2a were recognized on the basis of their different translation inhibitions after treatment with a reducing agent (DTT). The assay was

adapted to human serum and cleaved Stx2a has been identified for the first time in 5 out of 10 sera from STEC-infected patients. The developed method, allowing the detection of Stx2a at concentrations similar to those found with ELISA in the blood of STEC-infected patients, would be a useful tool for studying the contribution of the cleaved and uncleaved form of Stx2a in the pathogenesis of HUS and a possible relationship with clinical symptoms.

Since a growing body of evidence supports the idea that blood cell-derived microvesicles are implicated as crucial players in the pathogenesis of HUS, pathogenic microvesicles from Stx2a-challenged blood from healthy donors were isolated and characterized by identifying their origin and the presence of Stx2a.

Recently, we have identified the antibiotic NAB815, a polymyxin B derivative, as inhibitor of the binding of Stx2a to TLR4 in circulating cells. The antibiotic was found to be significantly effective in inhibiting not only the binding to neutrophils and the formation of leukocyte-platelet aggregates, but also in impairing the formation of platelet-derived and leukocyte-derived microvesicles containing Stx2a. The protective effect of NAB815 on the formation of blood cell derived-microvesicles containing Stx2a was also assessed in cellular models. Microvesicles isolated from blood treated with Stx2a in the presence of NAB815 showed reduced toxicity on Vero cells (protein synthesis inhibition and cell death) than those purified by blood challenged with Stx2a. Since Stx2a associated with microvesicles via TLR4 appears in the blood of patients the day before the development of HUS, administration of NAB815 in patients with STEC infection could be an innovative treatment for the prevention of HUS.

INTRODUCTION

1. Hemolytic uremic syndrome (HUS)

1.1. STEC-associated HUS

STEC-associated hemolytic uremic syndrome (STEC-HUS), or typical HUS, is a complex disease characterized by thrombotic microangiopathy, which occurs as a severe life-threatening sequela of gastrointestinal infections caused by Shiga toxin-producing *Escherichia coli* (STEC) strains. These pathogenic bacteria release potent exotoxins called Shiga toxins (Stx) as major virulence factors.

About 15% of STEC-infected pediatric patients develop the syndrome with a mortality rate of 3-5% (Johnson & Taylor, 2008). HUS is considered the leading cause of acute renal failure in early childhood (<3 years) and is also characterized by the simultaneous development of hemolytic anemia and thrombocytopenia (Detzner, Pohlentz, & Müthing, 2020; Lynn; M. Noris & Remuzzi, 2005; Tarr, Gordon, & Chandler, 2005; Varrone, Carnicelli, & Brigotti, 2021)

1.2. STEC infection and transmission

STEC are zoonotic pathogens that affect humans as a result of the consumption of contaminated food or water. In particular, the most common STEC O157:H7-related outbreaks were caused by the consumption of contaminated bovine-derived products, undercooked meat, fruit, vegetables and unpasteurized juice or milk (Karpman, Loos, Tati, & Arvidsson, 2017). Since STEC strains have been isolated from pets and many different human-associated animal species, it is clear that animals are the most significant carriers of this infection.

Ruminants have been identified as primary natural reservoir; indeed, they are asymptomatic carriers of these bacteria, and cattle represent the most important source of human infections (Detzner, Pohlentz, et al., 2020; Kim, Lee, & Kim, 2020). Smaller ruminants, such as sheep and goats, are also important carriers due to their ability to harbor STEC. They can encounter STEC by eating contaminated food, drinking contaminated water, or coming in contact with the bacterium via feces of other animals.

In addition, an increased number of animals from wildlife and aquaculture industries have been identified as possible reservoirs or spillover hosts of STEC (Espinosa, Gray, Duffy, Fanning, & McMahon, 2018; Kim et al., 2020). Transmission by direct contact with animals bearing the strain (or their specimens), direct transmission from human to human and mother-to-child transmission have been described and require a very low number of bacteria.

1.3. STEC serogroups and outbreaks

Epidemiological studies have shown different virulent STEC serogroups strongly associated with the development of HUS: the serotype responsible for most of the cases of STEC infection around the world is O157:H7 (STEC expressing somatic (O) antigen 157 and flagellar (H) antigen 7) (Tarr et al., 2005), although different non-O157 serogroups (O26, O45, O103, O104, O111, O121 and O145) have been emerging as additional dangerous pathogens worldwide (Karmali, 2009; Terajima, Iyoda, Ohnishi, & Watanabe, 2014).

HUS can occur as sporadic cases or in epidemic form (Karpman et al., 2017). Since 1982, a total of 740 outbreaks caused by STEC O157:H7 were reported in the USA and most of them were foodborne (Kim et al., 2020). Between 1998 and 2016, 35 STEC outbreaks in the Western Pacific region and 176 STEC outbreaks in Europe were recorded (Kim et al., 2020). The largest O157 STEC outbreak ever documented occurred in Japan in 1996 with 12,680 symptomatic individuals, of whom 121 (0.95%) developed HUS and 3 died (Fukushima et al., 1999; Terajima et al., 2014).

Although STEC O157 is the most important strain involved in Stx–related disease, more than 50 non-O157 STEC serogroups are also involved in human illnesses and are responsible for several outbreaks. The Center for Disease Control and Prevention estimates that in the USA from 1990 to 2010 only 36% of STEC infections were caused by O157 and the others were non-O157 (Scallan et al., 2011). Moreover, 11 different serogroups were responsible for 47 non-O157 STEC outbreaks. The most commonly isolated serogroups responsible for more than 60% of outbreaks are O111 and O26 (Brooks et al., 2005; Luna-Gierke et al., 2014). Interestingly, although non-O157 strains cause more infections than O157, they cause fewer outbreaks (Kim et al., 2020; Scallan et al., 2011).

The most severe and devastating non-O157 STEC outbreak occurred in Germany in 2011 and was caused by the unusual serotype O104:H4. Despite the smaller number of infected patients (3816) than in the Japan outbreak, 845 HUS cases and 54 deaths were reported (Trachtman, Austin, Lewinski, & Stahl, 2012). Interestingly, although HUS develops mostly in young children, most of the infected people were middle-aged adults, predominantly women (Frank et al., 2011). Furthermore, the strain responsible for this devastating outbreak has no known animal reservoir (Detzner, Pohlentz, & Müthing, 2022). In addition, sporadic illness and smaller outbreaks have been reported in different countries also by less common serotypes.

1.4. STEC epidemiology

Despite the severity of the syndrome and the significant public health implications, the epidemiology of STEC-HUS is not well documented (Ardissino, Salardi, et al., 2016). The lack of diagnostic tools that are easy to use in routine laboratories and the absence of surveillance networks in many nations make it difficult to compare the situation in different countries and to assess the annual incidence of STEC-associated HUS. Moreover, the incidence rate could have a wide variation depending also on the source of data and on the considered population. In global terms, the incidence of STEC infection cases varies widely, mainly in relation to environmental local conditions, agricultural factors, density of cattle, and eating habits which could have a significant role in favoring the contact of humans with STEC (Ardissino, Salardi, et al., 2016). In some countries the incidence of HUS is directly recorded by specific surveillance systems, while in others only the incidence of STEC infections is monitored. As a consequence, in the latter case, the incidence of HUS could be calculated on the basis of the assumption that nearly 15% of STEC-infected patients would develop HUS, as previously shown by strong epidemiological data (Tarr et al., 2005).

From the beginning of the year 2020, many efforts have been made by health authorities to cope with the COVID19 pandemic hence causing a reduction in the efficiency of the surveillance systems devoted to other communicable diseases. Due to the possibility that this situation would have resulted in an underestimating of the incidence of STEC infections or HUS, it is better to evaluate the epidemiological data in a year preceding the COVID19 pandemic (2017), as shown in Tables 1 and 2. The first estimate of the global incidence of STEC-related illnesses was achieved in 2014 (Majowicz et al., 2014) by

recording data from 21 countries belonging to 10 of the 14 WHO Sub-Regions. The results clearly indicated that STEC infections are a global public health issue:

2,801,000 acute illnesses per year (95% Cr.I.: 1,710,000; 5,227,000)

3890 cases of HUS per year (95% Cr.I.: 2400; 6700)

270 cases of end-stage renal disease (95% Cr.I.: 20; 800)

230 deaths per year (95% Cr.I.: 130; 420).

Sensitivity analyses indicate these estimates are likely conservative. According to a recent WHO report (FAO/WHO, 2019), 957 STEC outbreaks have been described in 27 countries in the Region of the Americas (the large majority), the European Region and the West Pacific Region between 1998 and 2017.

In Latin America there is a high intake of raw meat and STEC infection is endemic, with most of the cases located in the south of the continent: Argentina, Chile, Uruguay (Figure 1). STEC infections in South America cause approximately 2% of acute diarrhea cases and 20-30% of bloody diarrhea cases. As a consequence, in Argentina the incidence of HUS is 10-fold higher than any other industrialized country (Karpman et al., 2017; Rivas, Chinen, Miliwebsky, & Masana, 2014; Torres et al., 2018).

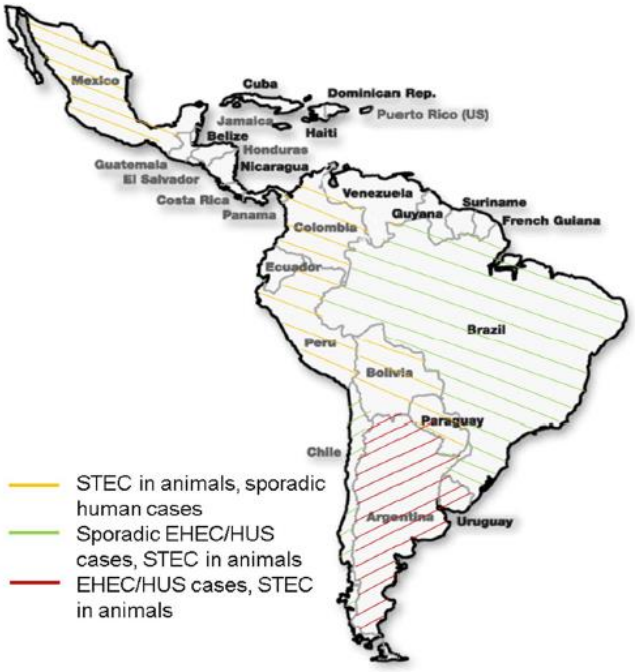

Figure 1: Distribution of HUS cases and STEC isolates (humans and animals) in Latin America. Adapted from (Torres et al., 2018).

Table 1: Epidemiology of STEC infections and HUS in Europe (2017) *

	Population	*STEC infection cases*	*HUS cases*
Austria	8,819,901	250	15
Belgium	11,419,748	123	24
Bulgaria	7,102,444	0	0
Croatia	4,182,857	7	- (1)
Cyprus	1,179,678	0	0
Czechia	10,641,034	37	5
Denmark	5,732,274	263	5
Estonia	1,319,390	3	0
Finland	5,511,371	123	- (18)
France	64,842,509	260	121
Germany	82,658,409	2065	72
Greece	10,569,450	3	0
Hungary	9,729,823	12	7
Iceland	334,393	3	- (0)
Ireland	4,753,279	795	26
Italy	60,673,701	92	67
Latvia	1,951,097	1	1
Lithuania	2,845,414	0	0
Luxemburg	591,910	1	- (0)
Malta	437,933	9	- (1)
Netherlands	17,021,347	392	12
Norway	5,296,326	381	5
Poland	37,953,580	4	1
Portugal	10,288,527	1	1
Romania	19,653,969	11	6
Slovakia	5,447,900	3	- (0)
Slovenia	2,076,394	33	2
Spain	46,647,428	86	2
Sweden	9,904,896	504	18
UK	66,727,461	993	34
EU		**6455**	**424**
EU + calculated cases			**444**

In the absence of available data, the value (in red) was calculated according to (Tarr et al., 2005): HUS cases=15% of STEC infections

* Data from STEC infections and HUS are from the Surveillance Atlas of infectious disease (ECDC) https://www.ecdc.europa.eu/en/surveillance-atlas-infectious-diseases, population data are from https://www.worldometers.info/population

The burden of STEC infections and the deriving HUS cases occurring in Europe in 2017 are depicted in Table 1. Of note, the highest number of STEC infection cases was observed in Germany and in the UK, while HUS cases peaked in France. The global burden of STEC infections is represented by the data depicted in Table 2 on the Americas (USA, Canada, Argentina), Europe and China, accounting for ~2.5-billion population. It is worth noting that the average cost of HUS per patient is 2150 US dollars, as recently estimated in China (Feng et al., 2022).

In conclusion, STEC infections and their life-threatening sequela HUS are a significant public health issue worldwide.

Table 2: Worldwide epidemiology of STEC infections and HUS (2017)*

	Population	***STEC infection cases***	***HUS cases***
USA	325,084,756	6034	905
Canada	36,732,095	808	121
Argentina	43,397,140	1880	282
EU	745,414,735	6455	444
China*	1,414,049,351	62218	9333
Total		**77395**	**11085**

In the absence of available data, the value (in red) was calculated according to (Tarr et al., 2005): HUS cases=15% of STEC infections.
USA; data were from the CDC annual report: https://www.cdc.gov/ecoli/surv2017/index.html
Canada; data were from the National Enteric Surveillance Program ("Public Health Agency of Canada: National Enteric Surveillance Program (NESP), Annual summary 2017", 2019)
Argentina; data were from the National Surveillance System (*Ministerio de Salud y Desarrollo Social de la Nación, Boletín Integrado de Vigilancia 463 SE 34/219*, 2019)
EU; data were from Table 1
*China; data from the first population-based study on the incidence of HUS are related to 2016 (Feng et al., 2022).
Population data are from https://www.worldometers.info/population.

1.5. Complement-related HUS

Although STEC are the most common cause of HUS (~90% of cases) there is also an atypical form of the syndrome (approximately 10% of cases) that is associated with dysfunctional complement regulation resulting in an uncontrolled activation of the complement system on host cells, via the alternative pathway (Karpman et al., 2017; Marina Noris & Remuzzi, 2009).

The majority of atypical HUS cases occur as a result of genetic mutation of complement factors, such as complement factor H (CFH), which is the main regulator of the alternative pathway; complement factor I (CFI), a serine protease which cleaves C3b to iC3b; membrane cofactor protein (MCP/CD46), a cofactor necessary for the cleavage of C3b; thrombomodulin (THBD); C3; complement factor B (CFB), which is a C3 convertase protein, resulting in an uncontrolled activation of the alternative complement pathway (Karpman et al., 2017).

The uncontrolled activation of the alternative complement pathway leads to an overproduction of C5a and of the membrane attack complex C5b/C9 which causes endothelial cell death. As a consequence, prothrombotic substances are exposed and this activates the coagulation system determining the formation of microthrombi, obstruction of the vessels and erythrocyte fragmentation, as well as inflammation (Canpolat, 2015). In a small group of patients (5-6%), atypical HUS occurs as a result of antibodies against complement proteins. Factor H mutations are the most common genetic defects found in about 70% of patients with complement-related HUS.

2. Pathogenesis of HUS

2.1. Main steps of HUS pathogenesis

After ingestion of contaminated food or water, STEC enter the human body selectively colonizing the intestine without being invasive. In fact, in the course of the following systemic phase, the bacteria can be detected in the gut and not in extra-intestinal tissues (Menge, 2020). During the intestinal phase, intimate interactions and tight associations of the pathogens with the epithelial cells of the gut mucosa cause the so-called attaching and effacing lesions which alter the absorption properties of the enterocytes, determining watery diarrhea (Stevens & Frankel, 2014). Most STEC carry the locus of enterocyte effacement (LEE) and express the adhesin intimin (encoded by the *eae* gene) which mediates their adhesion to the epithelial lining of the intestine. These injuries are independent of Stx effect (Law, 1994) and the resulting watery diarrhea starts about 3 days after the intake of contaminated food (Canpolat, 2015). Afterwards, STEC synthesize and release Stx (free or enclosed in bacterial-derived vesicles), which cross the intestinal

mucosa and reach the lamina propria, hence producing lesions to the microvasculature of the gut. The deriving histopathological changes are edema, necrosis, hemorrhage, as well as thrombotic microangiopathy and inflammation, culminating in bloody diarrhea. (Bielaszewska & Karch, 2005; Richardson, Karmali, Becker, & Smith, 1988; Stevens & Frankel, 2014). Typically, in 90% of cases bloody diarrhea appears 1-3 days after watery diarrhea (Tarr et al., 2005).

The damage to the endothelial lining of the gut allows Stx to enter the circulation and the onset of an inflammatory response in the intestine leads to an upregulation of the specific Stx receptors (see below) on target endothelial cells (van de Kar, Monnens, Karmali, & van Hinsbergh, 1992). Toxins are transported in the bloodstream causing injuries mainly to the endothelial cells of the target organs, kidney and brain (Richardson et al., 1988; Tarr et al., 2005; Varrone et al., 2021). HUS develops 6-7 days after the prodromal intestinal phase in 15% of STEC infected pediatric patients, while in 85% of cases there is spontaneous resolution (Johnson & Taylor, 2008; Tarr et al., 2005). The timeline for STEC disease from ingestion to HUS or resolution are depicted in Figure 2.

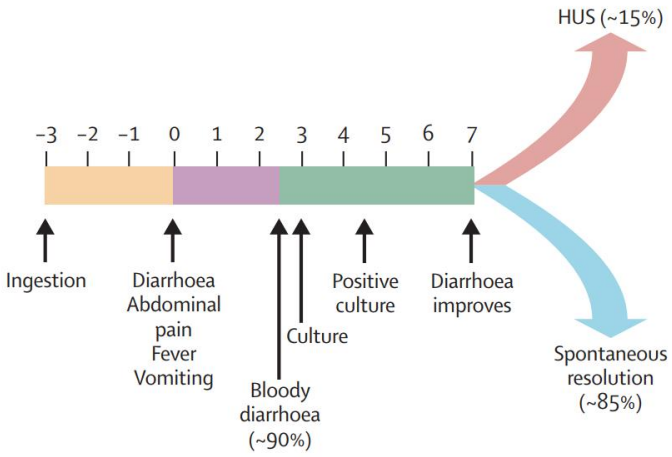

Figure 2: Progression of *E. coli* O157:H7 infections in children (Tarr et al., 2005).

2.2. Thrombotic microangiopathic lesions

Stx-related endothelial injuries cause thrombotic microangiopathic lesions in target organs, determining the onset of a symptomatic triad which is the hallmark of HUS: acute renal failure, hemolytic anemia and thrombocytopenia.

The massive presence of microthrombi in the glomerulus narrows the microvascular lumen of renal glomerular capillaries causing acute renal failure, thereby passing

erythrocytes are damaged and fragmented due to the partial or complete obstruction of the vessel lumen (Detzner, Pohlentz, et al., 2020). In addition, the binding of Stx to a receptor known as Pk antigen expressed by red blood cells activates the deposition and the activation of complement factors inducing hemolysis (Arvidsson, Stahl, et al., 2015). Furthermore, evidence have been obtained showing that Stx is capable of inducing morphological alterations and injuries in developing erythrocytes (Betz et al., 2016; Maloney & Lingwood, 2003). In conclusion, erythrocyte loss is mostly due to a passive mechanical damage and also to direct Stx-mediated mechanisms (Detzner, Pohlentz, et al., 2020).

Injuries to endothelial cells induced by the toxins trigger the recruitment of platelets to the damaged site. The interaction of platelets with fibrinogen, collagen and von Willebrand factor leads to their activation and to the formation of aggregates initiating microvascular thrombus formation and leading to vessel occlusion in glomeruli. This process triggers platelet consumption, and it is well known that low platelets count correlates with renal dysfunction. In addition, the toxin itself affects not only glomerular endothelial cells but also different renal cells inducing an acute renal injury (Karpman & Ståhl, 2014; Varrone et al., 2021). Indeed, the inhibition of protein synthesis and the induction of apoptosis induced by Stx in tubular cells leads to altered water absorption across tubular epithelial cells contributing to renal injury (Trachtman et al., 2012).

2.3. Main target organs and clinical features

The kidney and the brain are the two principal target organs in patients with STEC-HUS, and the kidney is the most affected site. Stx bind to specific receptors (see below) expressed by glomerular endothelial cells, renal tubular cells, podocytes and mesangial cells (Chaisri et al., 2001; Cheung, 2014).

As a result, patients manifest different degrees of renal failure, according to the severity of the damage. The presence of hematuria, proteinuria and increased serum creatinine, as well as hypertension are important indicators of renal damage (Canpolat, 2015). A large percentage of patients (40-50%) undergo dialysis for nearly 10 days (Scheiring, Rosales, & Zimmerhackl, 2010) and, in the most critical cases, kidney transplant is required. In addition, although neurological complications are not as common as renal ones, also cerebral microvascular endothelial cells are targeted by Stx, leading to thrombotic microangiopathic lesions and dysfunction of the endothelial blood–brain barrier. Moreover, Stx seem to have a direct toxic action on neural cells that express the specific toxin receptor

(Obata, 2008). The damage to the brain results in mild symptoms to serious neurological complications, such as coma or stroke in approximately 30% of cases, and it is also the main cause of acute mortality (Detzner, Pohlentz, et al., 2020; Karpman et al., 2017).

3. Shiga toxins (Stx)

3.1. Stx family

Stx are a family of AB5 bacterial toxins of about 70 kDa consisting of two main types, Stx1 and Stx2, and several subtypes (4 for Stx1, and 12 for Stx2) with different receptor preference and toxic potency. Stx2a seems to be the subtype mainly involved in the development of HUS in humans (Friedrich et al., 2002). Among the other subtypes, Stx2b is associated with a milder disease, Stx2c and Stx2d show a reduced toxic effect on Vero cells, but Stx2d has the same toxic effect as Stx2a when injected in animals (Lindgren, Samuel, Schmitt, & O'Brien, 1994; Melton-Celsa, 2014). After activation by the elastase present in the intestinal mucus, Stx2d-act (activatable) shows an increased toxic effect on Vero cells and is associated with severe symptoms in STEC infection and often with HUS. However, it is not commonly found in serogroups most frequently associated with STEC outbreaks (Bielaszewska, Friedrich, Aldick, Schürk-Bulgrin, & Karch, 2006; Bunger, Melton-Celsa, & O'Brien, 2013; Melton-Celsa, Darnell, & O'Brien, 1996; Melton-Celsa, Kokai-Kun, & O'Brien, 2002; Melton-Celsa, O'Brien, & Feng, 2015). Finally, Stx2e, Stx2f, Stx2g are produced by STEC harbored by animals, but only Stx2e is associated with symptoms, in particular edema in pigs (Melton-Celsa, 2014). Both Stx1 and Stx2 are encoded by genes present in bacteriophages. STEC strains with more than one bacteriophage can produce more than one toxin type (Fürst et al., 2000; Menge, 2020). The induction of Stx phage with mitomycin has been coupled with an increased production of Stx which is followed by a phage release during lytic growth in both *in vitro* and *in vivo* experiments (Yokoyama et al., 2000). Strains which produce only Stx1 are not usually associated with STEC-HUS (Khalid & Andreoli, 2019) or are associated with mild symptoms (Melton-Celsa, 2014). In addition, HUS has been reported to occur much more frequently in individuals infected with STEC strains expressing Stx2 than in those infected with strains carrying Stx1 and Stx2 at the same time (Detzner et al., 2022).

The amino acid homology between Stx1 and Stx2 is nearly 50%, more precisely 55% for the A subunit and 57% for the B subunits (Melton-Celsa, 2014). However, the enzymatic activity and the molecular mechanism of the two toxins are the same. The main difference between the two subtypes is in their receptor binding sites in the B subunits, resulting in a different affinity for the specific receptor. Moreover, the A1 fragment of Stx2 has higher affinity for ribosomes hence inhibiting translation in human cells at a significantly higher level, thus explaining the greater potency and severity of the tissue damages induced by this toxin subtype (Menge, 2020).

3.2. Structure and mechanism of action

Stx are composed of a single 32 kDa-A chain, non-covalently bound to five identical B chains (7,7 kDa each) forming a pentameric ring (Figure 3, Figure 4A) (Detzner, Pohlentz, et al., 2020).

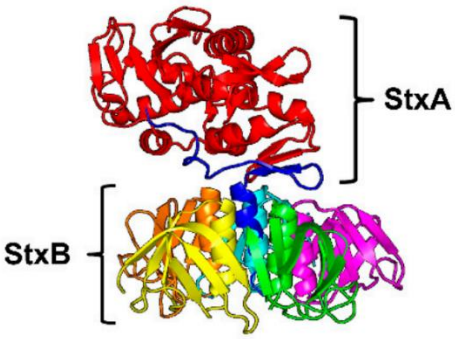

Figure 3: Stx2 crystal structure (Detzner et al., 2022)

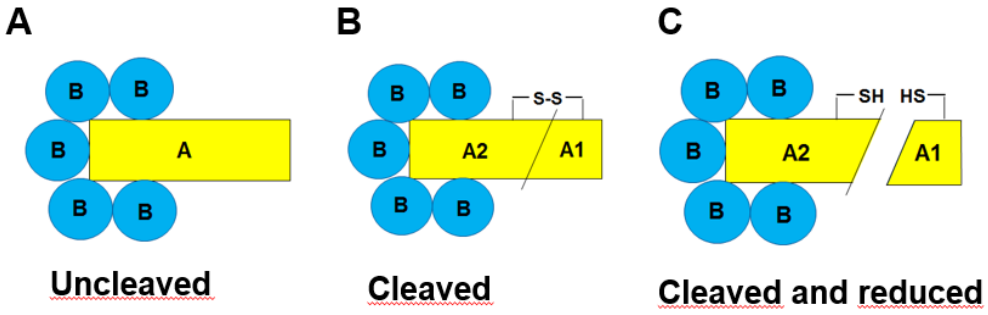

Figure 4: Structure of Stx2. (A) Native form composed of an A chain non-covalently bound to five identical B chains; (B) Cleaved form composed of A1 and A2 fragments linked by a disulfide bound. The A2 fragment is connected to the B pentameric ring; (C) Cleaved and reduced form.

When they are translated, the initial product consists of 2 polypeptide chains, having a 22- or 19-20-amino acid N-terminal signaling sequence for A or B subunits, respectively. The signal sequences are cleaved off during the transfer of the proteins into the periplasmic space of STEC by signal peptidase I present in the membrane (Menge, 2020).

The A chain is a proenzyme that is enzymatically cleaved at arginine residues 248 or 251 into two fragments linked by a disulfide bond; A1, the 27,5 kDa enzymatically active fragment, and the 4,5 kDa A2 fragment connected to the B pentameric ring (Figure 4B). The disulfide bond is reduced (Figure 4C), usually within cells, permitting the A1 fragment to express its deadenylating activity on 28S rRNA in ribosomes, resulting in a decreased ribosomal affinity for eukaryotic elongation factors (eEF1 and eEF2) and leading to irreversible arrest of translation. Another intracellular target of Stx is DNA in chromatin that is serially deadenylated leading to the formation of nuclear apurinic sites (Detzner, Pohlentz, et al., 2020; Menge, 2020). In target cells, proteolytic cleavage of the A chain can occur in the course of cellular intoxication, during the retrograde transport (see below), by the protease furin which recognizes the sensitive region (Arg-X-X-Arg), the consensus motif that is also recognized by trypsin. However, a cleavage activity, although different, has also been found in the intestinal mucus (Melton-Celsa et al., 1996) or can be induced by bacterial proteases released after the lysis of bacteria (Detzner, Pohlentz, et al., 2020; Menge, 2020).

In any case, it is not clear when and where the toxin is cleaved and whether the A subunit is still intact or already cleaved when the holotoxins enter circulation and challenge the human blood components.

4. Stx receptor-dependent toxicity

4.1. Glycosphingolipid receptors: Gb3Cer and Gb4Cer

To affect target cells (especially the endothelial cells lining of the microvasculature of kidneys and brain) and to exert their toxicity, Stx need to bind to a specific member of globoseries (GSLs) glycosphingolipids receptors: globotriaosylceramide (Gb3Cer) and, to a lesser extent, to globotetraosylceramide (Gb4Cer) (Figure 5) (Detzner et al., 2021; Legros, Pohlentz, Steil, & Müthing, 2018). Cell lines and mice that don’t express these

receptors are not sensitive to the toxic action of Stx (Jacewicz et al., 1994; Okuda et al., 2006).

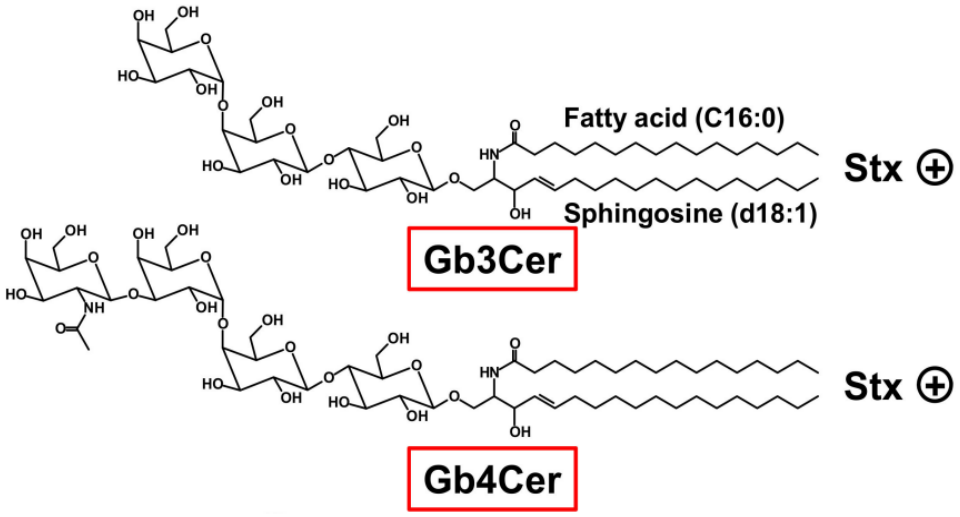

Figure 5: Structure of Gb3Cer and Gb4Cer. Modified from (Detzner, Pohlentz, et al., 2020).

GSLs are amphipathic molecules with a structure composed of a hydrophilic oligosaccharide moiety and of a twin-tailed hydrophobic lipid anchor known as ceramide (Cer) carrying sphingosine (d18:1) and a fatty acyl chain such as C16:0 (Figure 5) (Detzner, Pohlentz, et al., 2020). While the most prevalent component of the ceramide in GSLs is sphingosine (d18:1), the fatty acyl chain can have different lengths (from C14 to C26), resulting in a variety of GSL lipoforms. Cer (d18:1, C22:0) and Cer (d18:1, C24:1/C24:0) were identified as other dominant lipoforms present in Gb3Cer and Gb4Cer of primary human renal cortical epithelial cells (pHRCEpiCs) and of primary endothelial cells of the human brain (pHBMECs) (Detzner et al., 2021; Detzner, Steil, et al., 2020; Lindberg et al., 1987; Waddell, Head, Petric, Cohen, & Lingwood, 1988). The common precursor of the mammalian GSL families is lactosylceramide (Lc2Cer). It is produced by the transfer of galactose to glucosylceramide (GlcCer) by the action of a β1,4-galactosyltransferase (β1,4GalT). In Gb3Cer, Lc2Cer is connected to galactose in α1-4-configuration by the action of a α1,4-galactosyltransferase (α1,4GalT). The resulting structure includes Galα1-4Galβ1-4Glcβ1-1Cer (Gb3Cer) which carries a terminally α1-4-linked Gal molecule. Then, GalNAcβ1-3Galα1-4Galβ1-4Glcβ1-1Cer (Gb4Cer) is synthesized by action of a β1,3-N-acetylgalactosaminyltransferase (β1,3GalNAcT) being equivalent to GalNAc-elongated Gb3Cer and contains a subterminal α1-4-linked Gal molecule (Figure 6) (Detzner, Pohlentz, et al., 2020).

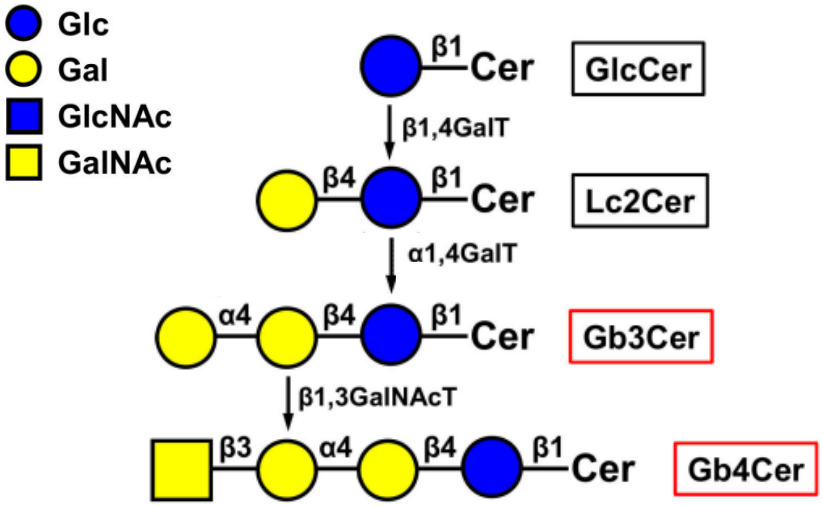

Figure 6: Biosynthesis of Gb3Cer and Gb4Cer. Modified from (Detzner, Pohlentz, et al., 2020).

In Stx-sensitive cells it has been estimated a number of receptors ranging between $1x10^6$ to $1x10^7$ (Menge, 2020). These receptors are localized in membrane microdomains called lipid rafts which are very rich in cholesterol. The organization and density of Gb3Cer receptors in lipid rafts are crucial factors for the effective binding and internalization of Stx. Effective binding and subsequent internalization of Stx depend on the positioning of surface-exposed GSL receptors in lipid rafts (Legros et al., 2018). The fatty acid chain length and the saturating state of the lipid component of Gb3Cer also influence the toxin binding. In addition, after the binding of the B subunits of the toxin to a single receptor, more receptor molecules are recruited in the raft to promote the interaction of Stx with the cell (Detzner et al., 2021; Melton-Celsa, 2014). Subtypes Stx1a and Stx2a preferentially bind to Gb3Cer or interact, although weakly, with the Gb4Cer receptor via their B-binding subunits (Legros et al., 2018). They don't interact with Gb5Cer at all. The gradual elongation of the oligosaccharide moiety of Gb3Cer to Gb4Cer and to Gb5Cer correlates with the rapidly diminishing attachment of Stx1a and Stx2a. The subtype Stx2e is unique in showing a specific and pronounced preference towards Gb4Cer (DeGrandis, Law, Brunton, Gyles, & Lingwood, 1989).

Therefore, the significant variations in tissue distribution of these glycolipid receptors and their expression by intestinal, renal and cerebral endothelial cells and by other cells in the kidney (mesangial cells, tubular cells and glomerular epithelial cells) explain why the damage is focused on selected organs. The localization of Gb3Cer is indeed a predictive

feature of the cellular site susceptible to toxin action. Moreover, the relative number of receptors correlates with the sensitivity of cells to specific Stx subtypes (Detzner, Pohlentz, et al., 2020; Müthing, Schweppe, Karch, & Friedrich, 2009; Trachtman et al., 2012).

4.2. Retrograde trafficking of Stx

After the binding of the pentameric B subunit to target cell surface-exposed Gb3Cer, the Stx/receptor complex is internalized by endocytosis. A specific retrograde transport route allows the toxin to reach the Golgi apparatus and the endoplasmic reticulum. Within the host cell, the cleavage of the A subunit by furin occurs and, in the endoplasmic reticulum, the disulfide bond connecting A1 and A2 fragments is reduced so that the catalytically active A1 fragment is released into the cytosol hence expressing its toxic action.

4.3. Effects of Stx on target cells

The effect of Stx on target cells is not only the irreversible inhibition of translation with subsequent activation of the apoptotic program and cell death, but also the triggering of a broad spectrum of responses caused by the damage to the ribosome called “ribotoxic stress response” (D. M. Jandhyala, Thorpe, C. M., & Magun, B. , 2012).

More specifically, the structural alteration of the ribosome induces the activation of multiple stress signaling pathways involving stress protein kinase cascades (SAPK/JNK, MAPKp38, PKC, PI3K/Akt/mTOR pathway) and leading to the transcription of pro-inflammatory genes. As a consequence, there is the release of proinflammatory cytokines triggering the inflammation process which, if excessive, promotes further damage. In addition, some of the Stx-induced pro-inflammatory mediators up-regulate the expression of toxin receptors on target cells thereby increasing the severity of organ injury during HUS (D. M. Jandhyala, Thorpe, & Magun, 2012; Lee & Tesh, 2019; Menge, 2020; Tesh, 2012; C. Zoja, Buelli, & Morigi, 2010).

5. Interaction of Stx with soluble factors present in the blood

5.1. HuSAP and soluble TLR4

Human serum amyloid P component (HuSAP) is present in soluble form at constant concentration in the human blood. This blood factor composed of a pair of pentameric subunits is considered a negative modulating factor of Stx2. Each subunit binds specifically to Stx2 and not to Stx1, impairing its interaction with Gb3Cer receptors and thus inhibiting its cytotoxic activity (Armstrong et al., 2006; Kimura, Tani, Matsumoto Yi, & Takeda, 2001; Marcato, Vander Helm, Mulvey, & Armstrong, 2003). At the same time, HuSAP stimulates the binding of Stx2 to Toll-like receptor 4 (TLR4), which is mostly expressed by neutrophils (Griener, Mulvey, Marcato, & Armstrong, 2007).

In humans the presence of pathogen-associated molecular patterns (PAMPs), such as lipopolysaccharide (LPS), stimulates and activates the cells of the innate immunity through Toll-like receptors (TLRs). As a consequence, the cells release the soluble forms of TLR2 and TLR4 in order to capture the specific stimulating PAMP and reduce the responses of monocytes, macrophages and neutrophils hence preventing an excessive stimulation of the innate immune response (Iwami et al., 2000). The soluble form of TLR4 derives from an alternative mRNA splicing or the conversion of the internalized receptor in a truncated form then released by exocytosis (Jaresová et al., 2007). The soluble form of TLR4 might be considered a positive modulator of Stx2. It interacts with Stx2 avoiding the capture by HuSAP which would inhibit the interaction with Gb3Cer, thus allowing the toxin to target and damage human cells (M. Brigotti, Arfilli, et al., 2018). However, once Stx2 interacts with HuSAP and form a complex, soluble TLR4 is no longer able to displace HuSAP. Moreover, considering the physiological concentrations of HuSAP it is unlikely that soluble TLR4 would be able to prevent the formation of the complex between Stx2 and HuSAP in blood (M. Brigotti, Arfilli, et al., 2018).

6. Cleaved and uncleaved forms of Stx

Recently, it was found that the functional and biological properties of Stx change according to modifications of the structure of the toxins: in fact, cleaved and uncleaved forms of the toxins bind to circulating cells and to host serum components differently, and have a different effect on the formation of aggregates (M. Brigotti et al., 2019; Dorothea Orth et al., 2009).

Cleaved unreduced Stx (which have a single nick in the A chain resulting in two fragments, A1 and A2, connected by a disulfide bridge) do not bind to human neutrophils through TLR4 and to the same receptor on monocytes and platelets, whereas it is fully active in binding to complement factor H; uncleaved toxins show opposite features and stimulate the formation of aggregates between leukocytes and platelets (M. Brigotti et al., 2019; Dorothea Orth et al., 2009).

The lack of interaction of the cleaved form of Stx with human neutrophils suggests that the binding site for neutrophils is probably very close to the A subunit cleavage site, but does not correspond to the active site of the toxin. Indeed, both cleaved and uncleaved Stx show similar cytotoxicity for Vero and Raji cells. In addition, the induction of the formation of neutrophil/platelet and monocyte/platelet aggregates by the uncleaved form indicates that TLR4 has an important role in this process, given that all the involved cells express this receptor. Only the cleaved form of Stx is instead able to bind to factor H.

Concerning HuSAP, cleaved and uncleaved Stx seems to have the same behaviors. Indeed, both forms interact with this blood protein which prevents their binding to Gb3Cer receptor and thus promotes the interaction with TLR4 (M. Brigotti et al., 2019).

To sum up, these observations suggest that to bind to neutrophils, Stx has to be uncleaved since these cells do not express a Gb3Cer receptor in humans. The toxin then has to be cleaved to interact with factor H. The other circulating cells involved in toxin binding (platelets and monocytes) can interact with both forms as they express both Gb3Cer and TLR4. The outcome of STEC infections and the consequent onset of HUS could therefore be influenced by the percentages of uncleaved or cleaved toxin circulating in the patient blood, since the two forms of toxin could determine different amounts of aggregates and pathogenic microvesicles (see below). Thus, the characterization of the structure of the toxin present in the blood of patients could be useful for a better understanding of the pathogenesis of HUS.

7. Stx-induced inflammation

Inflammation plays a key role in the pathogenesis of HUS. High levels of inflammatory and prothrombotic mediators have been found in STEC-infected and HUS patients. Examples are cytokines, chemokines, tissue factor, complement factors, cytokine receptors, growth factors and these have been correlated with the progression of renal damage (Kamitsuji et al., 2000; C. Litalien et al., 1999; Petruzziello-Pellegrini et al., 2012; Proulx, Seidman, & Karpman, 2001; Proulx et al., 2002).

7.1. Chemokines and cytokines

Infected cells release different types of chemokines which contribute to the recruitment of inflammatory cells in target organs. Treatment of endothelial cells with Stx leads to an increased level of mRNA and protein expression of genes associated with inflammation (A. Matussek et al., 2003; Carla Zoja et al., 2002). Even renal epithelial cells can be stimulated by Stx to release chemokines. Elevated levels of chemokines such as IL-8, a powerful activator and chemoattractant of neutrophils, and MCP-1 (monocyte chemoattractant peptide-1) have been found in urine samples and in the serum of HUS patients (van Setten et al., 1998).

Experiments conducted with mice exposed to Stx showed higher level of chemokines such as MCP-1, MIP-1α (macrophage inflammatory protein α) and RANTES (regulated on activation normal T-cell expressed) and an increased recruitment of mononuclear cells in target organs, especially in the kidney, while the treatment with antibodies to neutralize chemokines reduced the renal damage. These results imply that the recruitment of these cells contribute to the renal damage associated with HUS (Cheung, 2014; Keepers, Gross, & Obrig, 2007). Different *in vivo* experiments with baboons treated with Stx also identified high mRNA levels for IL-8, MCP-1 and MIP-1α in renal cells (Stearns-Kurosawa et al., 2013). Similarly, neutrophil infiltrates and high level of IL-8 were shown in the kidney of rabbits treated with Stx (García et al., 2008).

In conclusion, it is likely that the chemokines IL-8, MCP-1 and MIP-1α are involved in the pathogenesis of HUS thanks to the recruitment and activation of neutrophils, monocytes and macrophages. Additionally, chemokine receptors seem to be involved in the formation of leukocyte infiltrates in the kidney. Indeed, in experiments with chemokine receptor 1 (CCR1) knockout mice where HUS was induced by Stx, reduced neutrophil and monocyte

counts were observed, as well as reduced renal infiltration of inflammatory cells associated to mild renal damage (Ramos MV, 2007). The treatment of human microvascular endothelial cells with Stx induced the expression of CXCR4, CXCR7 and stromal derived factor-1 (SDF-1), a potent chemoattractant cytokine that, via interaction with CXCR4, modulates inflammatory cell infiltration. In a mouse model of HUS, the inhibition of CXCR4/SDF-1 interaction decreased kidney injury. Interestingly, STEC-infected patients who developed HUS had higher plasma concentrations of SDF-1 compared to children who did not develop the syndrome (Petruzziello-Pellegrini et al., 2012).

In STEC-infected patients who developed HUS, high neutrophil counts at presentation and their renal influx are associated with a poor outcome and with increased mortality (Barbour, 2012; Inward et al., 1997). Neutrophils give a direct contribution to the inflammatory response by releasing proinflammatory cytokines, even though monocytes have a more important role. Isolated monocytes incubated with Stx produce cytokines such as IL-1β, IL-6, IL-8, and TNF-α (M. Brigotti, Carnicelli, et al., 2018; van Setten, Monnens, Verstraten, van den Heuvel, & van Hinsbergh, 1996) and incubation of human endothelial cells with TNF-α or IL-1 results in a higher expression of Gb3Cer receptors and an increased sensitivity of cells to Stx (Van de Kar, Monnens, & Van Hinsbergh, 1993). Consistently, high levels of circulating IL-6 and IL-10 correlate with more severe symptoms and complications in children (C. Litalien et al., 1999). STEC-infected children who progressed to severe renal dysfunction had a 10-fold increase in IL-6 (Catherine Litalien et al., 1999) and elevated concentrations of IL-6 and soluble TNF receptor 1, associated with encephalopathy (Shiraishi et al., 2008). Results obtained in animal models corroborated these findings since mice infected with *E. coli* O157:H7 and treated with TNFα showed severe damage to the kidney whereas specific inhibition of this cytokine led to a reduction of the damage (Harel et al., 1993).

Taken together these results highlight the important role of cytokines, chemokines and their receptors in the inflammatory response associated with HUS.

7.2. Complement system

The complement system is part of the innate immunity and is composed of different plasma or membrane-bound proteins activated by a proteolytic cascade related to three different pathways, (namely the classical, alternative and lectin-binding pathway), while several regulatory proteins control the process. In particular, factor H is considered one of

the most important regulators of the complement alternative pathway because of its inhibitory activity on C3 convertase in virtue of its binding to C3b which prevents its interaction with factor B. Numerous studies have been conducted to determine how complement components affect the development of HUS. Stx activate the alternative complement pathway in the fluid phase and thus increase plasma levels of complement components but, at the same time, bind to factor H leading to impaired complement regulation hence reducing its protective effect on cell membranes (Walsh & Johnson, 2019). Laboratory findings and clinical studies have shown that complement activation via the alternative pathway occurs during STEC-associated HUS (Walsh & Johnson, 2019). Orth et al. have provided the most conclusive evidence of *in vitro* complement activation by Stx. Wherein, incubation of Stx with normal human serum resulted in the activation of the final common complement pathway. Co-incubation with EGTA (a classical pathway blocker) did not inhibit complement activation whereas EDTA totally prevented it, indicating that the toxin triggers the alternative pathway (Dorothea Orth et al., 2009; Walsh & Johnson, 2019).

The activation of C3 and the generation of C3a by Stx was also demonstrated in *in vitro* experiments with microvascular endothelial cells and *in vivo* by using a mouse model of STEC–HUS (Morigi et al., 2011) and it has also been shown that this setting induces damage to podocytes in mice (Locatelli et al., 2014).

HUS patients show low levels of C3 and increased plasma levels of products of complement activation such as C3a, C3b, C5a, breakdown products C3c and C3d, factor Bb and C5b-9 during the acute phase of the disease (Thurman et al., 2009; Trachtman et al., 2003; Walsh & Johnson, 2019). In particular, C3a and C5a interact with monocytes and macrophages stimulating the release of cytokines and chemokines (Markiewski & Lambris, 2007) which are involved in HUS-associated inflammation, as described above.

It is worth noting that C3a and C5a and other factors of the complement system can activate platelets and favor the thrombotic process (Rawish, Sauter, Sauter, Nording, & Langer, 2021). Furthermore, the presence of C5b-9 on endothelial cells enhances the expression of tissue factor, thus concurring to thrombosis (Buteau et al., 2000). Moreover, Stx can have an effect not only by directly activating the complement system, but also by altering its regulation by interfering with complement controllers such as factor H. In fact, Stx bind to factor H and impair the interaction between factor H and the cell surface. As a consequence the activity of factor H is delayed leading to complement activation on the

cell surface without appropriate control, whereas fluid phase control is preserved (Dorothea Orth et al., 2009).

As evidence of complement activation/dysregulation, the deposition of C3b and C5b-9 in the renal endothelium has been observed (Cheung, 2014; Koster, Boonpucknavig, Sujaho, Gilman, & Rahaman, 1984), as well as decreased levels of mRNA of the membrane attack regulator CD59 in glomerular endothelial cells treated with Stx (Ehrlenbach et al., 2013). In addition, it has been demonstrated that Stx significantly increase P selectin expression on the surface of a human endothelial cell line (human microvascular endothelial cells, HMEC-1). The presence of an anti-P selectin antibody decreased both C3 deposition and thrombus development, indicating the ability of this receptor to bind to and activate the circulating C3 and to promote thrombus formation (Morigi et al., 2011).

The activation of the alternative pathway of the complement system by Stx, as part of the innate immune response, is considered one of the key steps in the development of renal injuries (Dorothea Orth et al., 2009).

8. Interaction of Stx with circulating blood cells

8.1. Interaction of Stx with circulating blood cells

A critical phase of HUS pathogenesis is the release of the toxin into the bloodstream and its dissemination to target organs. Free Stx have been found in the bloodstream during late toxemia and before the onset of HUS, while they have been rarely detected in patients with HUS (M. Brigotti et al., 2011; He et al., 2015).

Different human circulating cells (erythrocytes, monocytes and platelets) express Gb3Cer or similar lipoforms, and thus interact with Stx (Bitzan et al., 1994; M. Brigotti, 2012; Karpman et al., 2001; van Setten et al., 1996). However, neutrophils specifically bind to Stx as well, even though they lack the expression of the receptor (Detzner, Pohlentz, et al., 2020; Macher & Klock, 1980). As a matter of fact, neutrophils are not targeted by Stx and instead recognize these bacterial toxins through Toll-like receptor 4 (TLR4) which interacts with the Stx A chain allowing the toxin to circulate bound to their cell membrane

(Arfilli et al., 2010; M. Brigotti et al., 2013; Macher & Klock, 1980). In humans, TLR4 is also expressed by monocytes and platelets (M. Brigotti, 2012).

8.2. The role of neutrophils, monocytes and platelets in the pathogenesis of HUS

The role of neutrophils after their specific interaction with the Stx A chain via TLR4 has stimulated intense debate: on the one hand, they could exert a protective action as they might capture free toxins (sponge effect) preventing the binding to target cells; on the other hand, neutrophils can be considered the major carrier cells of the toxins in circulation, delivering them to target organs. (M. Brigotti, 2012; M. Brigotti, Arfilli, et al., 2018; M. Brigotti et al., 2010). Consistently, Stx bind to TLR4 on neutrophils with a lower affinity than that for Gb3Cer on endothelial cells and this feature makes them good candidates for the delivery and subsequent transfer of the toxin to endothelia in target organs (Griener et al., 2007; te Loo et al., 2000).

The study of the Stx kinetics in HUS patients during the natural course of STEC-infections showed a positive relationship between the amount of the toxin in the intestine and in the bloodstream. Stx were detected on neutrophils for several days after the onset of diarrhea, when they were no longer detectable in stools, despite the blood half-life of neutrophils is nearly 6-7 h and they survive for 1-2 days only (Maurizio Brigotti et al., 2006). Two observations explain this neutrophil behavior: the interaction with Stx delays the apoptotic program of neutrophils, and the transfer of Stx between neutrophils has been documented *in vitro* suggesting that the toxins move from older circulating neutrophils to new neutrophils entering the circulation from the bone marrow (M. Brigotti et al., 2008). Finally, the transmigration of neutrophils carrying Stx through an endothelial monolayer showed a direct correlation between the amount of Stx bound to neutrophils and the damage to endothelial cells, while an indirect correlation was observed with the release of proinflammatory cytokines (M. Brigotti et al., 2010). Specifically, neutrophils carrying higher toxin amounts induced a massive endothelial injury whereas cytokine production was blocked (M. Brigotti et al., 2010; M. Brigotti et al., 2011). On the contrary, lower amounts of Stx bound to neutrophils induced less severe toxic effects on endothelial cells while triggering the release of higher levels of proinflammatory cytokines and chemokines such as IL-6, IL-8, TNF-α and IL-1β (Geelen, van der Velden, van den Heuvel, & Monnens, 2007; van Setten et al., 1996) hence triggering inflammation that ultimately contributes to

tissue damage (M. Brigotti et al., 2010; M. Brigotti et al., 2011). This suggests that the level of toxins bound to neutrophils might be related to different clinical presentations, also considering that elevated neutrophil counts are associated with a worse prognosis (Robson, Fick, & Wilson, 1988).

The interaction of the A subunit of Stx with TLR4 allows the B subunits to be available for the binding to Gb3Cer expressed by target cells. In contrast, when the toxins are bound to Gb3Cer (Karpman & Ståhl, 2014) the B pentamer is not available for the binding to the Gb3Cer expressed by target cells.

Platelet activation can be induced by a direct effect of Stx, by cytokines and chemokines released by Stx-stimulated monocytes or by Stx-induced endothelial cell damage. However, Stx preferentially bind to Gb3Cer in activated platelets, then the toxins are rapidly internalized causing structural changes, for example increasing the capacity of binding fibrinogen and thus the formation of thrombi. The consumption of platelets leads to thrombocytopenia, in particular, platelet counts lower than 150 x 10^9/l are considered pathologic during STEC-HUS (Trachtman et al., 2012). Platelets are also involved in inflammation beside their role in thrombosis. Once activated, platelets can interact with neutrophils and monocytes and release chemokines (Karpman & Ståhl, 2014).

8.3. Blood cells and complement activation

The binding and activation of blood cells by the action of Stx is also accompanied by the activation and deposition of the complement system. Evidence from different studies demonstrated the activation of the complement on circulating platelets and leukocytes. STEC-HUS patients also presented high levels of C3a in plasma and C3, C9 and C5b-9 on the surfaces of these blood cells. Focusing on platelets, after the stimulation of blood cells with Stx, the presence of C3c, iC3b, C3b, C9 and C5b-9 was found on their surface. C3b can bind to platelets via P-selectin and to neutrophils and monocytes through CR1, while iC3b binds via CR3. In addition, the formation of the C5b-9 complex on platelets promotes the formation of the prothrombinase complex, which allow the generation of thrombin and expose negatively charged phospholipids on the membrane which are used as scaffold for clotting and subsequent thrombus formation (Stahl, Sartz, & Karpman, 2011).

8.4. Formation of platelet/leukocyte aggregates

When Stx come in contact with and bind to platelets and leucocytes, their activation leads to the formation of platelet-monocyte and platelet-neutrophil aggregates containing Stx. This was observed in children with HUS during the acute phase of the disease and in STEC-infected patients, but not after recovery. Under normal conditions, platelets and leukocytes do not interact in the circulation. Hence, the formation of aggregates between these blood components in STEC-infected patients could play an important role in the formation of thrombi (Varrone et al., 2021).

9. Stx-derived blood cell microvesicles

9.1. Evidence on other mechanisms by which Stx can affect target cells

As explained above, when Stx are released in the bloodstream, preferentially bind to platelets, neutrophils and monocytes and stimulate them to form aggregates. Afterwards, in order to affect target cells, it is necessary that Stx are released from blood cells to target renal endothelial cells through the high-affinity Gb3Cer receptor.

However there are evidence suggesting that Stx affect target cells through different Gb3Cer-independent mechanisms: human intestinal cells may develop injuries caused by the action of the toxin even though they don’t express Gb3Cer receptors (Schüller, Frankel, & Phillips, 2004). Murine glomerular cells may be damaged although they lack Gb3Cer (Keepers, Psotka, Gross, & Obrig, 2006).

On the whole, these findings suggest that other mechanisms exist by which Stx exert their cytotoxic activity in target regardless of the binding to Gb3Cer receptors.

9.2. Formation of blood cell-derived microvesicles

Recently, a novel mechanism of transfer of Stx and other bacterial virulence factors to target cells has been described (Ståhl et al., 2015). This mechanism is centered on the

Gb3Cer-dependent uptake of toxin by endocytosis of blood cell-derived microvesicles containing Stx. For this process, it is necessary the binding of Stx to receptors expressed on blood cells leading to their activation, the Stx' internalization within platelets (Karpman et al., 2001) or monocyte (Falguières et al., 2001) or their presence on neutrophil membrane and then their release within or on the surface of microvesicles.

9.3. Classification of extracellular vesicles

Extracellular vesicles are cell-derived membrane particles including microvesicles, exosomes and apoptotic bodies, whose classification is based on their size and their mechanism of generation. In addition, they can be differentiated on the basis of cellular markers which reveal from which parent cells they are released (Figure 7).

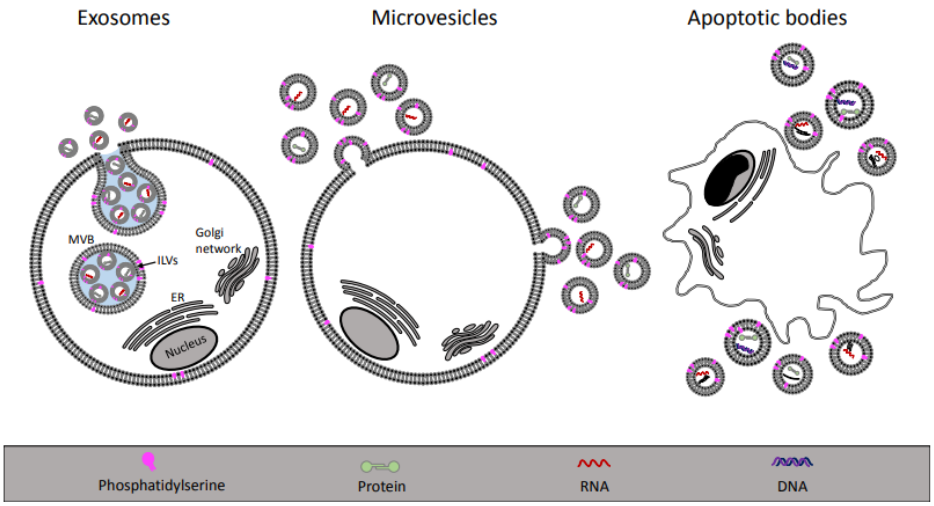

Figure 7: Mechanisms of generation of extracellular vesicles (Villysson, Tontanahal, & Karpman, 2017)

9.3.1. Microvesicles

Microvesicles are a subtype of extracellular vesicles shed and released directly from the plasma membrane of a cell by budding upon activation, stress or apoptosis (Figure 8). Indeed, shedding of microvesicles is a process which occurs spontaneously in resting cells (Ratajczak, Wysoczynski, Hayek, Janowska-Wieczorek, & Ratajczak, 2006), but it is increased as a result of particular stimuli. They have a diameter ranging from 100 to 1000 nm and are generally greater than exosomes. They can be originated from blood cells (Angelillo-Scherrer, 2012; Flaumenhaft et al., 2009; Olivier Rubin, Canellini, Delobel, Lion, & Tissot, 2012) as well as from non-circulating cells (Turco et al., 2016) and are

enriched of components of the parent cells, such as proteins, RNAs, microRNAs, lipids. Their content reflects the biological status of the parental cell and depends on the cell of origin (Sapet et al., 2006). In addition, there are evidence showing that their contents, within the particle or on its surface, are not randomly generated but that microvesicle components are packaged in a selective way by a controlled mechanism consisting in the action of a regulatory protein, ADP-ribosylation factor 6, which selects the protein cargo. Interestingly, the same cells can origin microvesicles with different contents and with components having higher concentrations than those in parent cells, thus enhancing their potency (Biró et al., 2005; Lai et al., 2016).

Thanks to their structure they are able to transfer substances from one cell to another which can be close or distant (Figure 8). In fact, microvesicles participate in various physiological processes and normally contribute to intercellular communication, and also maintain the integrity of the cell by removing unwanted and harmful components (Abid Hussein, Böing, Sturk, Hau, & Nieuwland, 2007; Camussi, Deregibus, Bruno, Cantaluppi, & Biancone, 2010; Raposo & Stoorvogel, 2013; Ståhl, Johansson, Mossberg, Kahn, & Karpman, 2019). However, they can be released even upon cellular activation, senescence and apoptosis (Ståhl et al., 2019) and elevated levels of microvesicles are involved in pathological process (Arraud et al., 2014).

The uptake of microvesicles could depend on the type of recipient cell and the recognition of different ligands or receptors expressed by microvesicles or target cells (Mulcahy, Pink, & Carter, 2014; Ståhl et al., 2019). The most common mechanism is endocytosis which can be mediated by receptor-ligand interactions and can be clathrin-dependent or independent, caveolin-dependent, associated to micropinocytosis and phagocytosis or mediated by lipid-rafts. In any case, the fusion of microvesicles with the membrane of the recipient target cell is a dynamic process which depends on the presence of specific receptors or proteins recognized by ligands, a reorganization of lipid composition and proteins in order to allow the formation of a microvesicle-cell complex and the transfer of the content in the cell cytosol (Podbilewicz, 2014). As example of specific uptake, platelet-derived microvesicles can transfer tissue factor to monocytes and endothelial cells but not to neutrophils (Lösche, Scholz, Temmler, Oberle, & Claus, 2004; Ståhl et al., 2015). Another important aspect is that, once transferred, the materials present within or on the surface of microvesicles, can influence the phenotype of the recipient cell.

The other possible mechanism for microvesicles uptake is fusion, where the membrane of microvesicles fuses with the membrane of the target cell and, in this way, the content can be transferred (Ståhl et al., 2019). An example are monocyte-derived microvesicles which can transfer tissue factor to platelets expressing P-selectin by fusion, activating platelets and increasing their ability to initiate coagulation (Del Conde, Shrimpton, Thiagarajan, & López, 2005).

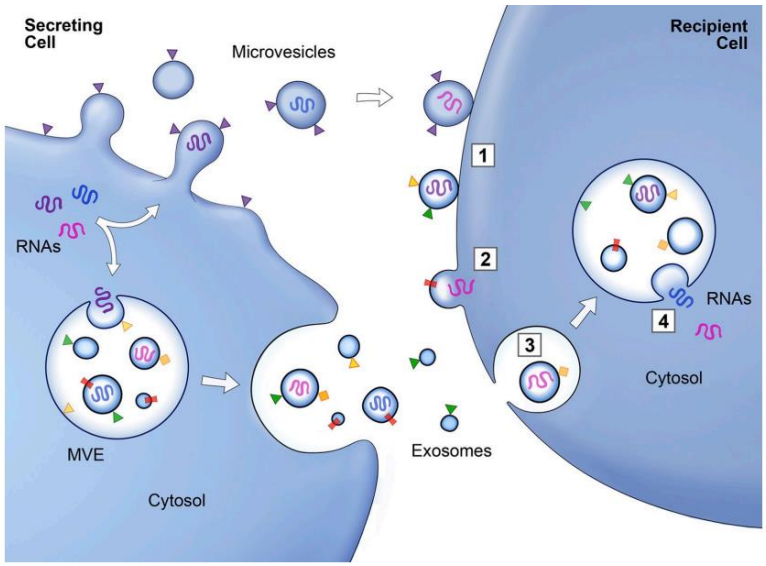

Figure 8: Protein and RNA transfer to cells by microvesicles. Microvesicles may dock to the target cell's plasma membrane. (1) Binding of microvesicles and (2) direct fusion with the plasma membrane (3) or endocytoses. (4) After endocytoses, fusion of the microvesicles with the delimiting membrane of an endocytic compartment. Both pathways result in the delivery of proteins and RNA into the membrane or cytosol of the target cell (Raposo & Stoorvogel, 2013).

9.3.2. Exosomes

Exosomes are small vesicles (diameter of 30 to 100 nm) formed by budding into early endosomes and a subset of late endosomes called multivesicular bodies. Exosomes are released by fusion of the external membrane of multivescicular bodies with the plasma membrane (Colombo, Raposo, & Théry, 2014; Ståhl et al., 2019). They are different from the other subtypes of extracellular vesicles because they origin from an endosome and thus they have a unique composition of lipids and proteins. Indeed, they have much more cholesterol, glycosphingolipids, sphingomyelin and phosphatidylserine than their parent cells (Skotland, Sandvig, & Llorente, 2017).

9.3.3. Apoptotic bodies

Apoptotic bodies are the largest vesicles with a diameter about 1-5 μm formed by the breakdown of cells during the activation of the apoptotic program (György et al., 2011).

9.4. Methods for the detection of extracellular vesicles

The interest in extracellular vesicles is growing because of their role in many physiological processes and their contribution to the pathogenesis of different diseases, such as HUS. However, our knowledge about extracellular vesicles is limited and hindered by the availability of few suitable methods for their accurate quantification and characterization. Indeed, it is very difficult to study their features such as size, morphology, phenotype, cell of origin, concentration, density and protein composition (Arraud et al., 2014). Nowadays the classification is based on their size and mechanism of generation, as explained above. For this reason, it is very important to establish and standardize methods for the isolation and characterization of extracellular vesicles.

Extracellular vesicles are usually isolated from the supernatant of cultured cells or from whole blood or plasma by differential ultracentrifugation and exploiting their differences in floatation velocity. Then they can be analyzed and characterized by immunoblotting or mass spectrometry or imaging techniques. In addition, in order to know the molecular composition and the cell of origin, SDS-PAGE followed by protein staining, immunoblotting or proteomic analysis has to be performed (Raposo & Stoorvogel, 2013).

9.4.1. Transmission electron microscopy (TEM)

Transmission electron microscopy associated with cryo-preparation is the gold standard and the most eligible method of analysis. This high-resolution technique preserves the integrity of membranes and reveal the morphology and the size of extracellular vesicles. Thanks to a direct visual inspection of the vesicles, it is possible to obtain a more accurate measure of the size compared with other methods, such as flow cytometry or nanoparticle tracking (Headland, Jones, D'Sa, Perretti, & Norling, 2014; Raposo & Stoorvogel, 2013).

Different studies have showed that microvesicles have a rounded shape (Arraud et al., 2014) in particular, the extracellular vesicles involved in the pathogenesis of HUS analyzed with this technique showed a rounded shape and a 1 μm diameter (Ståhl et al., 2015). A weak point of transmission electron microscopy is that it is difficult to ascertain whether

the detected vesicles are typical or rare structures. Therefore, it is recommended to supplement TEM with an additional method, allowing detection and analysis of the whole vesicle population since TEM is not quantitative (Dragovic et al., 2011).

9.4.2. Dynamic light scattering (DLS)

Dynamic light scattering (DLS) allows to have information about the size by analyzing the light scattered by particles in suspension, such as isolated extracellular vesicles, under Brownian motion. The analyzed vesicles are in suspension without any type of treatment or fixation of the sample thus artefacts are unlikely (Dragovic et al., 2011). However, it is difficult to detect particles equal to or larger than 1 μm diameter and to resolve mixture of particles of different size such as microvesicles and exosomes. In fact, the scattered light deriving from all the particles is collected simultaneously, as a consequence the detection of bigger particles is biased, thus the estimate of particle size and distribution is difficult (Dragovic et al., 2011).

9.4.3. Nanoparticles tracking analysis (NTA)

In order to have information about the size, the distribution and quantification of isolated extracellular vesicles, the nanoparticle tracking analysis (NTA) is the preferred technique based on the analysis of the Brownian motion of extracellular vesicles in suspension. In addition, it allows a real-time visualization because microvesicles can be monitored by light microscopy. A video is recorded to track the motion of individual vesicles, and by using an appropriate software it is easy to evaluate the rate of Brownian motion and to determine the size of the vesicles and their total concentration (Dragovic et al., 2011). Compared to DLS, this technique allows to accurately resolve heterogeneous mixture of vesicles. However, the detection limit is nearly 1 μm diameter since above this size the Brownian motion is too slow (Dragovic et al., 2011; Headland et al., 2014). NTA is more rapid than electron microscopy and it is possible to analyze a higher number of vesicles.

9.4.4. Flow cytometry

Flow cytometry is a technique which allows to detect microvesicles thanks to their expression of phosphatidylserine (recognized by annexin V) and their subpopulation thanks to the expression of antigens belonging to parent cells (recognized by multiple labelled antibodies). Flow cytometry is not sensitive and accurate for the analysis of microvesicles

as they have a size very close to the lower detection limit of the instrument (~ 300 nm). As a result, extracellular vesicles are difficult to distinguish and many smaller particles are undetectable. In fact, small extracellular vesicles could have a limited number of binding site for antibodies and this could restrict the staining, as a consequence the expression of antigens on their surface can be underestimated (Ståhl et al., 2019).

9.5. Studies on STEC-infected patients before HUS development

A recent clinical study has shown that Stx2 associated to blood cell-derived microvesicles is the main pathogenic factor responsible for the transition from bloody diarrhea to life-threatening HUS in children (Brigotti M., 2020). The study analyzed the journey of Stx in the blood of 20 STEC-infected patients not during the acute phase of HUS but a step before, from the onset of bloody diarrhea to the development of HUS. In this study 2846 pediatric patients were analyzed in a screening program for the detection of Stx in the stools of children with bloody diarrhea, which involved 56 pediatric units. STEC infection was found in 5% of patients (155 cases) and, according to stringent clinical-laboratory criteria (other evidence of STEC-infection, absence of the HUS triad), 20 of them were enrolled in the study and admitted to the hospital where 3 children developed HUS during the observation (15%). In contrast to studies on patients in the acute phase of HUS in whom free Stx were rarely found in serum, the enrolled patients showed free Stx in blood detected by ELISA at concentrations ranging from 2 to 6 ng/ml. Therefore, the mere presence of free Stx in serum (100% of patients) was not a sufficient condition for the development of the syndrome.

In addition, most of STEC-infected patients (55%) and those who developed HUS showed Stx bound to neutrophils, a reservoir of cell-associated toxic molecules ready for delivery. However, also patients who recovered belonged to this group hence the presence of Stx bound to neutrophils is not sufficient to trigger HUS. The toxin amounts bound to leukocytes decreased over time, as shown by kinetic analyses, followed by an increase in the concentration of functionally active Stx in patients' sera.

It is worth to note that the distinctive feature observed in patients who developed HUS the day before the onset of the HUS triad was the presence of microvesicles containing the toxin, during the decreasing phase of toxin associated to leukocytes.

During HUS the involvement of the brain occurs in the most critical cases. Neurological complications seem to be associated to a direct action of the toxin rather than a consequence of renal failure (uremic encephalopathy). Indeed, in 15% of HUS patients these symptoms appear before the typical HUS triad (Goldstein, Nuñez-Goluboay, & Pinto, 2021). Moreover, it has been shown that the presence of high concentrations of Stx on neutrophils during the acute phase of HUS promotes the development of neurologic complications (M. Brigotti, 2012; M. Brigotti et al., 2011), whereas HUS appears in STEC-infected patients when the toxin bound to neutrophils is reduced.

It can be hypothesized that cerebral endothelial cells composing the blood-brain barrier are differently affected with respect to glomerular endothelial cells and that higher amounts of blood Stx could be required to damage them rather than the release of lower amounts of toxins by microvesicles.

Stx dock target cells through microvesicles that also contain other pathogenic factors involved in HUS development. High levels of platelet and leucocyte-derived microvesicles were found in plasma during the acute phase of HUS (Ståhl et al., 2015). Moreover, microvesicles containing Stx have been found in the renal cortex of a patient with HUS as strong evidence of the pivotal role of microvesicles in delivering Stx *in vivo* (Ståhl et al., 2015).

9.6. Other evidence of microvesicle involvement in HUS from *in vitro* and *in vivo* studies

The findings observed in HUS patients were also reproduced in *in vitro* experiments and *in vivo* animal models. *In vitro* studies have shown that the stimulation of whole human blood with Stx2 induces a significant increase in the production and release of blood cell-derived microvesicles compared to controls and deriving from circulating cells such as monocytes, neutrophils, erythrocytes and platelets. In addition, most of them contained the toxin. The incubation of Stx-containing blood cell-derived microvesicles with glomerular endothelial cells induced cell death because of the transfer of Stx leading to inhibition of protein synthesis. Furthermore, in mice infected with Stx-producing *E. coli* O157:H7 high level of circulating platelet- and leukocyte-derived microvesicles carrying Stx were detected. In the kidneys of the infected mice extensive damage in glomerular endothelial and tubular epithelial cells was observed, as well as injuries in glomerular and tubular basement membranes and in podocytes (Ståhl et al., 2015).

9.7. Features of blood cell-derived microvesicles in HUS

Blood cells are not sensitive to the cytotoxic effects of the toxin, because of the lack of Gb3Cer receptors (neutrophils), lack or low level of protein synthesis (red blood cells and platelets, respectively) or resistance to translation inhibition by Stx (monocytes). However, they contribute to the pathogenesis of HUS since they can be activated and stimulated to release microvesicles containing Stx (Figure 9).

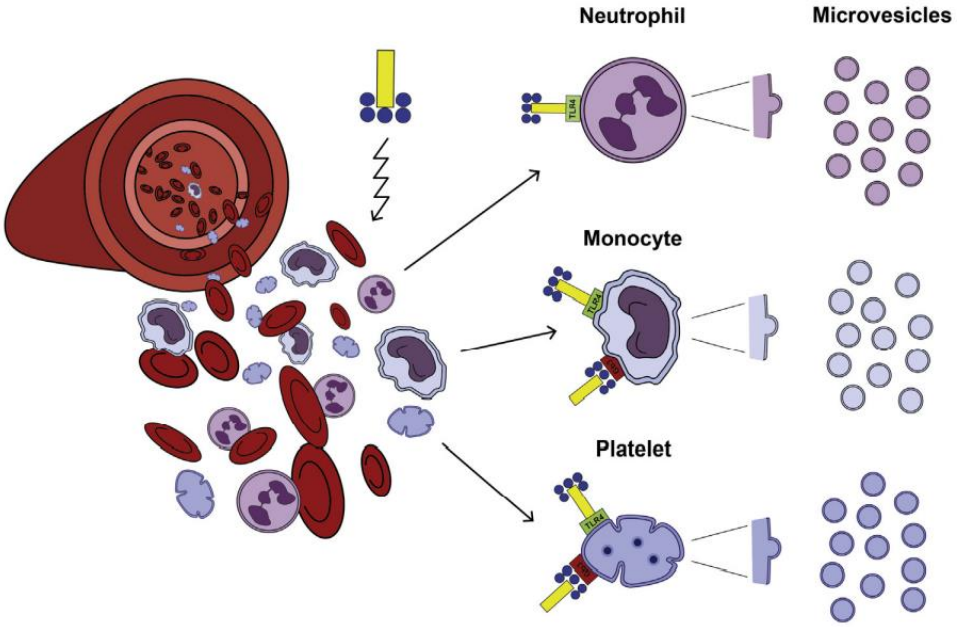

Figure 9: Stx2 induces the release of blood cell-derived microvesicles containing the toxin. STEC-infected patients' blood cells challenged by Shiga toxins (Stx) and their toxin-specific receptors. Stx (left), which consists of a single A chain (yellow rectangle) and five B chains (blue circles), interacts with platelets and blood circulating cells (zigzag arrow) via two different receptors: globotriaosylceramide (Gb3Cer; red rectangle) and Toll-like receptor 4 (TLR4; green rectangle) on monocytes, platelets, and neutrophils, respectively. On the surface of circulating cells and platelets, interactions of the Gb3Cer/Stx B chain and the TLR4/Stx A chain are displayed. (Varrone et al., 2021)

Concerning the localization of Stx in microvesicles, a study suggests that they are mainly concentrated within microvesicles since permeabilization is required for their detection (Ståhl et al., 2015). However, other evidence showed that toxins are also localized on the outer membrane, as Stx circulating in the blood of patients can be detected by using monoclonal antibody and this means that part of the toxic cargo is not localized within the microvesicles (Brigotti M., 2020). In addition, a recent paper showed that Stx can be transferred from the outer surface to the interior of microvesicles (Willysson et al., 2020).

Microvesicles expose phosphatidylserine on the outer leaflet of the membrane and the generated negative charge promotes the binding of prothrombin, factor Va and factor Xa

favoring a prothrombotic activity (Bevers & Williamson, 2016). Another factor carried by platelet- and monocyte-derived microvesicles is tissue factor and this finding suggests that not only aggregates of these blood cells but also the derived microvesicles could contribute to a prothrombotic state (Stahl et al., 2011). Microvesicles bearing complement factors C3 and C9, as well as C5b-9 complex are released especially from platelets. In addition, C3c, iC3b, C3b and C4 are bound to the surface of microvesicles. The deposition of C5b-9 was also observed on red blood cell-derived microvesicles (Ståhl, Sartz, & Karpman, 2011). This complement-derived complex contributes to red blood cells' hemolysis and to the release of red blood cell-derived microvesicles coated by the same complex (Arvidsson, Ståhl, et al., 2015). Microvesicles carrying tissue factor and complement factors reflect the presence of complement activation in the cell of origin and are capable of activating the coagulation pathway further enhancing the inflammatory and thrombotic process (O. Rubin et al., 2013).

It is worth to note that microvesicles can transfer to target endothelial cells not only Stx but also the other pathogenic factors they are carrying. In this regard, an emerging concept is the microvesicle pathotype (Figure 10) (Varrone et al., 2021). The development of HUS in STEC-infected patients could be influenced not only by the number or by the type of microvesicle-generating cells, which confer them some of the cellular features, but also by a specific combination of virulence factors present in microvesicles, the so called pathotype. In other words, the simultaneous presence of the virulence factors (Stx, activated complement factors, tissue factor) and their relative proportion could render the microvesicle fully pathogenic. As a consequence, it should be important to determine the microvesicle pathotype rather than refer to the cellular source of the microvesicles (Varrone et al., 2021).

Microvesicle can transfer their toxic cargo by interacting with target cells in different ways:

1. non-receptor-mediated endocytosis or fusion, in which is not necessary the specific binding of Stx to a receptor. However, this model does not explain the selected damage to specific target organs expressing Gb3Cer receptors as observed in HUS patients. Rather this unspecific transfer could explain the presence of more rare injuries to other organs, such as pancreas, heart and skeletal muscles which lack this receptor.

2. Receptor-mediated endocytosis better explains the specific targeting of Gb3Cer-expressing organs. Stx present on the surface of microvesicles are bound to Gb3Cer receptor through B-binding subunits thus exposing the A-chain or to TLR4 through the A chain and thus exposing the B-binding subunits. Microvesicles derived from platelets or monocytes have both these possibilities, and given that renal endothelial cells express both these receptors (Gb3Cer and TLR4), they can interact in both ways. Accordingly, *in vitro* experiments showed that when renal endothelial cells are targeted by soluble Stx, TLR4 cooperates in the binding of the toxin (Torgersen et al., 2011). Therefore, the presence of both chains of Stx (A chain or B-binding chains) exposed on the surface of microvesicles could favor the intoxication of target cells, even though the specificity of toxin action is due to the B chain/Gb3Cer interaction. Neutrophils, because they lack Gb3Cer receptors, bind Stx only through TLR4 and consequently interact with the A chain exposing the B-binding subunits available for the Gb3Cer receptors expressed by target cells.

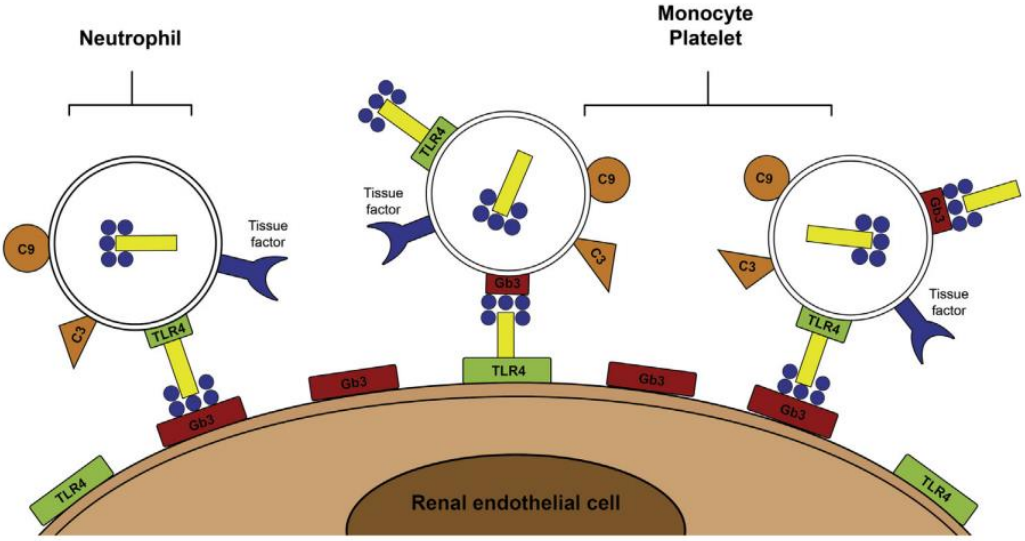

Figure 10: Microvesicles released by platelets, monocytes, and neutrophils after Shiga toxins (Stx) challenge and their interactions with renal endothelial cell. In addition to Stx, which is present both within and on the surface of the microvesicles, they also include complement factors 3 (orange triangle) and 9 (orange circles), as well as tissue factor (blue cup). Stx A chain (rectangle in yellow) binds to Toll-like receptor 4 (TLR4; rectangle in green), while Stx B chains (blue circles) interact with globotriaosylceramide (Gb3Cer; red rectangle). These receptors are expressed by target endothelial cells and are found on the surface of microvesicles. The key event in the pathogenesis of hemolytic uremic syndrome is considered the targeting of Gb3Cer-expressing endothelial cells by Stx and/or Stx associated with microvesicles. Docking of microvesicles to renal endothelial cells depends on the origin of microvesicle (neutrophil or monocyte/platelet derived) and on the Stx chain involved in the interaction with microvesicle receptors. Through the B chains of TLR4-anchored Stx and the A chain of Gb3Cer-anchored Stx, monocyte/platelet-derived microvesicles can interact with endothelial Gb3Cer and TLR4. In neutrophil-derived microvesicles, lacking Gb3Cer, only the first mechanism is present. Stx and other pathogenic factors are successfully released from microvesicles into target cells as a result of their initial contact with the endothelium surface (Varrone et al., 2021).

After the interaction with the receptors, microvesicles transfer the associated virulence factors. These findings were observed in the plasma of 12 children during the acute phase of HUS (Stahl et al., 2011): C3 and C9 were detected on the surface of circulating blood cell-derived microvesicles and, in a patients with HUS, C3 was found on 30% of the platelet-monocyte aggregates and on 15% of platelet-neutrophil aggregates from which microvesicles were originated (Stahl et al., 2011). In addition, the presence of tissue factor on microvesicles was observed in the whole blood of 4 children with HUS during the acute phase, as well as bound to platelet-leukocyte aggregates (Stahl, Sartz, Nelsson, Bekassy, & Karpman, 2009).

Another important feature is that toxins within microvesicles evade host immune recognition by covering itself with the membrane of the vesicles. In fact, the host blood cell-derived microvesicles containing virulence factors, such as Stx, are recognized as self-components while outer membrane vesicles produced by pathogens, such as STEC, cannot avoid the attack by the immune system since they are considered non-self-components (Bielaszewska et al., 2017; Ståhl et al., 2015).

10. Diagnosis, methods and problems

The diagnosis of HUS is based on the observation of the symptomatic triad (hemolytic anemia, thrombocytopenia and acute renal failure) (Tarr et al., 2005). Despite the similar presentation, there are different etiologies leading to HUS and it is important to discriminate between STEC-related HUS and HUS related to complement dysregulation since treatment and outcome of the disease are quite different (Wijnsma et al., 2016).

Currently, the diagnosis of STEC infections consists in the identification in stool samples of STEC genes coding for virulence factors (*stx* genes, the attaching and effacing gene (*eae*) and hemolysin gene (*hly*)) by polymerase chain reaction (PCR) (Gould et al., 2009). These methods replaced the time-consuming Vero cell cytotoxicity assay, aimed at detecting fecal toxins, used as a gold test in the past. In addition, fecal specimens are simultaneous plated on Sorbitol MacConkey agar plates in order to identify STEC colonies. By the latter methods the presence of STEC can be identified only in few patients with

HUS (30-69%), while the use of PCR for the detection of Stx genes allows the identification in 70% of cases (Chui et al., 2013; Heuvelink, Van de Kar, Van Der Velden, Chart, & Monnens, 1999; Qin et al., 2015; Wijnsma et al., 2016). However, bacteria and toxins can be detected in the stool of patients for a short period of time after the onset of the disease, indeed their presence in the intestine declines during the first 6-7 days (Tarr et al., 1990). In addition, they depend on the availability of fecal material. In most cases diarrhea occurs before the onset of HUS and this makes the detection of the pathogen difficult, and often many stool collections are required. For this reason, another strategy for the diagnosis of STEC infections is the detection in blood samples of antibodies against LPS belonging to the main STEC serogroups. This method allows diagnosis in 60-94% of patients who have clinical sign of HUS also when stool culture is negative (Heuvelink et al., 1999; Ludwig, Sarkim, et al., 2002).

The choice of the method depends on the timeframe between the onset of the symptoms and the analysis. In fact, the identification of STEC in stool samples is possible at the beginning of the disease a few days after the manifestation of intestinal symptoms, therefore it is mandatory to collect early the fecal sample. In contrast, IgM against LPS are detectable by 5 days up to 2 months after the onset of the disease, hence it is necessary to collect the blood sample not too early (Chart, Perry, Cheasty, & Wright, 2002; Ludwig, Bitzan, Bobrowski, & Müller-Wiefel, 2002).

However, these microbiological and serological diagnostic methods have high detection limits. Additionally, they are very expensive in term of time and costs. Often the analysis of the samples requires complex pre-treatments and the specimens have to be sent to specialized laboratories, thus delaying the diagnosis and the treatment of the infection.

In conclusion, the early detection of Stx in STEC-infected patients to prevent HUS development is very difficult. The search for new rapid diagnostic methods for the early detection of Stx during the phase preceding HUS in order to start as soon as possible the supportive managements would be an important goal.

11. Therapies

To date, there are no effective and specific therapies for the treatment of STEC-HUS and management is only supportive (hyperhydration, blood transfusions, hemodialysis or peritoneal dialysis, anti-hypertensive drugs). The patients with HUS usually present a clinically relevant renal involvement with different degree of severity, and approximately 50% of patients require renal replacement therapy (Khalid & Andreoli, 2019).

As a result of renal failure, 40-50% of STEC-HUS patients require dialysis for almost 10 days (Scheiring et al., 2010). In the most critical cases, (up to 20%) long-term renal damage occurs with permanent dysfunction and kidney transplantation is required.

11.1. Volume expansion

Currently, a hyperhydration protocol is recommended because it has been found to reduce the progression to HUS in patients with early diagnosis of STEC infection (Ardissino, Tel, et al., 2016). It consists of the infusion of isotonic fluids to expand the volume and reduce the injuries to the kidney caused by the loss of fluid occurring during diarrhea, thus reducing the need for dialysis, formation of microthrombi, organ hypoperfusion and the consequent ischemic damage, and finally the development of HUS (Ardissino, Tel, et al., 2016; Karpman et al., 2017).

11.2. Plasma exchange

Plasma exchange is not considered to be beneficial, and when it was applied in Germany during the 2011 outbreak sustained by *E. coli* O104:H4 it was not associated with improved outcomes, worsening neurological symptoms and renal dysfunction (Trachtman et al., 2012). Similarly, in another study, a significant association between plasma exchange and the development of hypertension, neurological symptoms, and need for dialysis was found (Rosales et al., 2012).

However, this treatment was received by patients with severe disease, making it difficult to determine if the worsening of renal and neurological symptoms was related to plasma exchange or to the natural course of severe HUS. In other studies the infusion of plasma in severely affected HUS children showed no differences in the outcome (Gianviti et al., 1993; Rizzoni et al., 1988) or it was associated with beneficial effects (Colic, Dieperink, Titlestad,

& Tepel, 2011). However, it is not clear how plasma infusion could influence the course of the disease although it is likely that this treatment would determine the removal of toxic microvesicles and of prothrombotic and proinflammatory factors. Consequently it could be useful only in the case of early diagnosis and not after HUS development (Karpman et al., 2017).

In conclusion, caution should be used in considering plasma exchange as a beneficial therapy in STEC infections.

11.3. Eculizumab

Eculizumab is a humanized monoclonal antibody against C5 that inhibits its cleavage to C5a and C5b and prevents the formation of the terminal complement membrane attack complex C5b-9 (Mahat, Matar, & Rotz, 2019). In 2011, the antibody was approved by FDA for the therapy of complement-mediated atypical HUS with excellent outcomes.

The role of complement and its uncontrolled activation has been studied also in typical HUS and it plays an important role in the pathogenesis. The efficacy of eculizumab in the treatment of STEC-HUS, however, is controversial (Trachtman et al., 2012). The treatment of three 3-years patients who were unresponsive to plasma exchange was successful since it improved neurological and renal function (Lapeyraque et al., 2011).

Unfortunately, other subsequent studies indicated that treatment with eculizumab is not associated with a better outcome in STEC-HUS patients (Loos et al., 2017; Menne et al., 2012). Most of the clinical symptoms are a consequence of Stx action on the kidney and the role of complement can be quite different in different patients. It is conceivable that in the most severe cases, as those treated with eculizumab during the German outbreak, a strong activation of complement had occurred, hence explaining the higher efficacy of the antibody in these patients.

In conclusion, caution might be used in the use of eculizumab in STEC-infected patients (Würzner, Riedl, Rosales, & Orth-Höller, 2014), also considering that there are no reports on the use of eculizumab in patients with less severe symptoms (Mahat et al., 2019).

11.4. Antibiotics

The treatment of STEC-infection during the watery or bloody diarrhea phases is aimed at preventing the development of HUS. Most studies have shown that antibiotics should be avoided in routine treatment of STEC infections since they potentially increase the risk of HUS development by enhancing Stx expression and their release after bacterial lysis (Tarr & Freedman, 2022; Würzner et al., 2014). In fact, some antibiotics, especially those belonging to quinolone family, are potent inducers of bacterial SOS responses triggered by DNA damage. As a consequence, bacteriophages encoding Stx genes are induced enhancing the production of Stx and their release (Kakoullis, Papachristodoulou, Chra, & Panos, 2019; Kimmitt, Harwood, & Barer, 2000; Shaikh & Tarr, 2003; Walterspiel, Ashkenazi, Morrow, & Cleary, 1992). On the other hand, B-lactams, a class of antibiotics which prevent the synthesis of the bacteria cell-wall, promote the release of the toxin (Grif, Dierich, Karch, & Allerberger, 1998). Ciprofloxacin was shown to have an effect in increasing the production of Stx in a mouse model of STEC infection with *E. coli* O157:H7 (Zangari et al., 2014).

The current recommendation against antibiotics has been confirmed in different studies with patients infected by *E. coli* O157:H7 (Smith et al., 2012; Wong, Jelacic, Habeeb, Watkins, & Tarr, 2000; Zhang et al., 2000), who were treated with antibiotics during the diarrhea phase resulting in a 17-fold higher risk to develop HUS with respect to untreated patients. Data of this prospective study prove that antibiotics should not be administered to patients with diagnosed or putative STEC infections (Wong et al., 2000). This was demonstrated for B-lactams as well as for TMP-SMZ (trimethoprim-sulfamethoxazole) (Wong et al., 2000).

However, the treatment of STEC-infected patients with antibiotics is widely debated since the data are often controversial and require detailed analysis. For example, in 1996 during an outbreak in Japan, fosfomycin, a non B-lactam cell wall-synthesis inhibitor, was administered to STEC-infected patients during the bloody diarrhea phase, in particular on day 2, determining a 85% reduction of the relative risk to develop HUS (Ikeda et al., 1999). However, this was the only study reporting a striking beneficial effect of antibiotic treatment in STEC-infections. In addition, in this study children who received fosfomycin were compared to a control group that received other antibiotics. The absence of a control group with no antibiotic treatment did not allow to demonstrate a real reduced risk of developing HUS (Safdar, Said, Gangnon, & Maki, 2002). Finally, it is important to note

that after HUS development the treatment of patients with antibiotics showed no positive effects.

The only prospective randomized controlled trial on the use of antibiotics, TMP-SMZ, to study the prevention of HUS development in STEC-infected children showed that there were no significant difference between treated and untreated control patients in term of onset of symptoms, and duration/development of HUS (Proulx, Turgeon, Delage, Lafleur, & Chicoine, 1992). In addition, a recent study (McKee et al., 2020) on 866 STEC-infected children reported that antibiotics had an opposite effect, i.e. the treatment increased of the risk of HUS development.

The characterization of O104:H4 strain responsible of the major outbreak in Germany in 2011 spring showed that these bacteria were susceptible to common antibiotics. Data showed that, when O104:H4 isolated from two HUS patients was incubated with therapeutic concentrations of antibiotics such as ciprofloxacin, meropenem, fosfomycin or chloramphenicol, the subsequent release of Stx did not increase (Corogeanu et al., 2012). In addition, patients who received azithromycin eliminated STEC from their stool faster than the group of patients who did not receive antibiotics.

Antibiotics seem to be effective in alleviating the clinical manifestation induced by the O104:H4 strain, however the antibiotic treatment may be useful only against this particular strain. In addition, data reported in a 5-year prospective study showed that the influence of antibiotics on long-term outcome was not significant (Rosales et al., 2012). Thus, the role of antibiotic therapy in late illness or for gut decolonization after recovery from STEC-HUS is still uncertain and needs to be further studied (Trachtman et al., 2012).

In the light of these controversial data, the administration of antibiotics in patients with confirmed or suspected STEC infections is not recommended (Tarr & Freedman, 2022).

11.5. Novel therapies

In recent years progresses was made in the development of a variety of alternative treatment options for STEC infection which have been evaluating in *in vitro* and *in vivo* experiments or in clinical trial. These include monoclonal antibodies against Stx; Stx receptor (Gb3Cer) analogues; several vaccines (Karpman et al., 2017; Mühlen & Dersch, 2020).

11.5.1. Stx-targeted antibody therapy

The use of Stx-specific antibody aimed at neutralizing the toxin in the circulation has been found to block the cytotoxic action of the toxin in cell culture and, when administered immediately after the infection, to protect animals challenged with toxins from the development of symptoms (Cheng, Henderson, Patfield, Stanker, & He, 2013). Different specific antibodies against the A-subunits or the B-subunits have been produced, differing in their protecting efficacy or in their specificity to different Stx variants. In general, it was shown that the A-subunit specific antibodies are capable of neutralizing toxin actions better than the B-subunit specific antibodies (Tzipori, Sheoran, Akiyoshi, Donohue-Rolfe, & Trachtman, 2004).

However, these promising results are not easy to be transferred to humans. In fact, in order to be effective, the passive immunization has to be administered to humans with a proper dosage immediately after the onset of infection. Different times of administration or errors in dosages render this therapy ineffective (D. Orth, Grif, Zimmerhackl, & Würzner, 2008).

11.5.2. Toxin receptor analogs

The rationale of this strategy is to mimic the structure of Gb3Cer to prevent the binding of the toxin to this receptor thus blocking its toxicity and the Gb3Cer-related pathogenetic steps. In fact, Stx, once released from bacteria in the intestine, enter the circulation and can bind to Gb3Cer receptors expressed by circulating cells and target cells such as renal and cerebral endothelial cells. Therefore, interfering with the binding of Stx to the receptor is a promising approach which could be able to reduce the toxin-induced damage and the progression of the disease. Another interesting strategy is the use of Gb3Cer inhibitors, which interfere with the synthesis or the expression of Gb3Cer receptors (Mühlen & Dersch, 2020).

11.5.3. Vaccination strategies

Stx, once released from the bacteria and before coming in contact with target cells, enter the circulation and could be recognized by the host immune system. As a consequence, specific vaccines could protect from STEC infections by interfering with toxin interactions with circulating and target cells. Since Stx are considered the main virulence factor of STEC-HUS, they are the best candidates for the development of specific vaccination strategies. For example, inactive derivatives of Stx have been developed which are capable

of inducing the production of neutralizing antibodies when injected in animals protecting them from toxin actions and avoiding the development of symptoms. Other examples are hybrid subunit vaccines, consisting of the inactive Stx2 A subunit and of Stx1 B subunits which can protect from both type of toxins (Stx1 and Stx2); vector-based DNA vaccine which encodes the C-term sequence of Stx2 A and the complete B subunits; bacteria-based vaccines based on non-pathogenic STEC variants (Mühlen & Dersch, 2020).

11.6. Polymyxin B and derivatives

11.6.1. The antibiotic polymyxin B

Polymyxin B is an old antibiotic used against Gram negative bacteria and derived from *Bacillus polymyxia* which was abandoned as systemic therapy in 1970s and no longer used because of its high nephrotoxicity and increased availability of more effective antibiotics. Unfortunately, polymyxins are highly nephrotoxic when used systemically at conventional doses, inducing frequently acute kidney injury. For this reason, they cannot be used as continuous therapy and discontinuation is required (Tsuji et al., 2019).

However, up to day polymyxins are used in therapy as the last resort against multiresistant bacteria (M. Vaara, 2010; M. Vaara, Vaara, & Vingsbo Lundberg, 2018).

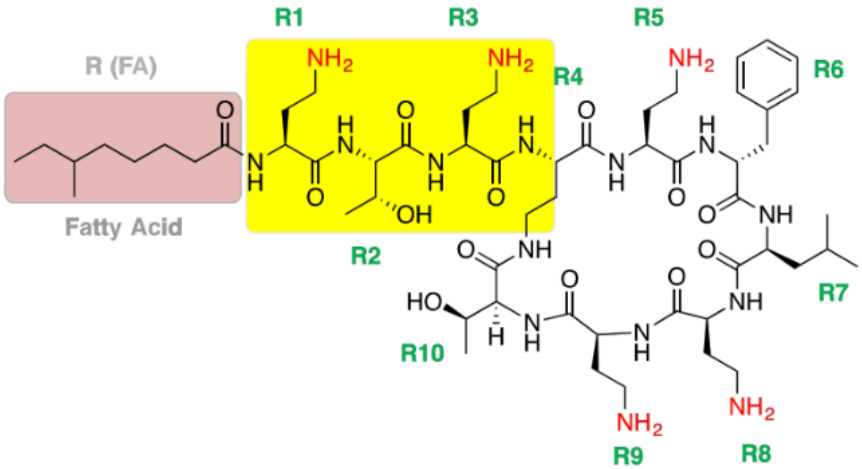

Figure 11: The structure of polymyxin B. The fatty acyl "tail" is highlighted in pink and the linear peptide part in yellow. The five free amino groups are marked in red. (M. Vaara et al., 2018)

Polymyxin B is composed of a cyclic heptapeptide part with three positive charges and a linear part with two positive charges, linked to a hydrophobic fatty acyl tail residue (Figure 11) (M. Vaara, 2010). This antibiotic, thanks to its amphipathic region, is capable of interacting with lipid A portion of LPS (Morrison & Jacobs, 1976; Srimal, Surolia, Balasubramanian, & Surolia, 1996) inducing perturbation and permeabilization of the outer membrane of Gram-negative bacteria, thus exerting its antimicrobial effect. In addition, it is able to impair the interaction between LPS and TLR4 expressed by innate immune cells, blocking their activation and response.

As described before, Stx A chain is also recognized by TLR4 expressed by human neutrophils, but also by monocytes and platelets, as well as endothelial cells resulting in their activation and release of proinflammatory mediators involved in the inflammation process. In the case of endothelial cells, the binding to TLR4 concurs to the internalization process if the toxins are bound also to Gb3Cer. Since Stx and LPS are sensed by the same receptor, it has been recently found that polymyxin B is also capable of impairing the interaction between Stx and TLR4 expressed by human neutrophils (Carnicelli et al., 2016). More specifically in this study it was discovered that polymyxin B inhibits the binding of the Stx A subunit to TLR4 expressed by neutrophils, avoiding their activation and inhibiting the release of IL-8. In addition, the antibiotic does not interact directly with B-chains having no effect in modifying the cytotoxicity of Stx to Gb3Cer expressing cells. Moreover, polymyxin B inhibits Stx enzymatic activity, evaluated through the inhibition of adenine release after incubation of a synthetic [^{3}H] DNA with Stx. Another important effect of polymyxin B is the significant inhibition of the formation of aggregates between neutrophils and platelets, and the non-significant lowering of the number of monocyte/platelet aggregates. Since the affinity of Stx for Gb3Cer is 10-fold higher than for TLR4, polymyxin B could have a milder effect on monocytes and platelets expressing both receptor with respect to human neutrophils which express only TLR4 (Carnicelli et al., 2016).

11.6.2. Polymyxin B derivatives

Antibiotic administration is not recommended for the treatment of STEC-infected patient during the intestinal phase as it increases the risk of HUS development. Moreover, the strong nephrotoxicity and neurotoxicity (M. Vaara, 2010; Martti Vaara, 2013) of polymyxin B further discourage its use as therapy. However, recently, nontoxic polymyxin

derivatives have been developed and they could be used at non-bactericidal concentrations as an effective treatment.

Thanks to the knowledge of the contribution of each amino acids of polymyxin B to its antimicrobial activity or to its LPS-binding activity, it was easy to change some of them for the development of new less toxic or non-bactericidal derivates, which are anyhow effective in the binding to LPS (Kanazawa et al., 2009). The idea is that hydrophobic interactions are the driving force for the association of polymyxin B with lipid A of LPS (Srimal et al., 1996). In addition, the toxic effect of polymyxin B, especially in the kidney, is due to the presence of the cationic charges. A different localization of the cationic functional groups or their reduction can influence both efficacy and nephrotoxicity of these drugs. Thus, the substitution of some positive charged amino acids with other amino acids would reduce the toxicity of polymyxin B derivatives (Yu, Qin, Lin, Fang, & Qiu, 2015).

An example is NAB739, developed by the Finland company Northern Antibiotics, which lacks the positive charges in the linear part and carry only three positive charges (M. Vaara, Vaara, & Tyrrell, 2017; M. Vaara et al., 2018). It is less toxic than polymyxin B but maintains its strong antimicrobial activity (Martti Vaara, 2013). Another candidate is NAB815 carrying two positive charges in the ring and a single positive charge in the liner part (M. Vaara et al., 2018). Both NAB739 and NAB815 are less nephrotoxic than polymyxin B in cynomolgus monkeys and can be used as therapy in murine *Escherichia coli* pyelonephritis at one-tenth doses of that needed for polymyxin B to be effective (M. Vaara et al., 2020; M. Vaara et al., 2018). The drugs are intravenously injected into the circulation to avoid their degradation by digestive enzymes.

Other examples are NAB7061 and NAB741, which are less toxic and devoid of a potent bactericidal action (Martti Vaara, 2013). Indeed, although they do not possess a powerful bactericidal action, they perturb the external bacterial membrane by interacting with LPS and thus increasing the permeability to other antibiotics (Martti Vaara, 2013).

In conclusion, some of these polymyxin derivatives appear to be promising drugs as their interactions with LPS, and probably with Stx, could be preserved without exerting a direct bactericidal action, which would be dangerous and contraindicated for STEC infected patients during the prodromal intestinal phase. *In vitro* assays have shown that NAB815, among the putative candidates, is the best polymyxin derivative to be used as an inhibitor of the interaction between the Stx and TRL4. The experiments have been previously described (2019, Italian patent 102019000025414; 2021, patent extended in EU,

USA, Canada, Japan and Brazil WO2021130700 (A1)) and showed that NAB815 binds directly to the A chain of Stx2 preventing the interaction of the toxin with TLR4 expressed by human circulating cells and inhibiting the formation of aggregates between white blood cells and platelets. Therefore, it is assumed that the subsequent phases of the pathogenesis of HUS, including the release of HUS-triggering microvesicles are impaired. A direct demonstration of the efficacy of NAB815 in preventing the formation of pathogenic blood cell-derived Stx2-containing microvesicles *in vitro* and in blocking the toxicity of Stx2 in cellular and animal models is needed.

12. HUS animal models

Several animal models of STEC-HUS have been developed to study the onset of HUS and, in particular, the renal damage.

The animal model required to study HUS should recapitulate the whole pathogenic process including intestinal STEC infection, toxin delivery in the blood and onset of the triad typical of HUS. However, it is not always possible to recapitulate all the stages of HUS in the different animal models.

The STEC-infected mouse model of HUS is capable of mimicking the pathogenesis of the syndrome from gastrointestinal infection to renal failure (Tarr et al., 2005). Alternatively, the toxin is directly injected into the circulation by intravenous administration or the animals treated with intraperitoneal injections, however bypassing enteric colonization.

In both cases, the presence on murine circulating cells of different receptors with respect to humans makes it difficult to clarify the early cellular events involved in the pathogenesis of HUS (Griener et al., 2007). Human neutrophils do not possess the complete set of enzymes required for the synthesis of Gb3Cer and Gb4Cer and hence express only TLR4 as the Stx receptor (M. Brigotti et al., 2013). In contrast, mouse neutrophils showed expression of both TLR4 and Gb3Cer. Consequently, in mice Stx preferentially bind via its B subunits to the Gb3 receptor rather than to TLR4 via its A subunits, and this is in keeping with the notion that Stx has a higher affinity for Gb3Cer than for TLR4, as in humans (M. Brigotti, 2012; te Loo et al., 2000).

Conversely, the presence of the same Gb3Cer receptors in renal and brain target cells (except glomerular endothelial cells) makes the mouse model useful for studying the damage to the main target organs.

Experiments using mice orally infected with STEC show clinical and pathological findings that mimic some aspects of human infection and of HUS: systemic and neurological symptoms 7-8 days after inoculation with intestinal and renal manifestations. Notably, fibrin deposition has been found in the glomeruli, as well as tubular and glomerular cell apoptosis (Békássy et al., 2011; Calderon Toledo et al., 2008; Karpman et al., 1998). Tubular damage can also be reproduced in mouse models with intraperitoneal or intravenous injection of Stx2 and lipopolysaccharide (LPS) (Psotka et al., 2009). However, in general, mouse models are characterized by less glomerular involvement and greater tubular damage than seen in human disease (Trachtman et al., 2012).

Given the different binding abilities of mouse and human circulating cells, suitable model allowing to study directly renal and cerebral damage can be obtained by inoculating in mice Stx-containing human microvesicles .

Furthermore, mice lack HuSAP that captures Stx2 in human blood (Varrone et al., 2021) and this feature is also required to adequately recapitulate the pathogenesis of human HUS in an animal model.

The best animal model to study the pathogenesis of HUS is the baboon as it more closely reproduces both the expression pattern of the receptors present on target organs and human circulating cells (Taylor et al., 1999).

In baboons, the amino acid sequence of TLR4 is 93.5% identical to humans in the extracellular domain, differing in the transmembrane domain by a single substitution and in the proximal cytoplasmic domain by only one residue; at the carboxyl terminus the homology is lower (Smirnova, Poltorak, Chan, McBride, & Beutler, 2000). No fundamental differences between humans and non-human primates in the pattern of TLR4 expression have been reported in blood cells, gut, and endothelial cells. Consequently, the baboon model reproduces the binding to circulating cells and the subsequent phases of HUS pathogenesis.

Finally, simian and human SAP are highly homologous and strongly immunologically cross-reactive.

Baboon models of HUS based on single or repeated doses of intravenously administered Stx are well known. Indeed, baboons treated with a single intravenous dose (10 to 50 ng/kg) of purified Stx2 show thrombocytopenia, microangiopathic hemolytic anemia, and renal thrombotic microangiopathy, thus reproducing the HUS triad (Stearns-Kurosawa, Collins, Freeman, Tesh, & Kurosawa, 2010).

Experimental infection with STEC as a model of HUS has not been described in baboons, whereas in Macaca radiata intragastric administration of STEC gave only intestinal symptoms without overt HUS (Kang et al., 2001).

AIMS

This thesis is focused (1) on the development of a new faster, more sensitive and more effective method for the early diagnosis of STEC-infections; (2) on the role of Stx in the pathogenesis of HUS, in particular on the journey of Stx once released into circulation, with the aim of better understanding its structural characteristics and properties; (3) on the identification of the origin and the features of blood-cell derived microvesicles involved in this critical phase of STEC infection that leads 15% of patients with hemorrhagic colitis to develop HUS, as well as on the search for new therapies using toxin binding inhibitors aimed at reducing the possibility of disease evolution.

1) Currently the gold standard strategies available for the diagnosis of STEC infections (microbiological and serological diagnostic methods) are very expensive, both in terms of work, as it is necessary to carry out the assays in specialized laboratories, and in terms of time, extending the timeframe from the onset to the diagnosis of disease hence delaying the treatment of the infection. Therefore, there is a strong need of identifying a faster more sensitive and more effective method for the early detection of Stx2a in STEC-infected patients.

   We sought to develop and validate a plasmonic biosensor as a new diagnostic tool for the early diagnosis of STEC infections, in collaboration with the physicists led by Dr Lucia Petti (CNR, Pozzuoli, Naples). This biosensor is capable of detecting Stx2a at low concentrations in the blood of STEC-infected patients. This method exploits the resolving power of SERS technology (Amplified Raman Spectroscopy on Surfaces) to detect Stx2a in different conditions: samples of toxin in water, PBS, or more complex biological samples.

2) During the pathogenesis of HUS, several toxin forms are transported in the bloodstream: free Stx, Stx bound to neutrophils and other circulating cells or associated to blood cell-derived microvesicles.

   Previous experiments in collaboration with a group of clinical microbiologists from the Medical University of Innsbruck (Austria) have shown that the toxin can have two different structures, according to the purification protocol used: uncleaved or cleaved, which have a single nick in the A chain resulting in two fragments, A1 and A2 connected by a disulfide bridge.

   The two forms have been recently found to be biologically active as they similarly intoxicate human cells expressing Gb3Cer, but functionally different. Indeed, they have different binding properties for circulating cells and host serum components (M. Brigotti et al., 2019). Although the structure, the mechanism of action and the different properties of the two forms of the toxin (uncleaved and

cleaved) are well known, whether the cleaved form can be found in the blood of STEC-infected patients and where the toxin is cleaved is unclear.

The outcome of STEC infections and the consequent onset of HUS could be influenced by the percentages of toxin present in uncleaved or cleaved form circulating in patients' blood.

We sought to develop a luminometric cell-free protein synthesis assay to detect the cleaved form of Stx2a in human serum. The presence of the cleaved form of the toxin in STEC-infected patients' sera was assessed by this method.

3) A growing body of evidence have been recently supporting the idea that blood cell derived-microvesicles produced in the blood of patients by toxin-challenged circulating monocytes, neutrophils, erythrocytes and platelets, are being implicated as crucial players in the pathogenesis of HUS.

From results obtained in a recent clinical study (Brigotti M., 2020) it emerged that the presence of the free toxin in the blood or bound to neutrophils does not constitute a discriminating and prognostic element for patients who develop HUS. The distinctive feature is the presence, on the day before the diagnosis of the syndrome, of microvesicle-associated Stx (particulate Stx) consisting of toxin associated with microvesicles through the binding of A chain to TLR4 or B chains to Gb3Cer.

It is therefore extremely important to identify the features and the origin of the pathogenic microvesicles and the subsets responsible for the development of HUS.

A better understanding of the pathogenesis would also allow to design therapies with toxin binding inhibitors that are intended to lower the likelihood of illness progression. No specific and established pharmacological treatment is currently available for HUS.

The antibiotic NAB815, a polymyxin B non-toxic derivative, constitutes a recent potential innovative treatment at non-bactericidal concentrations (approximately 60 times lower than that obtained with polymyxin B).

We sought to harvest pathogenic microvesicles from Stx2a-challenged human blood from healthy donors, to characterize the microvesicles by identifying their origin (by monocytes, platelets and neutrophils), and the presence of Stx2a. The protective effect of NAB815 on the formation of blood cell-derived microvesicles containing Stx2a will be assessed in cellular models.

MATERIALS AND METHODS

1. Shiga toxin 2a (Stx2a)

1.1. Stx2a purification

Stx2a was produced from strain C600ϕ933W, an *E. coli* K12 strain containing the bacteriophage carrying the Stx2a gene of the STEC EDL 933 strain, which was supplied by Dr. Alison O'Brien (Department of Microbiology and Immunology, Uniformed Services University of the Health Sciences, Bethesda, MD) (A. Matussek et al., 2003).

The bacteria were plated on agar and grown for 72 h. Then, the resulting colonies were added to 250 ml of sterile Luria Bertani (LB) medium and grown for 20 h in an orbital shaker at 120 rpm (pre-culture). Bacterial growth was evaluated by recording the absorbance at 540 nm with a spectrophotometer. The pre-culture was then inoculated in 4L of LB medium (culture) and incubated for 4-5 h at 37°C with shaking. Once A540 was ~0.6, mitomycin C (Sigma-Aldrich, Taufkirchen, Germany) was added at the final concentration 0.4 mg/L and incubated for 20 hours at 37°C with shaking to enhance Stx release from the bacteria. Finally, the bacterial culture was centrifuged at 16000 g for 15 min at 4°C and the supernatant containing the toxin was collected. The volume of the supernatant was measured and ammonium sulphate was added under constant stirring at 4°C to the final concentration 472 g/L corresponding to 70% saturation. The protein precipitate was spun down for 10 minutes at 16000 g (4°C) and the pellet resuspended in 15 ml of water. The suspension was then dialyzed against 10 mM Tris/HCl (tris(hydroxymethyl)aminomethane, pH 7.5) for 48 hours at 4°C.

The crude protein preparation was passed through a receptor analogue affinity column (1.5 cm x 0.6 cm, total volume 1 ml) in which bovine serum albumin (BSA) linked to a terminal galabiose (Galα1-4Galβ - O - spacer – BSA, Glycorex, Lund, Sweden) was coupled to cyanogen bromide– activated Sepharose 4B (Pharmacia, Uppsala, Sweden) (Andreas Matussek et al., 2003). Subsequently the column was washed with 200 ml of 10 mM sodium phosphate buffer (pH 7.5) containing 1 M NaCl to remove non-specifically bound proteins. Then the toxin was eluted with 4.5 M $MgCl_2$ (10 ml), a chaotropic agent which reversibly unfold the toxin detaching it from the column, and collected in 1 ml-fractions. The fractions 1-5 were pooled according to their high A280 values. To discard the eluent and concentrate the toxin, serial centrifugations of the pooled fractions over Amicon YA30 membranes (semipermeable membranes with pores allowing the passage of

molecules lower than 30,000 Da) were carried out at 4°C at 12167 g for 16 minutes. Repeated washing steps with phosphate buffered saline (PBS) in sterile endotoxin-low water were performed.

To remove traces of bacterial endotoxin a passage through ActiClean Etox Columns (Sterogene Bioseparations, Carlsbad, CA) was carried out. The toxin preparation (500 µl in PBS) was added to the column and, after washing with PBS, 500 µl-fractions were collected. The presence of Stx2a in each fraction was evaluated by applying 1 µl-aliquots to Immunostat EHEC plates (rapid test STX2, Meridian Bioscience). The fractions containing the toxin were pooled and stored at -80°C in aliquots.

1.2. Quantification of LPS

The Stx2a preparation was assayed by using the Toxin Sensor Endotoxin Detection System (Genscript, USA) to quantify the amount of lipopolysaccharide (LPS) in the sample. Stx2a was diluted in endotoxin-free water to obtain different dilution (1:16 to 1:1000). As controls different dilutions of *E. coli* endotoxin (0.5 to 0.0625 EU) were used. Endotoxin-free water was used as negative control. Then 100 µl of Limulus Amebocyte Lysate Pyrogent Plus (Cambrex, Walkersville, MD) were added to the samples. After 1 h incubation at 37°C, the presence of LPS was verified by inverting each vial and identifying the gelation of Limulus Amebocyte Lysate. A positive reaction is characterized by the formation of a firm gel that remains intact when the vial is inverted, while a negative reaction is characterized by the absence of a solid clot. The limit of detection of the test corresponded to the lowest concentration of LPS to which the test was positive. On this basis, the lowest dilution of the toxin to which the test was positive was identified hence obtaining the contaminant LPS value expressed in UE/ml. Knowing that 13 EU correspond to 1 ng of LPS, we calculated the amount of LPS/mg of toxin.

1.3. Stx2a quantification by Lowry assay

Purified Stx2a (20 µl aliquots) was quantified by using Lowry assay, with BSA (3-24 µg) as standard in 250 µl of water. After the addition of 625 µl of Lowry (Lowry reagent + $CuSO_4$ 0,1%) and 62.5 µl of Folin reagent, the mixture was incubated at room temperature for 30 minutes and the absorbance at 660 nm was recorded. The protein concentration of the Stx2a preparation was obtained by the standard curve.

1.4. Cleavage of Stx2a

In order to obtain the cleaved form of Stx2a, the toxin (4 µg) was treated with 50 ng of trypsin (1 mg/mL in 0.1 mM HCl, diluted to 0.05 ng/ml with PBS) in 10 µl PBS pH 7.5 and incubated for 1 h at 37°C. Then, in order to inactivate trypsin, 0.7 ng of the trypsin inhibitor phenilmethylsulfonil fluoride (PMSF, 1 mg/ml dissolved in absolute ethanol and diluted to 0.7 µg/ml with water) was added and incubated for 10 minutes at 37°C (M. Brigotti et al., 2019; Rocchetti et al., 2021).

2. Blood and serum

Whole blood from 5 healthy donors (males, median age 50 years) having different blood groups (B+, A+, AB+ and two 0-) was kindly provided by the Immunohematology and Transfusion Center (Maggiore Hospital, Bologna) after obtaining informed consent. Whole human blood was used for the preparation of blood cell-derived microvesicles after the addition of Stx2a and/or NAB815.

Serum samples from 10 STEC-infected patients (6 males and 4 females, median age 5.7 years), 3 with overt HUS, were collected and stored ad -20 °C. Parents of the children gave their informed consent for inclusion before they participated in the study. The study was conducted in accordance with the Declaration of Helsinki, and the protocol was approved by the Ethics Committee of the Fondazione IRCCS Ca' Granda Ospedale Maggiore Policlinico, Milan, Italy (18 May 2010). Serum samples were also available from three adults after obtaining informed consent. Sera were used for the detection of the cleaved form of Stx2a.

2.1. Treatment of human serum with protein G Sepharose

Human serum samples (125 µl) without or with different concentrations of Stx2a (0, 1.8, 3.6 or 6 ng/ml) were added to 375 µl of the resin suspension (Protein G Sepharose fast flow P3296, Merck Life Science, Milan, Italy) diluted with an equal volume of 20% ethanol and washed three times with PBS. After incubation for 15 minutes at room temperature (24 °C) in an orbital shaker, the mixture was centrifuged 4 min at 200 g at 4 °C in Eppendorf tubes and 100 µl of protein G-treated serum was collected (Rocchetti et al., 2021).

2.2. Concentration of human serum treated with protein G

Protein G-treated serum samples (100 μl) were concentrated 5 times by centrifugation on Centricon 30 ultra 0.5 mL centrifugation filters (Merck Life Science, Milan, Italy) for 1 h at 12000 g (Rocchetti et al., 2021).

3. Cells

3.1. Raji cells

Raji cells are human cells that express Gb3Cer receptor and are sensitive to the toxic action of Stx2a after short incubation times. They were cultured in RPMI 1640 medium (Lonza, Walkersville, MD) containing antibiotics (60 U/ml penicillin, 60 mg/ml streptomycin; Cambrex) and supplemented with 4 mM L-glutamine (Sigma-Aldrich) and 10% FBS (Lonza) and were used to assess the inhibition of protein synthesis induced by Stx2a.

3.2. Vero cells

Vero cells are simian renal Gb3Cer-expressing cells very sensitive to Stx2a after overnight exposure to the toxin. They were cultured in DMEM (Dulbecco modified essential medium containing glucose and L-glutamine; Euroclone ECGB 750L) supplemented with 10% FBS, 2 mM L-glutamine and 1% penicillin-streptomycin and used for the detection of inhibition of protein synthesis by Stx2a and by Stx2a-containing blood cell-derived microvesicles and for cell viability assays.

3.3. Human neutrophils

Neutrophils were isolated and purified in sterile conditions with low contamination of bacterial endotoxin from buffy coats of different healthy donors after centrifugation on Ficoll-Paque, sedimentation with dextran and hypotonic lysis of contaminating erythrocytes. The EasySep Human Neutrophil Enrichment Kit (Stemcell Technologies, Vancouver, BC, Canada) was used to achieve 99.7% purity and remove any contaminant

cells. Neutrophils were used to assess the binding capacity of the toxin to TLR4 (M. Brigotti et al., 2013; M. Brigotti et al., 2008).

4. Microvesicles

4.1. Isolation of blood cell-derived microvesicles

Whole blood from healthy donors (80 ml) diluted with an equal volume of DMEM and supplemented with 10 µM Gly-Pro-Arg-Pro Fibrin Polymerization Inhibitor (GPRP) (Merck) was incubated 4 h at 37 °C with 2 nM Stx2a or with NAB815 (0.01 µg/ml) or with Stx2 + NAB815 or in the presence of NAB815 alone or vehicle. Then, microvesicles were isolated by differential centrifugation of blood samples (2600 g for 35 minutes to remove blood cells and platelets; 10400 g for 25 minutes to remove cell debris and apoptotic bodies; 20800 g for 1 h to sediment microvesicles). Each pellet was resuspended in 1 ml of PBS and divided in two aliquots: 250 µl of the suspension were centrifuged at 20800 g for 40 minutes and the pellet frozen at – 80 °C in order to prepare microvesicle-derived proteins for further characterization; 750 µl of the suspension were centrifuged as above and the pellet resuspended in 200 µl and frozen at – 80°C (Ståhl et al., 2015; Villysson et al., 2017).

4.2. Identification of the size of microvesicles by DLS

The microvesicles were analyzed by using DLS, an instrument that detects the Brownian motion of these particles in solution according to their size.

4.3. Microvesicle lysis and protein extraction

Each pellet of microvesicles obtained by the 250 µl aliquot (see 4.1.) was lysed by adding 25 µl of RIPA buffer containing cOmplete protease inhibitors cocktail (Roche, Sigma-Aldrich, USA) and incubating for 10 minutes with occasional stirring. Then, each sample was centrifuged at 14000 g for 10 minutes at 4°C in order to discard membrane residues and the supernatant recovered and frozen at -80°C.

4.4. Protein quantification by Bradford assay

Microvesicle-derived proteins were quantified by using Bradford assay, with BSA as standard (1.25- 20 µg) in 1 ml water. After addition of 250 µl of Bradford reagent (Biorad, USA), the samples were mixed and incubated at room temperature for 5 minutes. The protein concentration was calculated by the absorbance at 595 nm.

4.5. Characterization of blood cell-derived microvesicles by WES

Microvesicles were characterized by WES (quantitative capillary Western Blot) performed on total proteins extracted from microvesicles. Each sample was prepared according to the manufacturers' instructions by diluting proteins with a provided sample diluent and a master mix containing DTT and incubated 5 minutes at 95°C. Then, the marker, the sample, the antibody diluent for the blocking step, the primary antibody, the secondary antibody, streptavidin-HRP and Luminol-Peroxide mix were added to each well of the plate. The plate and the capillaries were used to start the automated Western Blot analysis and the quantitative immunodetection (Protein Simple Western, Biotechne).

To characterize microvesicles, different primary antibodies were used: rabbit anti-Alix 1:50 (Novusbio) (microvesicle marker); mouse anti-CD45 1:250 (BD Transduction Laboratories) (leukocytes marker) and rabbit anti-CD42a 1:10 (Genetex) (platelet marker) to identify the origin of microvesicles; rabbit anti-Stx2 1:50 (Dr. Stefano Morabito, ISS Rome) to detect the toxin.

4.6. Analytical gel-filtration of microvesicles

A representative preparation of microvesicles (control microvesicles, Stx2a microvesicles and Stx2a+NAB815 microvesicles) was analyzed by gel-filtration column chromatography (Sephacryl S-500 HR, 0.5 cm x 28 cm, total volume 5.5 ml, 200 nm exclusion size) in order to evaluate the purity of the sample. After equilibration with 20 mM Tris-HCl (pH 7.4) containing 150 mM NaCl, 100 µl-aliquots of each sample were separately loaded on the column. Then 5 ml of the buffer were added and 250 µl-fractions were collected (Watanabe-Takahashi et al., 2018). Vero cell protein synthesis assay (see below) was used to detect Stx2a in the fractions.

5. Assays

5.1. Protein synthesis assay

5.1.1. Protein synthesis assay with Raji cells

Human Gb3Cer-expressing Raji cells were used for the detection of translation inhibition induced by Stx2a. Raji cells were seeded in a 24-wells plate (300,000 cells in 500 µl of medium). After 24 h, the cells were incubated with 5 µl of different concentrations of Stx2a for 3 h at 37 °C. Protein synthesis was measured as the rate of incorporation of [^{3}H] leucine into proteins during 60 minutes-incubation at 37 °C in complete medium. The content of each well was then transferred to a 2 ml Eppendorf tube and centrifuged for 5 minutes at 200 g at room temperature. The supernatant was removed and the cell pellet resuspended in 1 ml of 0.1 N KOH and incubated for 5 minutes at room temperature in order to cleave the bond between tRNAs and amino acids. Each sample was transferred to a 10 ml plastic tubes containing 20% TCA to precipitate the proteins which were subsequently collected on glass microfiber filters (Whatman GF/C) presoaked with 10 mM cold L-Leucine following filtration of the sample. The radioactivity associated with the filter was measured in a liquid scintillation β counter (Arfilli et al., 2010).

5.1.2. Protein synthesis assay with Vero cells

Vero cells were seeded in 24-wells plate (50,000 cells in 500 µl of medium). After 24 h, the cell monolayer was treated (Stx2a, STEC-infected patients' sera, microvesicles) and incubated for 18 h at 37 °C. Protein synthesis was measured as the rate of incorporation of [^{3}H] leucine in the new synthesized proteins in 60 minutes-incubation. The medium of each well was removed and cells were washed 3 times with 1 ml PBS and 3 times with 1 ml of TCA 10% to precipitate the cellular proteins. Then, the precipitated proteins were solubilized in 200 µl of 0.2 N KOH and transferred in a plastic tube. Radioactivity was measured in a liquid scintillation β counter. IC_{50} was calculated by the linear regression between mean percentage of translation and the log of inhibitor concentrations (Gentry & Dalrymple, 1980; Russo, Melton-Celsa, Smith, & O'Brien, 2014).

5.1.3. Cell-free protein synthesis assay

A luminometric acellular translation system derived from rabbit reticulocyte lysate, fractionated and reconstituted with human ribosomes that translate synthetic exogenous mRNA encoding the enzyme luciferase (*Renilla reniformis*) was used.

This assay involved the preparation of rabbit reticulocyte lysate and related fractions (S-140 post-ribosomal supernatant and salt wash), preparation of human ribosomes from Raji cells and reaction mixture of the luminometric translation system. In a final volume of 22 µl there were: 3 µl pre-incubation mix (containing PBS-BSA or Stx2a ± DTT with or without human serum), 4.4 µl 5X reaction mix (containing 150 mM Hepes / KOH, 400 mM KCl, 5 mM magnesium acetate, 250 µM of each amino acid, 10 mM ATP, 1.25 mM GTP, 25 mM creatine phosphate, 0.9 mg/ml creatine phosphokinase, 2.5 mM DTT, 2 mM spermidine), 8 µl of S-140, 0.9 µl of salt wash, 1 µl of mRNA-cap for *Renilla reniformis* luciferase (0.3 µg) transcribed from pRL-FL plasmid, 0.5 µl of placental RNAse inhibitor (PRI) and 2 µl of human or rabbit ribosomes (0.125 pmol), water up to the final volume. After 60 min at 30 ° C, the synthesis was stopped on ice and the luciferase activity was measured using the Dual-Luciferase Reporter assay (Promega, Milan, Italy) (Penzo, Carnicelli, Montanaro, & Brigotti, 2016).

5.2. Viability assay on Vero cells

A Luminescent Cell Viability Assay (Promega, Milan, Italy) was used to assess the number of live cells in culture by quantifying the amount of ATP as a product of metabolically active cells.

Vero cells were seeded in 24-wells plate (50,000 cells in 500 µl of medium). After 24 hours, the cell monolayer was treated (Stx2a, microvesicles) and incubated for 72 h at 37°C. Then the medium was removed and 150 µl of fresh medium and an equal volume of Cell Titer-Glo Reagent was added to each well. After 2 minutes shaking to induce cell lysis, 200 µl were transferred to a 96-wells plate. After 2 minutes shaking and 10 minutes of incubation at room temperature, a luminescent signal proportional to the amount of ATP present in the sample was measured. IC_{50} was calculated by the linear regression between mean percentage of viability and the inhibitor concentrations.

5.3. Adenine release from DNA assay

The enzymatic activity of Stx2a on radiolabeled DNA, as the removal of adenine bases from nucleic acids, was directly evaluated and measured by using as substrate the 2251-bp [^{3}H] DNA labeled in the purine ring of adenine obtained by PCR amplification of the 731–2981 region of the pBR322 plasmid (M. Brigotti et al., 1998).

Different amounts of Stx2a diluted in PBS-BSA 50 μg/ml were incubated for 40 minutes at 45˚C with [^{3}H] DNA. The enzymatic reactions were performed in 250 μl 1 M sodium acetate buffer (pH 4) containing 300 mM sucrose and 0.3 μg substrate corresponding to 205.5 pmol of adenine having a specific radioactivity of 3000 dpm/pmol. Then, DNA molecules were removed by passing the samples through Bond Elut NH2 columns that bind charged molecules but not the released neutral adenine. Radioactivity was measured in a liquid scintillation β counter (M. Brigotti et al., 1998).

5.4. Binding assay of Stx2a to TLR4 on neutrophils

Human neutrophils were isolated and purified under low endotoxin conditions. To prevent non-specific losses of toxins during binding experiments with Stx2a, Eppendorf tubes were pretreated with PBS containing 1% endotoxin-low bovine serum albumin (BSA) (Sigma-Aldrich) (van Setten et al., 1996). Neutrophils (500,000/ml) were incubated 90 minutes at 37˚C with Stx2a (60 nM) in 250 μl of PBS-BSA. Cells were then sedimented by centrifugation at 200 g for 5 minutes and washed three times with 100 ml of incubation buffer at 37˚C.

5.5. Detection of Stx2a bound to neutrophils

The detection of Stx2a bound to neutrophils was evaluated by incubation with a primary mouse monoclonal antibody anti-Stx2 in the presence of human serum to saturate FcRs on neutrophils (Tazzari et al., 2004). After washing with PBS, a secondary goat FITC anti-mouse IgG was added. Flow cytometric analysis was used to reveal the neutrophil-bound fluorescence. A cytogram that combined forward scatter versus 90° side scatter was used to identify cells, and a cytogram that combined 90° side scatter and fluorescence as well as a single-fluorescence histogram were used to examine fluorescence. Stx2a binding to neutrophils was quantitatively determined using the MCV parameter (mean channel value of fluorescence) of the produced fluorescence histograms. The values were calculated by

subtracting the control MCV (0.4–0.6), that is, the MCV of neutrophils from the same donor incubated with primary and secondary antibodies in the absence of the toxin. Neutrophils were examined by staining with monoclonal antibodies to antigens associated to neutrophils (FITC-CD16 and FITC-CD65, Beckman Coulter, Miami, FL) (Tazzari et al., 2004).

5.6. Plasmonic biosensor of nanostructured SERS substrates

Plasmonic biosensor consists of nanostructured SERS substrates fabricated by electron beam lithography technology that have an octupolar photonic crystal geometry, whose single unit cell is made up of three triangular nanocavities (Figure 12A). Each triangular nanocavities has a side (L) of 180 nm and is separated from the other triangular nanocavity by a minimum intercell distance (D) of 100 nm. The centers of each triangle are placed at the vertices of a virtual triangle (the cell) with side (S) of 230 nm and the lateral dimension of 430 nm. Shape, size, geometry, symmetry and composition of the material identified for the formation of the cells of the SERS substrates, are all factors which allow the development of plasmonic properties following the interaction with polarized light and to obtain SERS measurements carried out in reflection. Once the sample was adsorbed on the substrate, it was irradiated with a laser beam with a wavelength equal to 785 nm and following the interaction with the material, an amplified signal was generated by inelastic reflection formed by radiations of lesser energy than light, obtaining a characteristic spectrum (Figure 12B). The single reflected radiations depend on the presence of particular chemical groups or bonds of the molecule under study and this allowed to identify it on the basis of a specific spectrum (fingerprinting) (Rippa et al., 2022).

To perform SERS measurements, Stx2a was diluted in water or PBS from a 6.62 μM stock solution, to a final concentration of 0.04 nM. An aliquot (3 μl) of the diluted toxin corresponding to ~100 ng (~10^{12} molecules) of Stx2a (molecular mass of 68,000 Da) was directly deposited on the nanostructure sensor, dried at room temperature, and analyzed by SERS.

Subsequently the surface of the biosensor was pre-functionalized by the adsorption of 3 μl of different concentrations of an anti-Stx2 monoclonal antibody (5, 10 and 25 μg/mL) to obtain the specific capture of the toxin. After incubation, 5 washing steps were performed to remove unwashed excess antibody. The diluted toxin preparation was then added and

incubated for 1 h. After 5 washes with PBS and sample drying, SERS measurement was performed (Rippa et al., 2022).

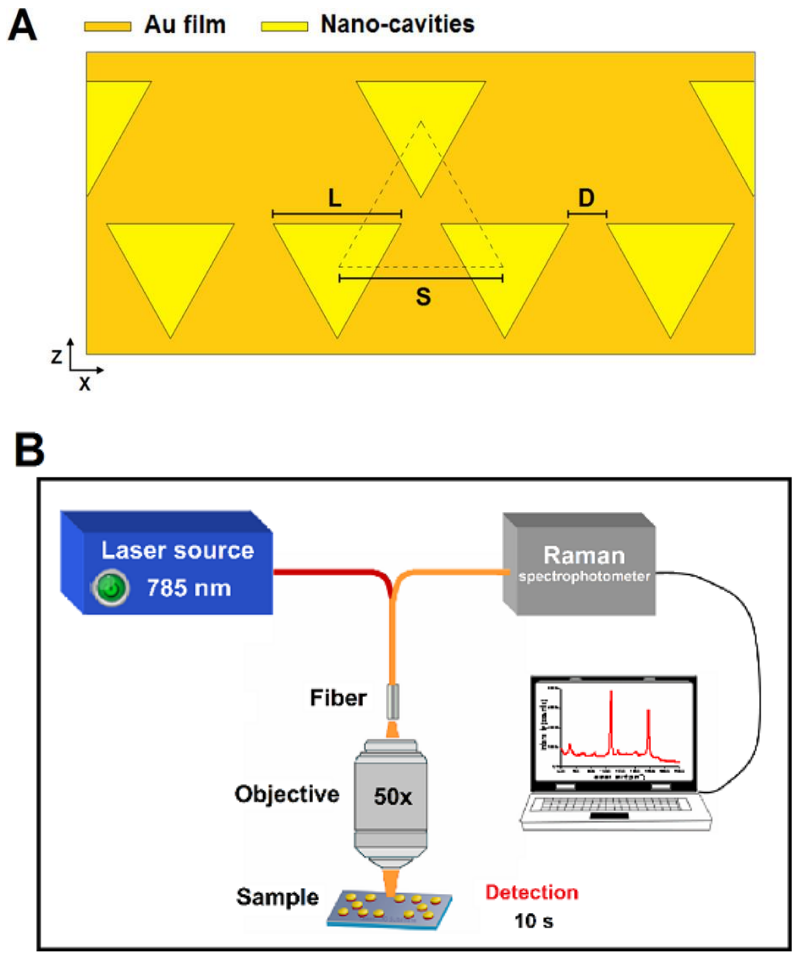

Figure 12: Structure of a plasmonic biosensor. A plasmonic biosensor consists of nanostructured surface enhanced Raman scattering (SERS) substrates manufactured by electron beam lithography with concavities on which the sample to be analyzed is deposited. (A) scheme of the octupolar cell unit of nanostructured SERS substrates. (B) procedural scheme of detection: once the sample to be analyzed is deposited, the surface is irradiated with a laser of suitable wavelength and by interpreting the characteristic spectrum obtained derived from the amplified signal, it is possible to identify the type of molecule and its features.

5.7. Enzyme-Linked Immunosorbent Assay (ELISA)

Enzyme-Linked Immunosorbent Assay (Eurofins Abraxis, Warminster, PA, USA) is an indirect immunoassay based on the detection of all variants of Stx2 by specific antibodies in different samples.

It was performed coating the plate with 5 µg/mL of capture antibody anti-Stx2 (which recognized the B-subunit of Stx2) for 16 h at 4 ◦C and then blocking with 5% nonfat skim milk at 37 ◦C for 1 h. Samples (0.75 µl) of different water-diluted Stx2a were added to the

ELISA plate and brought to the volume required for the assay (100 µL) with PBS−BSA 1% and incubated for 1 h at 37 ◦C. After a washing step, 100 µl of a second antibody anti-Stx2 which binds to Stx2a bound to the well were added and incubated for 30 minutes. After another washing step, 100 µl of horseradish peroxidase (HRP)-conjugated Ab which binds to the Stx2a/antibody anti-Stx2 complex were added and incubated at 37 °C for 30 minutes. After a washing step, 100 µL HRP substrate (SuperSignal Pico) were added and incubated for 20 minutes. Then 50 µl of stop solution were added and a color signal was generated and measured by recording the absorbance at 450 nm in a microplate ELISA photometer. The intensity of the blue color is proportional to the concentration of Stx2a. The concentrations of water-diluted Stx2a were estimated based on the equations obtained by the linear regression of the standard curve (He et al., 2018; Rippa et al., 2022).

6. Statistics

Statistical analysis was performed with GraphPad Prism 8 software. IC_{50} values were calculated by the least-squares method applied to the linear regression between percentage activity of protein synthesis and log of inhibitor concentrations or log of inhibitor volume (for protein synthesis assays) or between percentage of viable cells and volume (for viability assay). Differences in slopes and elevations of the different straight lines were tested by linear regression.

Differences in continuous variables (means, SD) were tested with a t-test after controlling the normality of their distribution, differences in proportions were assessed through the chi-square text or Fisher's exact test and correlation between variables was assessed by the Pearson correlation coefficient.

A p-value < 0.05 was considered statistically significant.

RESULTS

1. Stx2a isolation and properties

Stx2a was produced from C600ϕ933W strain, an *E. coli* K12 strain containing the bacteriophage carrying the Stx2a genes of the STEC EDL 933 strain. Ammonium sulfate precipitation, dialysis, and receptor analogue affinity chromatography with Galα1-4Galβ - O - spacer – BSA –Sepharose 4B were performed to isolate and purify the toxin present in the supernatant of the bacterial culture. To remove traces of bacterial endotoxin a passage through ActiClean Etox Columns was performed. The final Stx2a preparation was quantified using Lowry assay, obtaining a concentration of 7.2 µM and subsequently assayed by using the Limulus Amebocyte Lysate Pyrogent Plus showing a low amount of contaminant LPS (0.73 ng LPS /mg Stx2a).

Different assays were performed to evaluate whether the isolated toxin expressed its binding properties to Gb3Cer and TLR4 receptors and its enzymatic activity on ribosomes and DNA. The binding capacity to the Gb3Cer receptor was indirectly evaluated through the inhibition of protein synthesis (cell translation assay) with Gb3Cer-espressing Vero cells (IC_{50} = 0.013 pM). In addition, the toxic effect of Stx2a on the same cells after 72 h of incubation was evaluated using a Luminescent Cell Viability Assay (IC_{50} = 0.035 pM).

To evaluate directly the enzymatic deadenylating activity of Stx2a on DNA, the toxin was incubated for 40 minutes at 45˚C with [^{3}H] DNA labeled in the purine ring of adenine. The DNA deadenylating activity of the new preparation of Stx2a was similar to other preparations of the toxin obtained in our laboratory.

Furthermore, the binding of Stx2a to TLR4 expressed by human neutrophils was assessed by indirect flow cytometric analysis with a primary mouse anti-Stx2 monoclonal antibody and a secondary fluorescent FITC-IgG anti-mouse antibody. The results showed a full saturation of the neutrophil receptors by 60 nM Stx2a according to previous experiments.

Since the properties of the new toxin preparation were assessed (Gb3Cer and TLR4 binding activity, deadenylating activity on rRNA 28S within ribosomes and on DNA), the toxin was used for the experiments described in the thesis.

2. Validation of the biosensor for early detection of Stx2a

To validate the plasmonic biosensor produced by the physicists led by Dr Lucia Petti (CNR, Pozzuoli, Naples) and described in Materials and Methods 5.6., the purified Stx2a was diluted in water or in PBS to mimic the ionic and pH conditions typical of human plasma. Having to use low concentrations of toxin, a standard procedure for diluting the toxin in water or PBS up to the concentrations found in patients (2-6 ng/ml; 30-90 pM) was set up. However, Stx2a non-specifically binds to test tubes, and it is usually necessary to use a carrier (bovine serum albumin, BSA) during the dilution to avoid its loss. For this reason, each dilution of the toxin produced in water or PBS was compared to an identical dilution in PBS containing 1% BSA by using the Raji cells protein synthesis assay or the acellular translation system, described in Methods 5.1.1. and 5.1.3, respectively. Thanks to these assays, the real concentrations of Stx2a samples diluted in the absence of protein carrier and used in the following experiments was assessed (Table 3).

Table 3: Dilutions of Stx2a in water and PBS; real and expected concentrations. During the process of toxin dilution in water or PBS, its interaction with the test tubes causes a loss of toxin. Real concentration was assessed by comparing each dilution made in water with a similar dilution made in PBS containing 1% BSA and carrying out translation inhibition assays in acellular (dilutions A-C) or cellular (dilutions D-I) systems according to their limit of detection.

Dilutions	***Expected Stx2a concentrations (nM)***	***Real Stx2a concentrations (nM)***
A	550	154.542
B	165	47.119
C	55	23.085
D	33	16.470
E	16.5	9.010
F	5	1.571
G	1	0.443
H	0.2	0.034
I	0.04	0.005

Depending on the dilution, the toxin recovery was approximately 1/3 than the expected concentration and 1/6 for the highest dilutions. These data indicate the recovery of Stx2a to be used for the experiments with the plasmonic biosensor.

The toxin was detected using biosensors constituted by nanostructured SERS substrates fabricated by electron beam lithography technology that have an octupolar photonic crystal geometry, whose single unit cell is made up of triangular nanocavities. Once Stx2a was adsorbed directly on the substrate of the nanostructured sensor, it was irradiated with a laser

beam with a wavelength equal to 785 nm. The interactions with the material of the biosensor allowed to amplify bands directly associated with the protein and a specific spectrum (fingerprinting) of the toxin was recorded (Figure 13). Each peak was analyzed and attributed to a specific chemical group of the toxin, with the aim of understanding which are the toxin features that allow it to be identified even in more complex samples (Table 4). The plasmonic biosensor allowed to effectively detect the toxin, returning a characteristic and reproducible SERS spectrum (Figure 13).

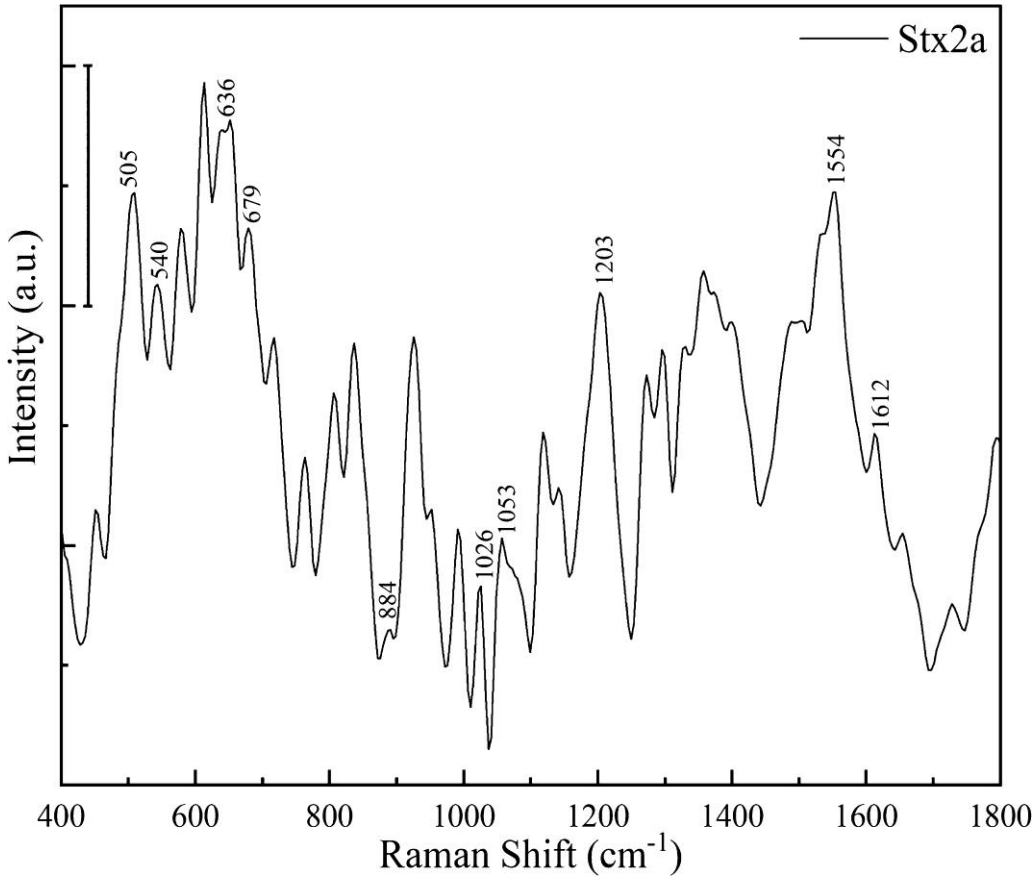

Figure 13: SERS measurements on Shiga toxins. Spectrum of Stx2a adsorbed on the octupolar nanostructure (154 nM) achieved by a mean of 10 different acquisitions. The scale bar represents 2000 au.

Table 4: Tentative assignation to the bands of Stx2a spectra and shared peaks between the toxin alone and the Ab + Stx2a complex.

Wavenumber cm^{-1}	*Assignation Stx2a*	*Shared with Ab+Stx2a*
505-540	Protein S-S	**500-550**
552	Trp	**552**
579	nd	579
613	Ring breathing	613
636	Tyr Ring deformation	**640**
652	Ring breathing	656
679	C-S Cystine	
717	Met C-S stretching	
764	Trp Ring breathing	**768**
810	nd	
837	Tyr	
856	Ring Tyr	**856**
883	PBS or Trp	
918	CC stretching	
995	Amide III	**995**
1026	In-plane ring CH def. Phe	**1022**
1053	Trp or Glu	**1053**
1115	stretching (CN) protein	1115
1203	Phe, Tyr	**1200**
1269	Amide III alpha helix	
1300	Amide III alpha helix	**1300**
1354	wagging (CH2, CH3)	1358
1392	Aromatic amino acids COO- stretching	**1392**
1554	Trp	
1612	bending C=C in Phe and Tyr	1616
1658	Amide I, alpha helix	1655

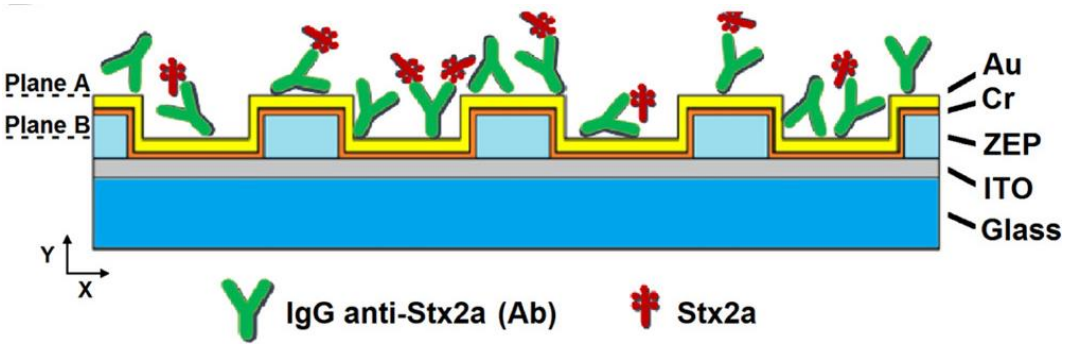

Figure 14: Capture of Stx2a by anti-Stx2 monoclonal antibody

We also proceeded to capture the toxin by using an anti-Stx2a monoclonal antibody against the B chain previously adsorbed on the biosensor (Figure 14). To optimize the capture, we tested three different antibody concentrations (5, 10, 25 µg/ml) and, after a washing step, we proceeded to add a sample of Stx2a for 1 h to react with the immune-surface. After incubation, another washing step was performed and the sample was finally tested to identify the toxin thanks to the signal amplification. The results showed that the optimal antibody concentration to have the highest signal amplification is equal to 10 µg/ml (7,5-fold higher than the sample with 5 µg/ml or 25 µg/ml) (Figure 15A).

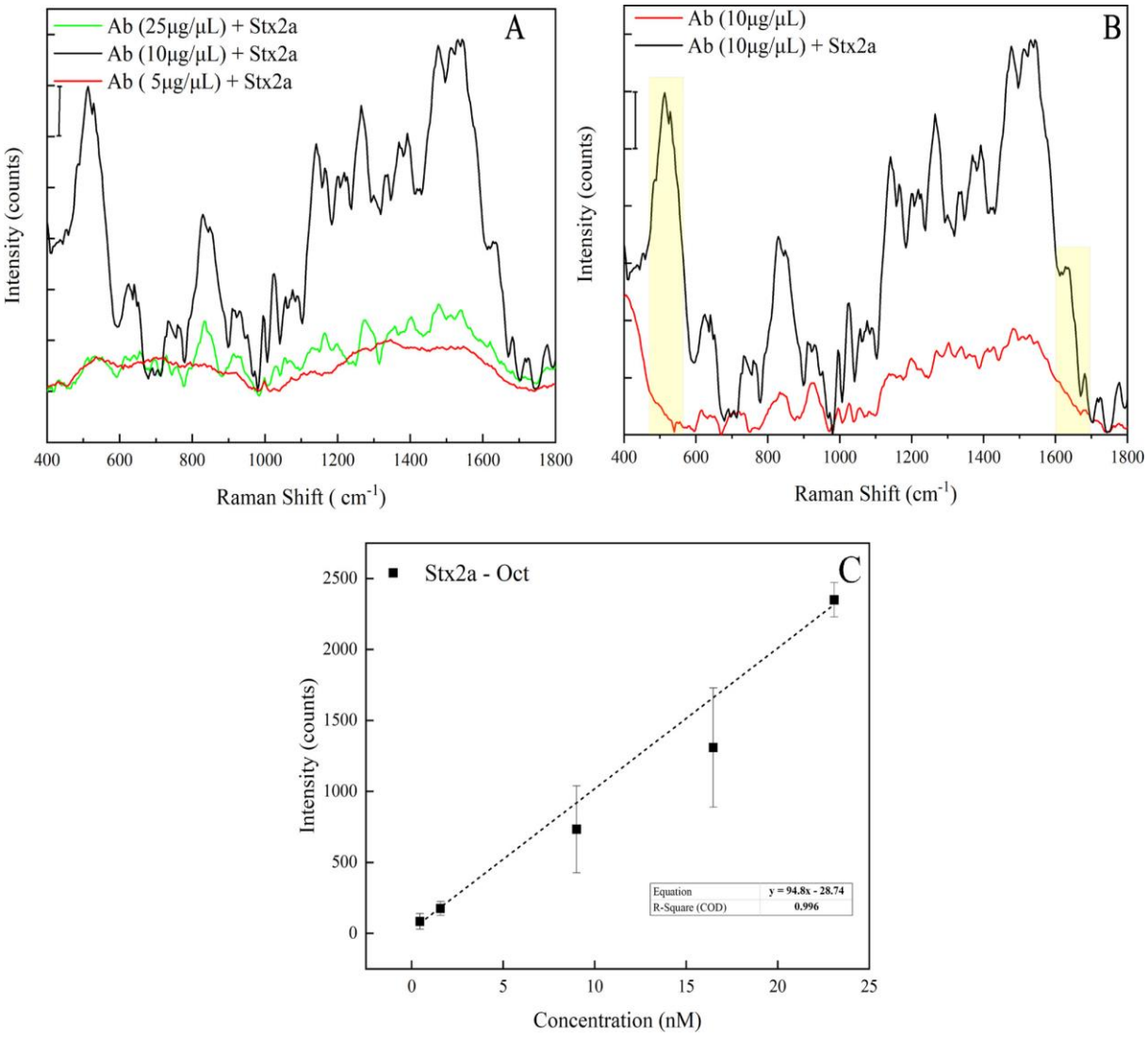

Figure 15: Comparison between spectra. (A) Comparison between the spectra of the toxin captured by the antibody (Ab + Stx2a) achieved with three different antibody (Ab) concentrations: 5, 10, and 25 µg/mL, the scale bar represents 2000 a.u. (B) Comparison between the spectra of Ab (10 µg/mL) and Ab + Stx2a (C) Calibration curve obtained by plotting the 1554 cm^{-1} peak intensity against the toxin concentrations.

In addition, comparison of the spectra obtained in the absence and in the presence of capturing antibodies (Figure 16), showed very similar profiles, indeed only a few peaks are lacking due to the involvement of some regions of the molecule in the formation of the complex Stx2a/Ab. The common peaks of the two spectra were identified and characterized, as depicted in Table 4.

To test the sensing performance of the immunosystem and identify the limit of detection (LOD), different toxin dilutions of Stx2a (1, 5, 16.5, 33, and 55 nM) corresponding to the real toxin concentrations (0.44, 1.57, 9.01, 16.47, and 23.09) were absorbed and the relative SERS spectra were recorded. The SERS signal of the whole spectrum was amplified more when the Stx2a was present in higher concentrations. To evaluate the LOD of the immunosurface, we chose to compare the amplification of the tryptophan-associated band, one of the aromatic amino acids much present in Stx2a, (centered at 1554 cm^{-1}, see Table 4). The calibration curve (Figure 15C) was obtained by plotting the peak intensity of 1554 cm^{-1} against toxin concentrations. The LOD was calculated from a residual standard deviation of the regression line and corresponded to 1.4 nM.

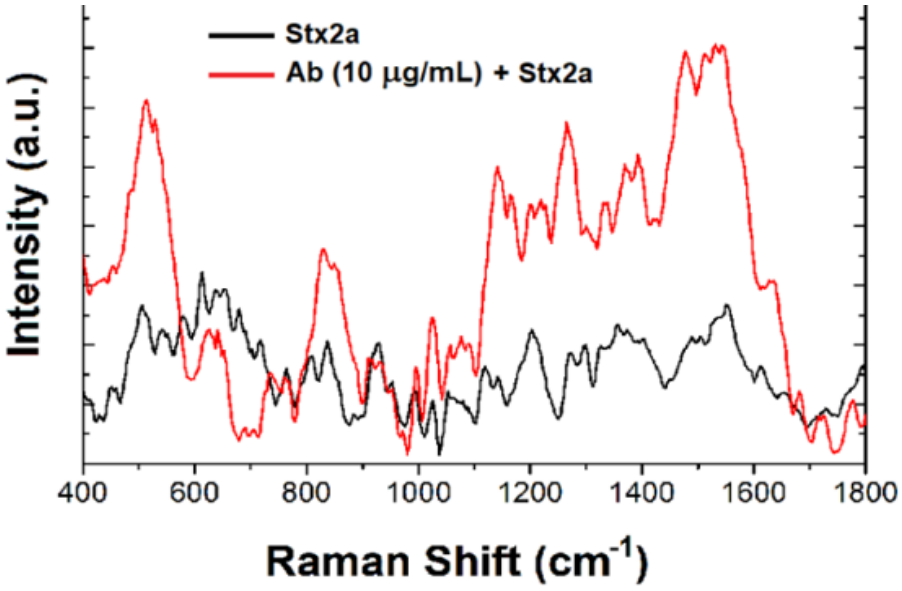

Figure 16: Fingerprinting of Stx2a and Stx2a captured by monoclonal anti-Stx2 antibody

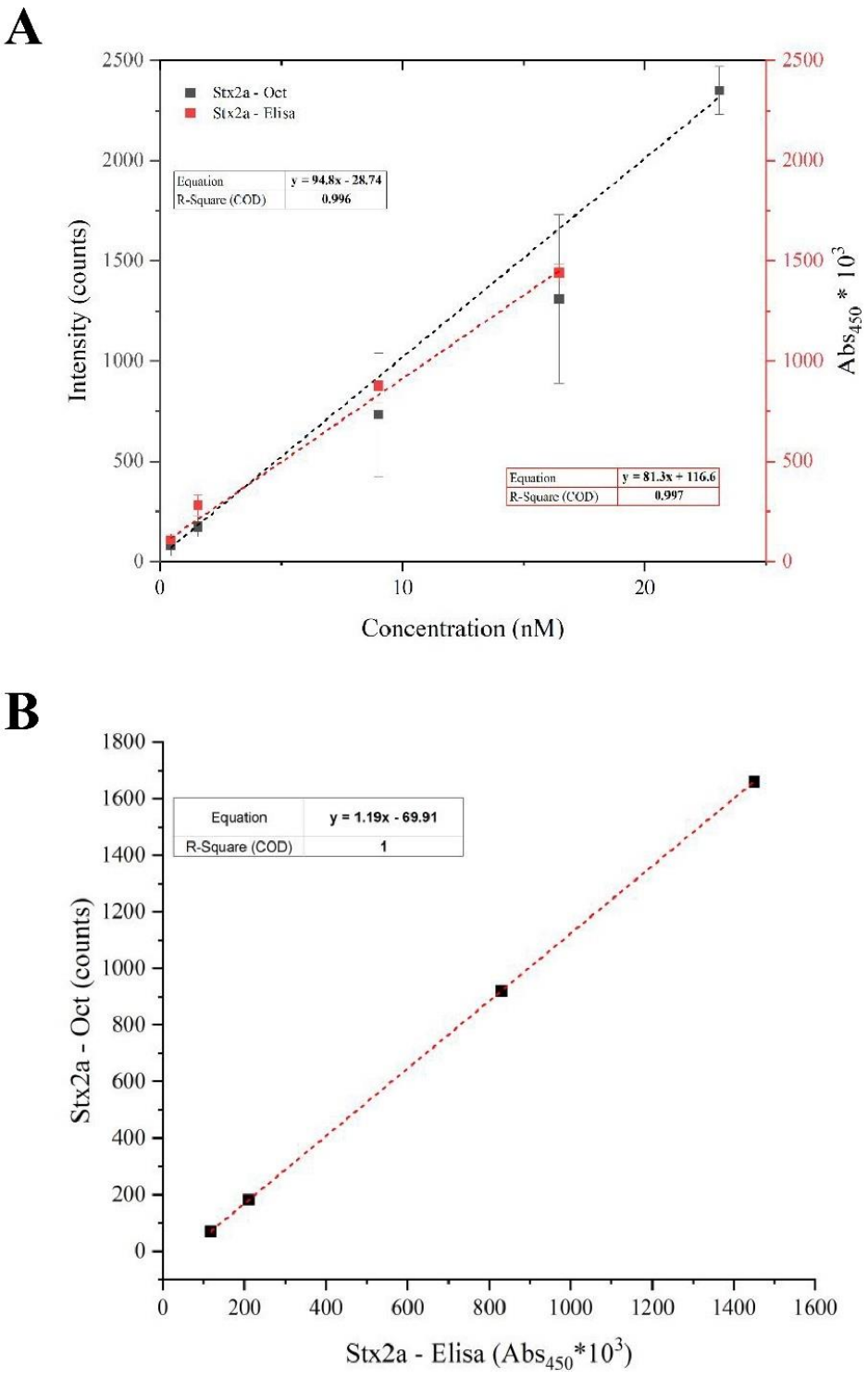

Figure 17: Comparison of SERS sensor and ELISA performances (A) Comparison of the regression lines produced when toxin samples were detected using the ELISA and SERS sensors. The water diluted Stx2a samples (theoretical concentrations) were assayed by the two methods. The real toxin concentrations were plotted against the ELISA signals (A450) and by SERS (counts). To compare the curves at the same order of magnitude, the absorbance values were multiplied by 10^3 (B) A scatter diagram that plots the weighted responses across the calibration concentrations is used to compare the performances of the two methods.

Subsequently, the assay performance of the developed antibody-dependent detection system was compared with a gold standard ELISA, specific for the detection of Stx2a (He et al., 2018). The latter assay is centered on a capture antibody anti-Stx2a (which recognized the B-subunit of Stx2a) and a HRP conjugated antibody which recognizes the complex Stx2a/anti-Stx2 Ab. The same dilutions of Stx2a in water (theoretical concentration) detected with the SERS sensor were also tested with the ELISA. The regression lines obtained with the two methods (Figure 17A, red for ELISA, black for SERS sensor) were very similar. Indeed, both curves were linear ($R^2 > 0.99$) with a very similar slope (b= 81.3 and b= 94.8).

The two analytical methods were compared with a regression graph (Figure 17B), in which each point represented on the x axis corresponds to the analytical response obtained by ELISA and on the y axis by SERS, each weighted by standard deviation at a given concentration. The $R^2=1$ shown in this graph indicates that the plasmonic sensor and ELISA results are linear. Moreover, the slope slightly higher than 1 (b = 1.2) indicates that the results of the two methods are proportional to each other, with a slight overestimation by the immunosensor (m>1).

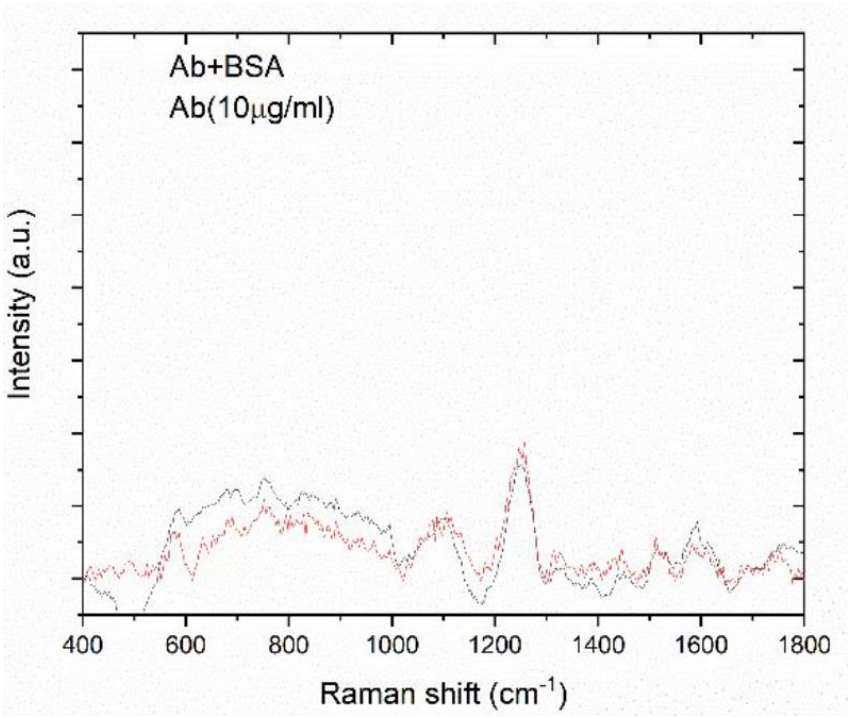

Figure 18: Specificity of the immunosurface of the biosensor. In red the SERS spectra of the antibody anti-Stx2a 10 µg/ml alone (Ab), in black the SERS spectra achieved with Ab anti-Stx2a+BSA.

Finally, to evaluate the specificity of the immunosurface, BSA, a non-target protein, was added and tested in an excess amount (about an order of magnitude higher than the maximum measured toxin concentration). The SERS spectra recorded in the presence of 4.5 μM BSA and anti-Stx2 antibody and that of anti-Stx2 antibody alone are nearly identical (Figure 18). The lack of capture of BSA by the immunosensor demonstrates the specificity of the immunosurface.

3. Studies on the cleaved form of Stx2a

The outcome of STEC infections and the consequent onset of HUS could be influenced by the percentages of toxin present in uncleaved or cleaved form (which have a single nick in the A chain resulting in two fragments, A1 and A2, connected by a disulfide bridge) circulating in the patients' blood. The two forms, while being biologically active and indistinguishable from the point of view of toxicity, bind very differently to circulating cells and to host serum components.

For a better understanding of the pathogenesis of HUS, a method to detect the cleaved and uncleaved forms of Stx2a in human serum based on the measurement of their different effect on protein synthesis was developed.

3.1. Determination of the percentage of cleaved Stx2a in a purified toxin sample using a cell-free translation system

Purified uncleaved or cleaved forms of Stx2a were tested using a luminometric cell-free protein synthesis system derived from rabbit reticulocytes, fractionated and reconstituted with human ribosomes that translate synthetic exogenous mRNA encoding the *Renilla reniformis* luciferase enzyme. Since in this system the two forms of Stx2a had similar inhibitory activities (as showed in Figure 20 in red), to increase the translation inhibition of the cleaved form of Stx2a and discriminate it from the uncleaved form, the reducing agent dithiothreitol (DTT) at different concentrations (12, 80 mM) was added directly to the system or during a pre-incubation step with the toxin (Figure 19).

The best reducing condition was identified when the cleaved form of Stx2a was pre-incubated with 80 mM DTT for 15 min at 30 °C in 3 µL final volume. This setting was used in the following experiments.

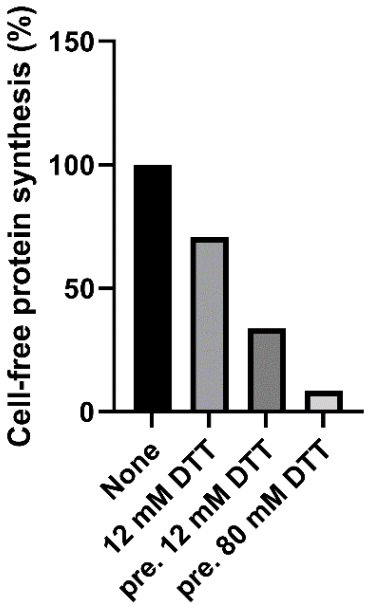

Figure 19: Effect on cell-free protein synthesis of the cleaved form of Stx2a in the presence or after pretreatment (pre.) of different concentrations of DTT.

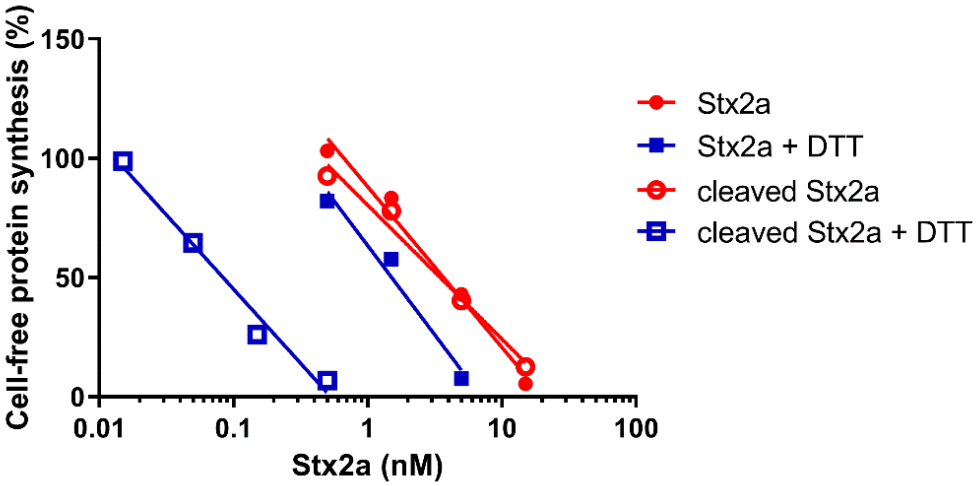

Figure 20: Effect on cell-free protein synthesis of the cleaved and uncleaved form of Stx2a under reducing (DTT 80 mM) and non-reducing conditions. The IC_{50} values calculated from the straight lines are reported in Table 5.

Table 5: IC_{50} of cleaved and uncleaved form of Stx2a under reducing (DTT 80 mM) and non-reducing conditions assayed in the cell-free translation system.

Additions	***IC_{50} (nM)***
Stx2a	3.680
Stx2a + DTT	1.511
cleaved Stx2a	3.475
cleaved Stx2a + DTT	0.083

In the presence of the reducing agent (80 mM DTT), the two different forms of Stx2a were recognized based on the different inhibition of protein synthesis. Figure 20 shows that, under reducing conditions, the cleaved form of the toxin has an inhibitory activity greater than the uncleaved form, as indicated by the lower IC_{50} values (concentration that allows the inhibition of 50% of the translation) for the cleaved toxin (picomolar) with respect to the uncleaved toxin (nanomolar) (Table 5). In fact, under these conditions, it is possible to break the disulfide bridge that connects the two fragments of the A chain already present in the cleaved form of the toxin, releasing the enzymatically active A1 fragment. In the case of the uncleaved toxin the effect induced by the reducing agent is negligible. After the reducing treatment the IC_{50} value of the cleaved form was decreased by 41.9 times while that of the uncleaved form by 2.4 times.

Therefore, this system allowed to discriminate between the cleaved and uncleaved form of Stx2a. Moreover, in purified Stx2a samples, on the basis of the translation inhibition and of the ratio between the IC_{50} obtained under non-reducing or reducing conditions, it was possible to calculate the percentage of fragment A1, which corresponded to the cleaved form of the toxin.

Assuming that the toxin used to set-up the assay was totally uncleaved, if in an unknown toxin sample 100% of the uncleaved form is present (A1 fragment = 0%) the corresponding variation of the IC_{50} under reducing conditions is 2.4-fold, whereas when all the toxin is in the cleaved form (A1 fragment = 100%) the variation of the IC_{50} under reducing condition is 41.9-fold.

The following equations describe how to determine the percentage of cleaved toxin in an unknown sample:

IC_{50} uncleaved Stx2a / IC_{50} uncleaved Stx2a + DTT = 2.4-fold decrease;

IC_{50} cleaved Stx2a / IC_{50} cleaved Stx2a + DTT = 41.9-fold decrease;

- If the reduction is ≤2.4, then A1 = 0% and only uncleaved toxin is present in the sample
- If the reduction is> 2.4 and <41.9, the following equation can be used to calculate the % of the A1 fragment and therefore of the cleaved form of the toxin present in the sample.

$$\frac{100\ x\ fold\ decrease}{41.9} = \%\ A1$$

- If the reduction is ≥41.9 A1 = 100%, only cleaved toxin is present.

3.2. Detection of the cleaved form of Stx2a added to human serum

Preliminary experiments were performed in the absence of toxin to check the effect of human serum added to the cell-free translation system. In the presence of human serum from healthy donors (2 µl in the final 22 µl-reaction) during the 3 µl pre-incubation step, the translation was strongly compromised under reducing and non-reducing conditions (Figure 21).

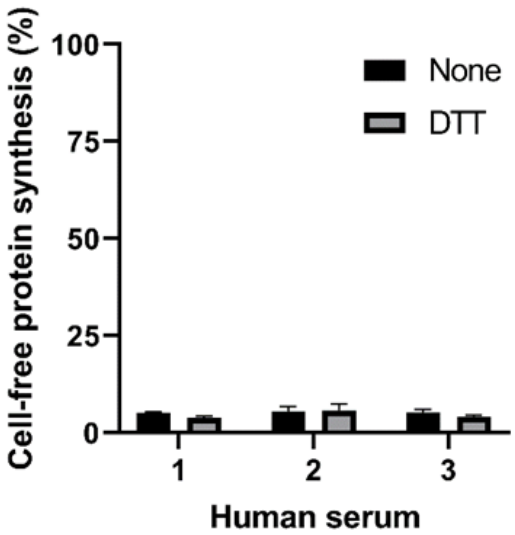

Figure 21: Effect of human serum derived from three different healthy donors on cell-free protein synthesis in the presence or in the absence of DTT.

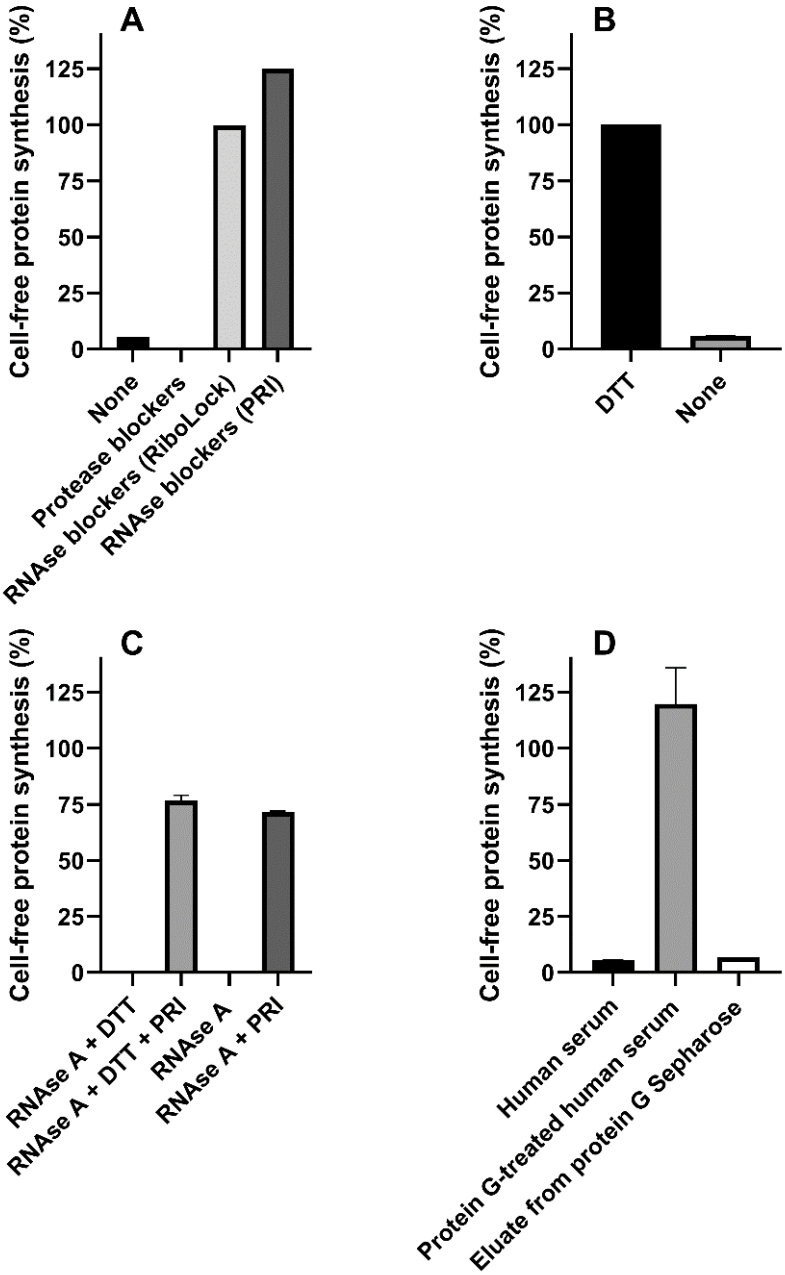

Figure 22: Effect of protease blockers, RNase blockers and Protein G-treated human serum added to the cell-free translation system. (A) Mixed sera from three healthy donors was assayed under reducing conditions (DTT) in the presence or absence or of protease blockers (1x cOmpleteTM) or different types of RNAse blockers (RiboLock or Placental RNAse Inhibitor (PRI)); (B) Mixed sera from three healthy donors was assayed in the presence of PRI under reducing and non-reducing conditions ($p < 0.0001$); (C) the use of RNAse A (10 ng) induces a strong inhibitory effects, while the addition of PRI induces a significant protective action both under reducing and non-reducing conditions ($p < 0.0001$); (D) Mixed sera from three healthy donors were treated with protein G Sepharose added to the assay and compared with the same untreated mix.

In human serum there were translation inhibitors that affected the results even after dialysis (6000-8000 molecular sieve) or gel-filtration (Microspin G-25 columns) of serum samples. These inhibitors were identified as high molecular mass components such as an RNase. They can be blocked by the addition of placental RNAse inhibitor (PRI) (20 U, Life Technology, Carlsbad, CA, USA), while the use of a different RNAse A, B and C inhibitor (RiboLock) (20 U, RiboLock, Thermo Scientific, Waltham, MA, USA) had a protective effect but partially interfered with protein synthesis. Addition of serin-, cysteine- and metal-protease blockers (1x cOmpleteTM, Sigma-Aldrich, St. Louis, MO, USA) had no protective effect (Figure 22A). Unexpectedly, even in the presence of PRI, the absence of DTT in the system restored the inhibitory action of human serum (Figure 22B). However, RNAse A from bovine pancreas both in the presence and in the absence of DTT, was completely inhibited by PRI in the translation system (Figure 22C). Therefore, additional inhibitors of cell-free protein synthesis were present in human sera, and high DTT concentrations impair their action. This translation inhibitor sensitive to DTT was identified as an immunoglobulin (probably an antibody-like molecule) and was cleared by pre-treatment of sera with immobilized G protein (protein G Sepharose). This treatment restored protein synthesis activity under non-reducing conditions and when the fraction eluted from protein G were added back into the system, it had an inhibitory effect similar to that of whole human serum (Figure 22 D).

On this basis, the experiments were then repeated and the uncleaved and cleaved forms of Stx2a were added to mixed sera from three healthy donors pre-treated with protein G Sepharose and the cell free protein synthesis assay was performed in the presence of PRI.

Under non-reducing conditions, in the presence of protein G-treated human serum, the uncleaved form and the cleaved form of the toxin exhibited the same ability to inhibit protein synthesis. Under reducing conditions (DTT 80 mM), the inhibition of protein synthesis of the cleaved toxin was found to be much greater than that of the uncleaved form. Furthermore, to demonstrate that the pre-treatment of sera with protein G had not altered or removed other components present in serum that can influence the activity of the toxin, the same experiments were carried out using sera not treated with protein G under reducing conditions, obtaining results comparable to those obtained using protein G treated sera (Figure 23).

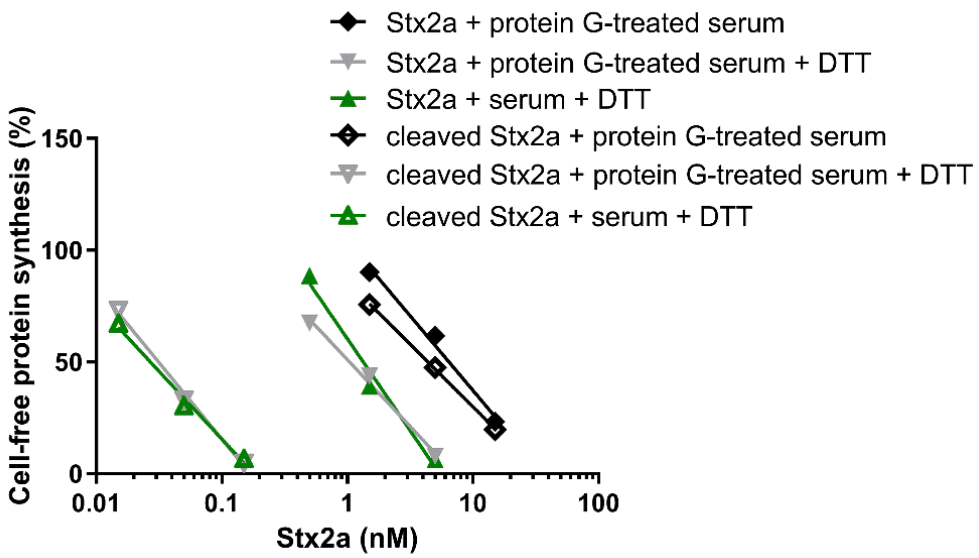

Figure 23: Effect of cleaved and uncleaved forms of Stx2a on cell-free protein synthesis under reducing and non-reducing conditions. The assay was performed in the presence of PRI and mixed sera from three healthy donors treated or not with protein G Sepharose. The IC_{50} values are calculated from the straight lines and are reported in Table 6.

To sum up, the activity of uncleaved Stx2a was nearly unchangeable regardless of the different conditions of the assay (Figure 24A). Conversely, preincubation of the cleaved toxin with DTT was the specific condition allowing the activity of the cleaved toxin to increase, either alone, in the presence of serum or in the presence of protein G-treated serum (Figure 24B). The IC_{50} of the cleaved form of the toxin showed an extremely significant decrease under reducing conditions, both in the presence and in the absence of serum, and the lowering was maximal in the presence of serum treated with protein G (~140 fold).

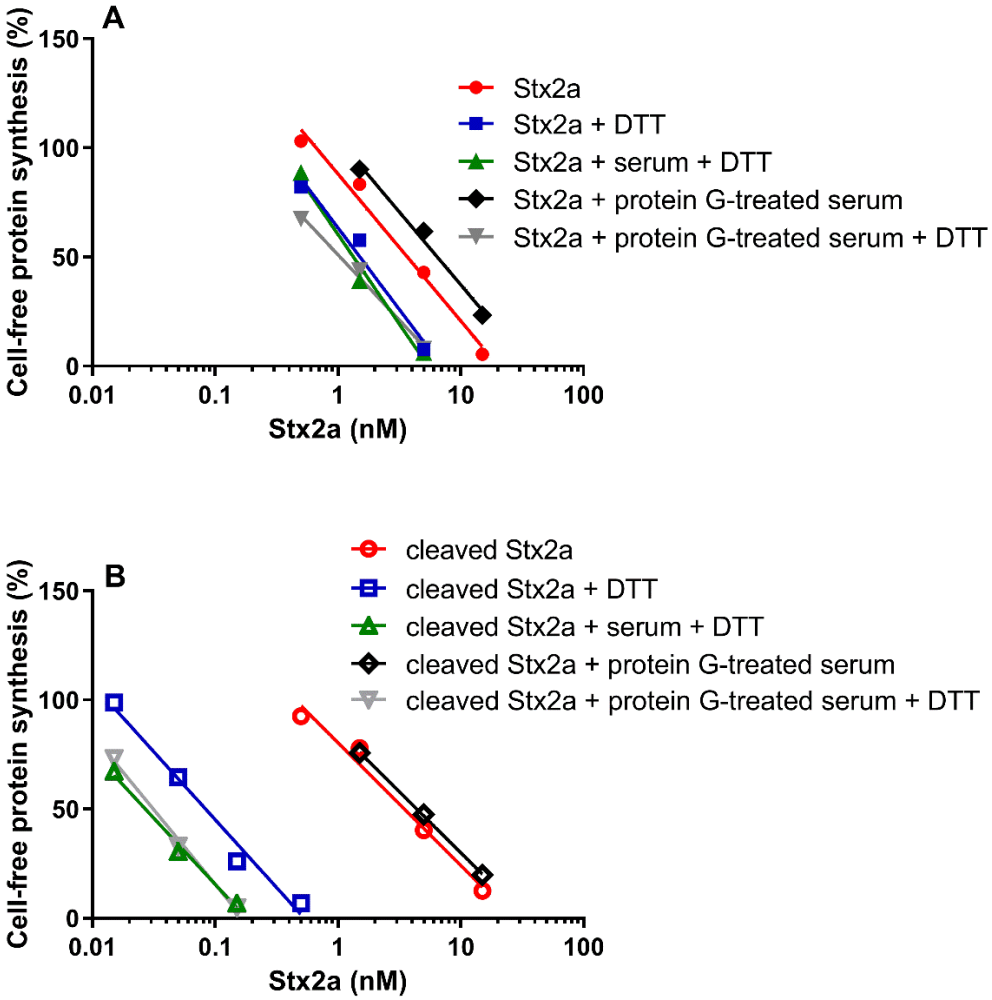

Figure 24: Summary of the effect of Stx2a on cell-free protein synthesis under reducing and non-reducing conditions. (A) Uncleaved form (B) Cleaved form of Stx2a. Experiments were performed in the presence or absence of mixed human sera from three healthy donors treated or not with protein G Sepharose. In the presence of sera, PRI was added.

Table 6: IC_{50} of cleaved and uncleaved form of Stx2a in different conditions (in the presence or absence of human serum treated or not with protein G Sepharose) and assayed in the cell-free translation system: equations and statistical analysis of the straight lines.

Additions	*IC_{50} (nM)*	*r^2*	*Equation*
Stx2a	3.680	0.9834	y = −67.31x + 88.09
Stx2a + DTT	1.511	0.9714	y = −74.79x + 63.41
Stx2a + protein G-treated serum	6.449	0.9878	y = −66.71x + 104.0
Stx2a + protein G-treated serum + DTT	1.042	0.9918	y = −59.81x + 51.06
Stx2a + serum + DTT	1.339	0.9798	y = −82.14x + 60.42
cleaved Stx2a	3.475	0.9796	y = −56.20x + 80.41
cleaved Stx2a + DTT	0.083	0.9804	y = −62.21x − 17.06
cleaved Stx2a + protein G-treated serum	4.389	0.9994	y = −55.89x + 85.90
cleaved Stx2a + protein G-treated serum + DTT	0.031	0.9944	y = −68.49x − 53.00
cleaved Stx2a + serum + DTT	0.027	0.9902	y = −60.66x − 45.13

Table 7: Ranges of detectable concentrations of cleaved and uncleaved form of Stx2a in protein G-treated serum calculated from the equations of the straight lines.

Stx2a + protein G-treated serum	1,213-27,095 ng/ml (10-100% inhibition)
Stx2a + protein G-treated serum + DTT	167-5,340 ng/ml (10-100% inhibition)
cleaved Stx2a + protein G-treated serum	632-25,754 ng/ml (10-100% inhibition)
cleaved Stx2a + protein G-treated serum + DTT	6-126 ng/ml (10-100% inhibition)

Considering that the toxin added to protein G-treated human serum was diluted 11 times when the assay was performed (2 µl of human serum in 22 µl final volume), according to the equations (Table 6), the detection of a translation inhibition ranging between 10% and 100% induced by cleaved Stx2a under reducing conditions was conceivable if the toxin was present at concentration 6–126 ng/ml (Table 7). The detection of Stx2a by ELISA in STEC-infected patients sera developing HUS was between 2 and 6 ng/ml (Brigotti M., 2020), hence only the highest concentration was close to the lower limit of detection of the assay.

To face this problem and allow to detect Stx2a at lower concentrations, 100 µl of human serum, containing different concentrations of cleaved Stx2a (1.8, 3.6 or 6 ng/ml) and treated with protein G, was concentrated 5 times by centrifugation on Centricon 30 (1 h at 12000x g). Under these conditions it was possible to detect cleaved Stx2a in the range of concentrations found in patients' sera.

The concentration of cleaved form of Stx2a can be determined according to these steps:

- Determinate the effect on translation of the protein G-treated patient's serum sample concentrated 5 times compared to a pool of protein G-treated healthy donors' sera under reducing condition (DTT).
- Calculate the % activity of protein synthesis
- Use the equation parameters of the straight line obtained with cleaved Stx2a + protein G-treated human serum under reducing condition (y = -68.49x – 53.00) to calculate the concentration of the cleaved form of Stx2a according to the formula:

$$10^{\frac{-53 - \%\mathrm{Act}}{68.49}} \times 68 \times 11 = \mathrm{ng/mL}$$

The assay could be a useful tool to study the contribution of the cleaved form of Stx2a in the pathogenesis of HUS.

3.3. Detection of the cleaved form of Stx2a in STEC-infected patients' sera

For a better understanding of the pathogenesis of HUS, it is useful to identify whether the cleaved form of the toxin is present in STEC-infected patients.

First, we verified the stability of Stx2a added to human serum by carrying out a protein synthesis inhibition assay on Vero cells. The activity of the toxin added to human serum samples was found to be equal to that of the toxin added to human blood from which serum was then obtained to treat cells. Furthermore, the storage conditions do not seem to alter the toxic activity since Stx2a added to human serum and incubated at room temperature for 2 days or stored at -20°C for 80 months did not change its activity on Vero cells.

To detect the cleaved form of circulating Stx2a in patients, human serum from STEC-infected patients was pretreated with immobilized protein G (protein G Sepharose) to eliminate immunoglobulins and with placental RNAse inhibitor (PRI), and concentrated 5 times by centrifugation on Centricon 30 (1 h at 12000 g).

Sera from 10 STEC-infected patients (4 females and 6 males, median age 5.7 years), were analyzed. At presentation the patients showed bloody diarrhea (BD, 8/10) and/or diarrhea (D, 7/10), hematuria (4/10), proteinuria (7/10). Three of them developed HUS. The presence of STEC infection was confirmed by identifying the gene encoding Stx2 in fecal extracts (RT-PCR) and by isolating the STEC strain. Furthermore, the concentration of the total serum toxin was assessed by ELISA as well as the presence of Stx2a bound to neutrophils (cytofluorimetric assay). The cleaved form of the toxin was detected in 5 out of 10 sera by using the method described above (Table 8 see below).

3.4. Detection of the cleaved form of Stx2a in STEC-infected patients' sera by Vero cells translation assay in the presence of an anti-cleaved Stx2 antibody

To confirm the results obtained on the identification of the cleaved form of Stx2a in STEC-infected patients' sera, a monoclonal antibody against the cleaved form of Stx2a developed by Prof. Reinhard Würzner and Prof. Dorothea Orth (Division of Hygiene and

Medical Microbiology, Medical University of Innsbruck, Austria) was associated to the Vero cells translation assay.

As depicted in Figure 25 (red box), this antibody recognizes specifically the cleaved form of Stx2a in quantitative capillary Western Blot by interacting with the C-terminal 263-272 region of the A1 fragment (CHHQGARSVR) before the A subunit cleavage. This region is not exposed in the uncleaved form of Stx2a hence preventing the binding of this antibody to the native whole form of the toxins (Figure 25).

Figure 25: Specificity of anti-cleaved Stx2 antibody. WES analysis showed that anti-cleaved Stx2 Ab recognizes only the cleaved form of Stx2a (10 ng/µl and 5 ng/µl) and not uncleaved Stx2a (red box).

Vero cells were challenged with protein G Sepharose-treated 5-fold concentrated serum samples (1 to 4 µl) belonging to selected patients (Table 8, pts 1, 2, 3, 4, 7, 8) with or without 20 µl of the specific anti-cleaved Stx2 antibody and assayed for translation inhibition compared to control sera from healthy donors as described in the method section. In the presence of anti-cleaved Stx2 antibody the total inhibition of protein synthesis induced by the sera of patients 1, 2 and 4 was reduced by nearly 50%, while no protection was observed in sera from patients 3, 7 and 8 (Figure 26).

In conclusion, the two detecting systems were found to be concordant in all sera tested, but one (pt 8) (Table 8).

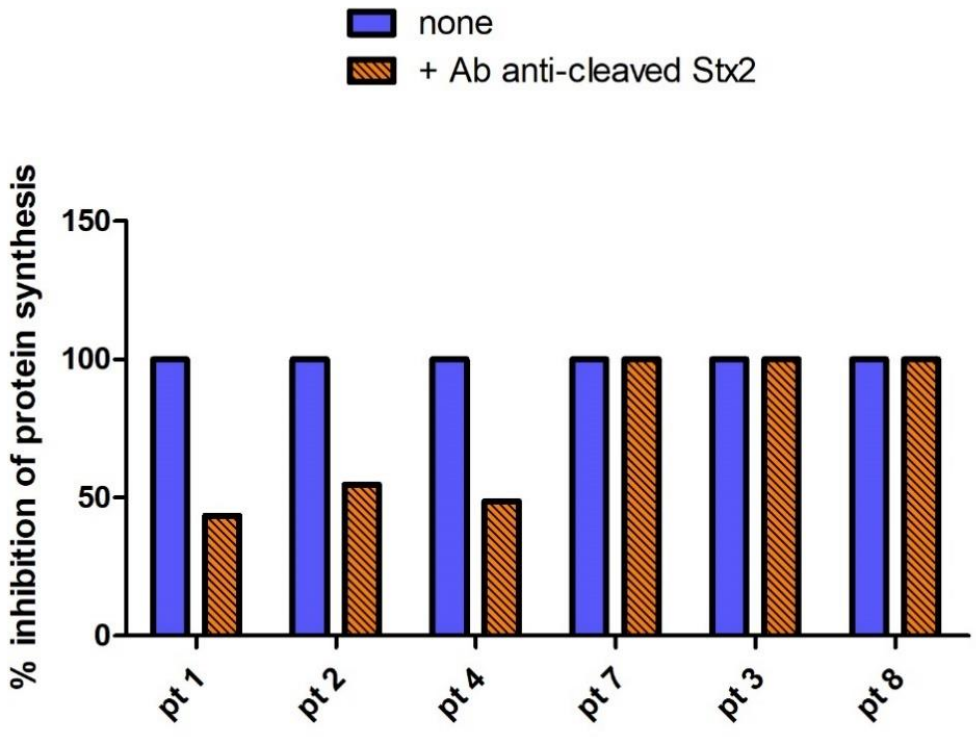

Figure 26: Detection of cleaved Stx2a in patients' sera by anti-cleaved Stx2 Ab using protein synthesis assay with Vero cells.
Sera of 6 patients (pt 1, pt 2, pt 4, pt 7, pt 3, pt 8) were used to intoxicate Vero cells in the presence or absence of anti-cleaved Stx2 Ab. Cleaved Stx2a was detected in pt 1, 2 and 4 by the reduction of protein synthesis inhibition induced by anti-cleaved Stx2 Ab.

Table 8: Detection of cleaved Stx2a in STEC infected patients' sera using the cell-free protein synthesis assay. Features of 10 STEC-infected patients: Sex, Age, toxin type, serum Stx2 detected by ELISA (ng/ml), neutrophil-bound Stx2, presence of the gene encoding Stx2 in fecal extracts identified by RT-PCR, isolation of *E. coli* serogroup, clinical symptoms, HUS, cleaved Stx2, concentrations of cleaved Stx2 (ng/ml).

Abbreviations: ELISA enzyme-linked immunosorbent assay; RT-PCR, real time-polymerase chain reaction: BD, bloody diarrhea; D, diarrhea; HUS, Hemolytic uremic syndrome.

Pt	Sex	Age (y)	Toxin type	Stx2 by ELISA (ng/ml)	Neutrophil-bound Stx2	RT-PCR Stx2 gene (feces)	*E. coli* serotype	Clinical symptoms	HUS	cleaved Stx2	cleaved Stx2 by cell-free assay (ng/ml)	cleaved Stx2 by Vero cells assay + anti-cleaved Stx2 Ab
1	f	1.7	Stx2	3.36	+	+	O26	BD, D, hematuria proteinuria	+	+	2,90	+
2	f	5.6	Stx2	3.37	+	+	O157	BD, D, proteinuria	+	+	11,45	+
3	m	8.3	Stx2	2.41	+	+	O127	BD, hematuria, proteinuria	+	-	-	-
4	f	10.2	Stx2	2.23	+	-	O145	BD, D, proteinuria	-	+	1,98	+
5	m	10.2	Stx2	2.38	-	+	O8	BD	-	-	-	nd
6	m	3.3	Stx2	2.13	-	-	nd	BD, D, proteinuria	-	-	-	nd
7	m	1.5	Stx1/Stx2	3.47	-	+	nd	BD, D	-	-	-	-
8	f	15.8	Stx1/Stx2	3.37	-	+	O157	BD, D	-	+	5,39	-
9	m	6.4	Stx2	3.00	+	+	O127	hematuria proteinuria	-	+	8,27	nd
10	m	5.7	Stx2	3.02	+	+	O127	D, hematuria proteinuria	-	-	-	nd

4. NAB815 impairs the release of blood-cell derived microvesicles in human blood treated with Stx2a

4.1. Stx2a induces the formation of platelet-derived and leukocyte-derived microvesicles containing Stx2a

To mimic what happens in STEC-infected patients when Stx2 enter the circulation and interacts with blood cells, whole blood (80 ml) from healthy donors was incubated for 4 h at 37°C with Stx2a (2nM) in the presence and in the absence of 0.01 µg/ml of NAB815, a concentration of the antibiotic that was proven to be effective in inhibiting the binding of the toxin to TLR4-expressing cells. At the end of the incubation, 1 µm-microvesicles were isolated by differential centrifugation as described in methods.

The size of microparticles based on their Brownian motion was analyzed by DLS showing that Stx2a added to human blood samples induced the formation of a population of vesicles with a diameter equal to 500-1000 nm, a size attributable to microvesicles.

Analysis by quantitative capillary Western Blot WES on the protein component extracted from the microvesicles showed that the expression of Alix, a specific marker of microvesicles, in the toxin-stimulated samples doubled compared to the controls (193.4% ± 25.8, $p < 0.0005$). As regards the origin of the microvesicles produced following the toxin trigger, a strong increase in the platelet antigen CD42a (252.1% ± 125.3, $p < 0.05$) and in the leukocyte antigen (CD45 144.6% ± 14.3 $p < 0.01$) was observed (Figure 27).

4.2. NAB815 impairs the formation of platelet-derived and leukocyte-derived microvesicles containing Stx2a

We identified the antibiotic NAB815, a polymyxin B derivative, as an inhibitor of the binding of Stx2a to TLR4 expressed by circulating cells, at concentrations ten times lower than the bactericidal ones. In previous experiments we had shown that it was effective in inhibiting the binding of Stx2a to TLR4-expressing circulating cells, hence blocking the formation of neutrophil-platelet aggregates (2019, Italian patent 102019000025414; 2021, patent extended in EU, USA, Canada, Japan and Brazil WO2021130700 (A1)).

The results described in this thesis showed that NAB815 has also an action in inhibiting the release of microvesicles by blood cells.

First, we demonstrated that the drug added to human blood did not have any effect on the basal release of microvesicles. Capillary Western Blot (WES) analysis showed the presence of a population of microvesicles with the same features as that of the control (Figure 27).

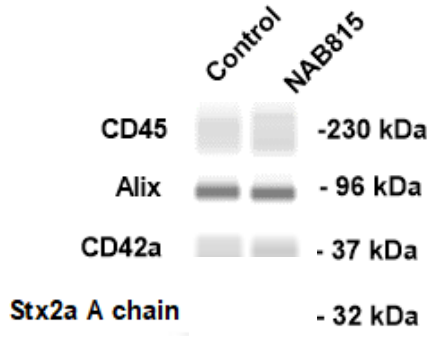

Figure 27: Characterization of blood cell-derived microvesicles. Analysis of Alix, CD45, CD42a and Stx2a by quantitative capillary Western Blot WES on the protein component extracted from the microvesicles present in control and NAB815-treated blood.

Then, we analyzed the blood cells-derived microvesicles produced by the treatment of the blood with Stx2a and Stx2a+NAB815. DLS analysis showed that the presence of NAB815 strongly reduced the population of 500-1000 nm microvesicles compared to those produced by the action of Stx2a alone.

Analysis by quantitative capillary Western Blot (WES) showed that NAB815 induced a strong reduction of the expression of Alix, as a marker of the whole microvesicles population. In fact, when the expression due to Stx2a action was set at 100%, a residual stimulation equal to 25.7% ± 24.3 ($p < 0.0005$) was observed. In addition, the antibiotic is effective in reducing the formation of platelet-derived and especially leukocyte-derived microvesicles, inducing a residual stimulation of 16.4% ± 27.4 ($p < 0.01$) for CD45 and 31.6% ± 36.7 ($p < 0.01$) for CD42a. Most importantly, Stx2a was found in microvesicles derived from blood treated with the toxin, whereas a strong significant reduction of toxin amount was observed if the toxin treatment was performed in the presence of NAB815 (residual % 12.3 ± 21.3, $p < 0.001$) (Figure 28).

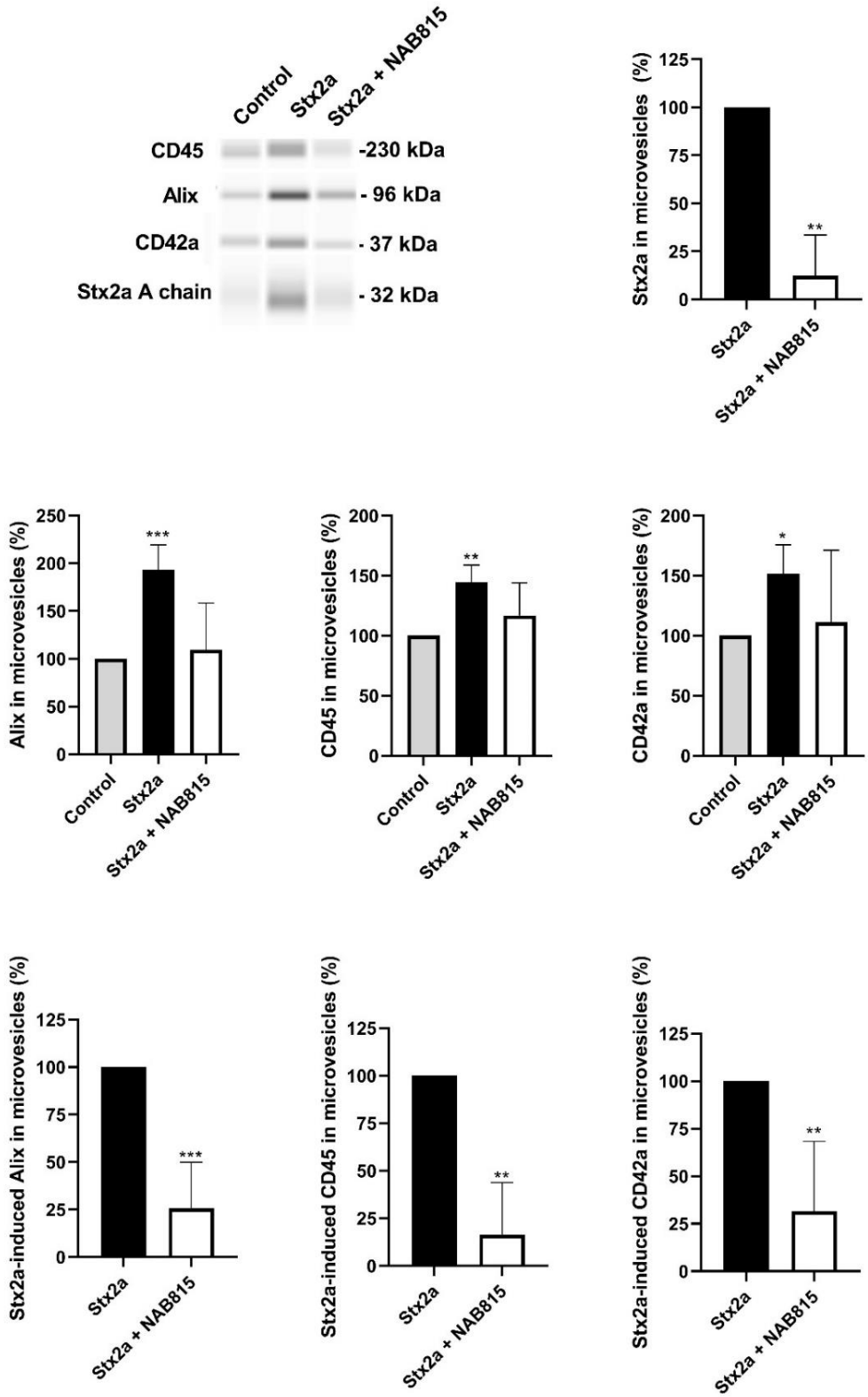

Figure 28: Characterization of blood cell-derived microvesicles. Expression of Alix, CD45, CD42a and Stx2a by quantitative capillary Western Blot WES on the protein component extracted from the microvesicles isolated from control, Stx2a-treated blood and blood treated with Stx2a+NAB815.

4.3. Gel-filtration analysis of the isolated microvesicles

To assess the purity of the isolated microvesicles and the inhibiting effect induced by NAB815 on their formation in the presence of Stx2a, each preparation of microvesicles (control, Stx2a and Stx2a+NAB815 microvesicles) was separated on Sephacryl S-500 gel filtration column (exclusion size 200 nm, total volume 5.5 ml) (Figure 29). The resin allowed the exclusion of microvesicles (1 μm) in the void volume whereas those molecules having sizes lower than 200 nm were separated during chromatography. Fractions (250 μl) were collected, the readings at A280 recorded and 50 μl-aliquots assayed for the presence of Stx2a by the Vero cell protein synthesis assay.

As depicted in Figure 28 (black squares), a single protein peak corresponding to the void volume was identified in each preparation. In the sample containing microvescicles from Stx2a-treated blood, we observed proteins in fractions 6-13 with a peak corresponding to fraction 7 (Figure 29B). In the presence of NAB815 (Figure 29C) proteins were found in the same fractions peaking at fraction 7 even though with a much lower A280 value, behaving as the control (Figure 29A).

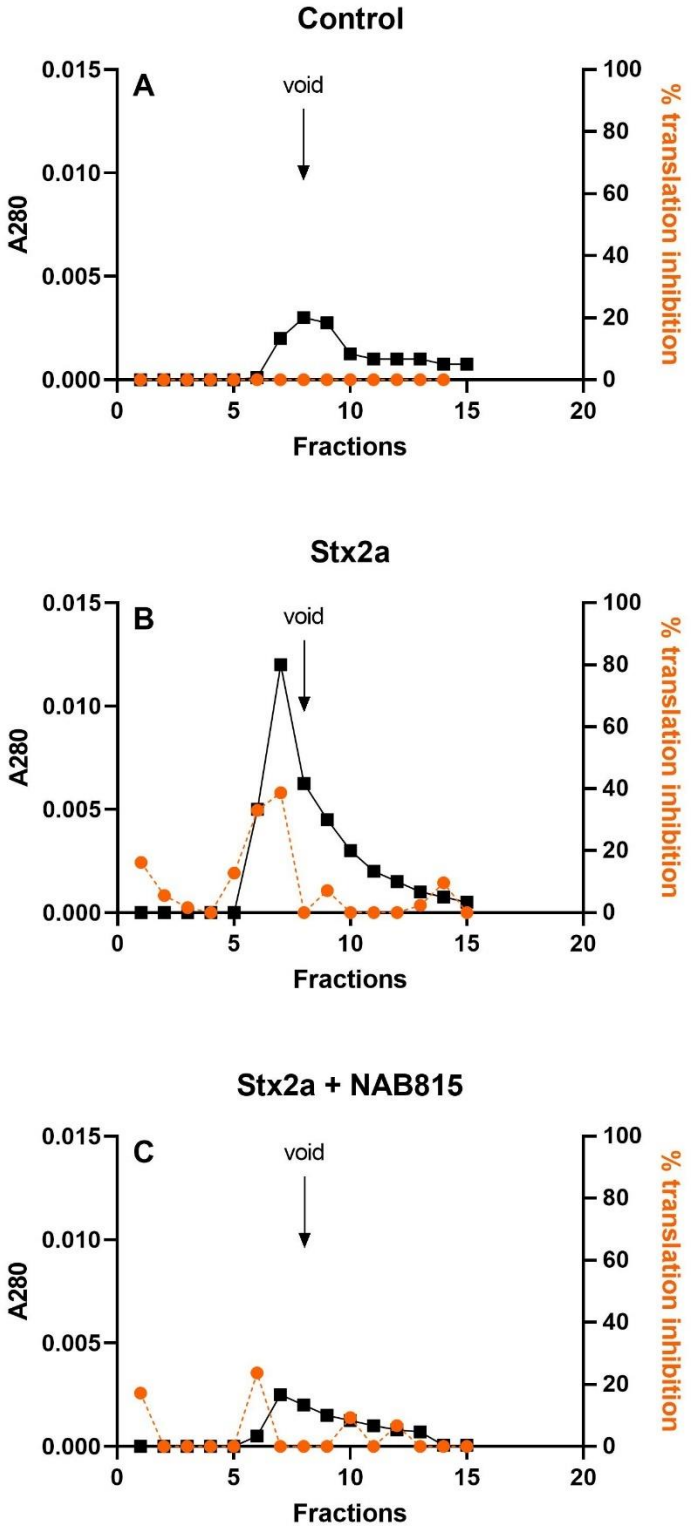

Figure 29: Gel-filtration chromatography of blood cell-derived microvesicles. (A) control (B) Stx2a (C) Stx2a+NAB815 microvesicles. In black, absorbance at 280 nm. In orange, the toxic activity of each fraction expressed as percent inhibition of protein synthesis by Vero cell protein synthesis assay. The arrow indicates the void volume of the column.

It should be noted that Stx2a (68,000) or the heaviest complex HuSAP-Stx2a (930,000), given their molecular masses, should not have been eluted in these fractions. In fact, the heaviest HuSAP-Stx2a complex, if globular, would have a ~13 nm diameter (according to the equation $r = 0.066 \times mass^{1/3}$) (Erickson, 2009), well below the exclusion limit of the resin. These observations suggest that the protein peak is related to proteins associated to whole microvesicles.

The translation inhibiting activity (orange circles) detected by the Vero cell assay was associated to the main protein peak of the Stx2-triggered microvesicles (fractions 5-7). In the presence of NAB815 the amount of Stx2a associated to extracellular vesicles was strongly reduced, peaking in fraction 6. No inhibition of protein synthesis was detected in control fractions.

To sum up, Stx2a was associated to microvesicles and their toxic cargo was strongly reduced in the presence of NAB815, suggesting that the antibiotic impaired the formation of Stx2a-containing microvesicles.

4.4. Effect of human blood-derived microvesicles on Vero cells

Microvesicles from control, Stx2a- and Stx2a+NAB815-treated blood from 5 different healthy donors were separately pooled and their toxicity tested on Vero cells by two different assays, i.e. protein synthesis assay and vitality assay. Control microvesicles did not affect protein synthesis, while Stx2a-triggered microvesicles were 3 times more toxic than those obtained in the presence of the toxin and NAB815, as indicated by the comparison of the IC_{50} values obtained in the two conditions (Figure 30). To evaluate the effect of microvesicles on cell viability after 72 h-incubation, a luminescent Cell Viability Assay on Vero cells was performed. Figure 31 clearly shows the protection induced by NAB815 on the toxic effect of microvesicle-associated Stx2a.

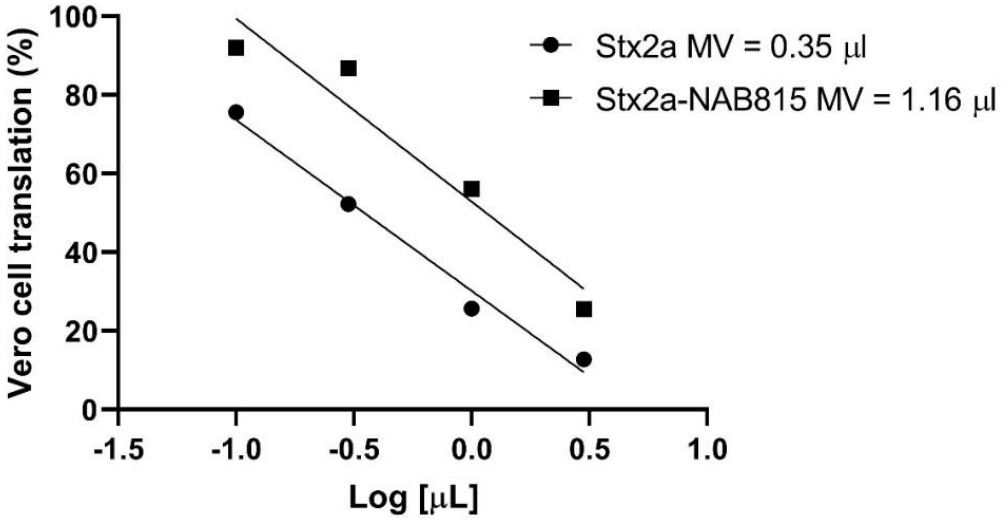

Figure 30: Effect of Stx2a microvesicles and Stx2a + NAB815 microvesicles on Vero cells protein synthesis. Different volume of the microvesicle (MV) samples (3 µl, 1 µl, 0.3 µl and 0.1 µl) was added to the cell monolayer.

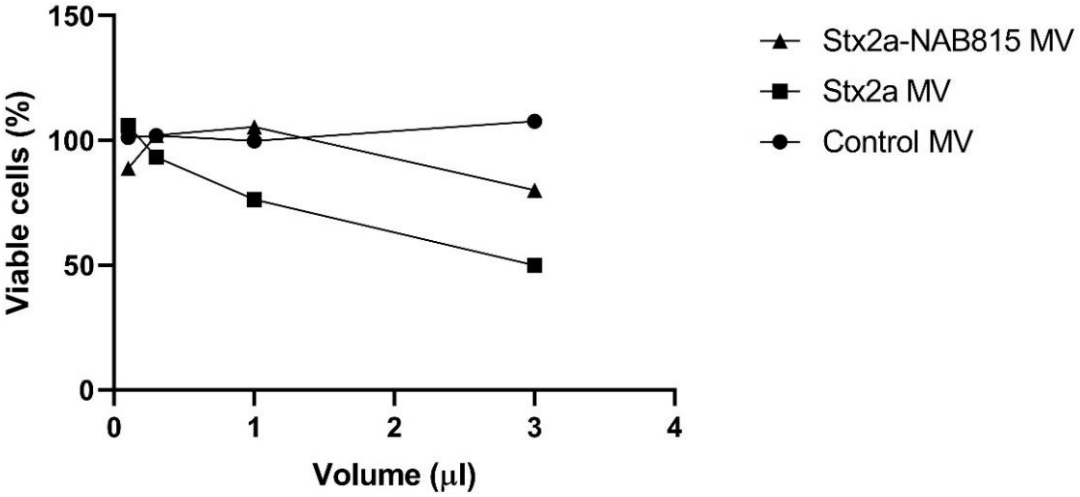

Figure 31: Effect of Stx2a microvesicles and Stx2a + NAB815 microvesicles on Vero cells viability. Different volume of the microvesicle (MV) samples (3 µl, 1 µl, 0.3 µl and 0.1 µl) was added to the cell monolayer.

DISCUSSION

1. Validation of the biosensor for the early detection of Stx2a

The developed plasmonic biosensor was able to effectively detect the toxin, returning a characteristic and reproducible SERS spectrum (Figure 13). The identification of specific peaks and their assignment to specific functional groups of the toxin, made the spectrum unique and characteristic (Table 4). For example, the peak 505 cm^{-1} and another minor peak (540 cm^{-1}) were identified as the 6 disulfide bonds characterizing the Stx2a structure (one in the A subunit and one in each of the B subunits) and having different conformation. The C−S stretching region was mainly occupied by the C−S bond vibration of cysteine (679 cm^{-1}) though the peak of methionine (717 cm^{-1}) was well represented. In addition, peaks corresponding to aromatic amino acids were identified: 552, 764, 883, 1053, 1554 cm^{-1} which correspond to the amino acid Trp; 636, 837, 856, 1203, 1612 cm^{-1} to Tyr and 1026, 1203, 1612 cm^{-1} to Phe. The peaks 837 and 856 cm^{-1} correspond to the typical Tyr doublet due to Fermi resonance. Another important feature was that, as expected, the alpha-helix conformation was well represented as we can infer from the amide III vibration well represented (1269 and 1300 cm^{-1}) in the spectra, and by the shoulder relative to the amide I mode (1658 cm^{-1}). These results were in agreement with crystallographic studies and circular dichroism analysis on Stx2a. Finally, it should be noted that the complexity of the final spectrum was the result of an average of repeated measurements of differently oriented Stx2a molecules bound to the nanostructure.

Regarding the anti-Stx2a capturing antibodies, the ideal concentration to have a resolved high-intensity spectrum was 10 µg/ml. The spectrum of Stx2a was not resolved at lower concentrations (5 µg/ml) because of the low amount of antibodies absorbed into the nanostructure. However, the highest tested concentration (25 µg/ml) was not optimal either, probably because of the saturation of the nanostructure.

Comparing the spectrum of the antibody and that of the antibody-bound Stx2a (Figure 15B), two bands at 460-590 cm^{-1} and 1616-1660 cm^{-1} were observed and these are related to the interaction with the toxin. In fact, it is likely that when Stx2a interacts with the antibody, conformational changes causing the formation of new peaks occurred. It is very interesting that in the presence of antibody-toxin interactions, the peak correlated to the disulfide bonds was more represented, probably because conformational changes lead the disulfide bonds to be more viable. Despite these differences, most of the peaks in the Stx2a

spectrum were shared with the antibody-Stx2 spectrum. This means that it is possible to recognize Stx2a even when it is captured by the immunosurface.

The LOD of the immunosystem was 1.4 nM. This was evaluated by the calibration curve obtained by the comparison of the amplification of the tryptophan-associated band (centered at 1554 cm^{-1}) corresponding to the spectra of different toxin concentrations. This value is higher than the concentrations of Stx2a detected in STEC-infected patient sera by ELISA (2-6 ng/ml corresponding to 30-90 pM). We are planning changes in the nanostructured biosensor allowing for further amplifications of the SERS system and enrichment steps on biological samples (concentration of human sera) to fill this gap. Despite the difference in LOD, the comparison of the performance of the developed SERS immunosensor with the gold standard ELISA assay showed that the two methods were comparable in terms of linearity, with a slight overestimation by the immunosensor.

Finally, the SERS spectra recorded in the presence of 4.5 μM BSA demonstrated that this non-target protein, well represented in sera, was not recognized and captured by the anti-Stx2 antibody, allowing to conclude that the immunosurface-based system was specific. Therefore, it could also be used to analyze more complex samples, as it was able to interact specifically with Stx2a.

The plasmonic biosensor based on this immunosensing strategy could be further developed as a new rapid and sensitive diagnostic tool for capturing and detecting the toxins present at low concentrations in the blood of STEC-infected patients or even in more complex biological samples. In addition, it could be utilized to create portable on-chip devices to use as point-of-care medical diagnostics.

2. Studies on the cleaved form of Stx2a

Recent findings highlighted that, the functional properties of Stx2a change according to the different structure of the toxin (uncleaved or cleaved with the A1 and A2 fragments held by a disulfide bridge), despite having the same toxic effect on cells. These two toxin forms bind to circulating cells and to serum components of the host very differently, and have a very different effect on the formation of aggregates. Specifically, the cleaved form of Stx2a is completely active in binding to complement factor H but does not bind to TLR4

on human neutrophils and to the same receptor on monocytes and platelets. The uncleaved form of Stx2a exhibits the opposite properties and promotes the formation of aggregates between leukocytes and platelets. As a consequence, the outcome of STEC infections and the onset of HUS could be also influenced by the percentages of toxin present in uncleaved or cleaved form circulating in the patient's blood.

By employing the above described luminometric cell-free protein synthesis method, the cleaved form of Stx2a can be discriminated from the uncleaved form due to its increased protein synthesis inhibition activity under reducing condition (pre-incubation with 80 mM DTT). This method was adapted for the toxin detection in serum samples to which the uncleaved or cleaved form were added. However, some factors in human serum strongly interfered with the cell-free protein synthesis system, directly inhibiting translation. They have been identified as an RNase, which may have some effect on the integrity of rRNA, mRNA or tRNA during protein synthesis, controlled by the addition of PRI to the assay. The other one is a factor which a high molecular mass component sensitive to DTT, which was eliminated by pre-treatment of sera with immobilized G protein. It has been hypothesized that the high molecular mass component probably consists of an immunoglubulin. Antibodies are well known to have a structure consisting of protein chains connected by disulfide bridges, and these bonds are necessary to maintain their integrity and allow their function. The high concentrations of DTT in the assay may have broken not only the disulfide bridge present between the A1 and A2 fragments of the toxin, but also the disulfide bonds between the antibody chains.

The toxin can be found bound to circulating cells, associated with microvesicles or in the free form once released in the circulation of patients. In particular, concentrations of Stx2a between 2 to 6 ng/ml circulating in the blood of 20 patients with STEC infection during the prodromal intestinal phase (bloody diarrhea) were detected by ELISA (Brigotti M., 2020). Our method could be useful for the detection of free Stx2a circulating in human blood, as its LOD allowed to identify concentrations very similar to those detected by ELISA. Indeed, ELISA is recommended to determine the presence of Stx2 quickly and quantitatively in the blood of patients and to diagnose STEC infections. However, ELISA does not discriminate between the two forms (uncleaved and cleaved) of toxin, whereas that is possible by using the newly described cell-free protein synthesis method.

To study and clarify the contribution of the two forms of Stx2a in the pathogenesis of HUS, it could be useful to use both methods: the total amount of toxin present in the blood

of patients can be identify by ELISA, while the percentage of toxin present in cleaved form can be easily established with the cell-free protein synthesis method.

The use of the newly developed method for the analysis of 10 STEC-infected patients' sera allowed to identify the cleaved form of Stx2a in 5 of them. The concentration of cleaved toxin was calculated through the equation described in the Methods. In 2 out of 5 cases, this was lower than the total concentration detected by ELISA, while in the remaining 3 patients the recorded toxin concentration was higher. This could be explained by the different features of the two methods. The toxin is recognized both in uncleaved and cleaved form by ELISA, however the capturing antibody binds to the B pentamer, consequently the free toxin is identified, as well as those toxin molecules interacting with TLR4 on the surface of microvescicles, but not the toxin bound to microvesicles via Gb3Cer. It is worth noting that Stx2a bound to Gb3Cer could be cleaved or uncleaved. By using the newly described cell-free protein synthesis method, when the toxin is bound via the B chain pentamer to the Gb3Cer expressed by microvesicles of platelet or monocyte derivation, it exposes the A subunit which, if present in cleaved form, is recorded by the system, similarly to free cleaved Stx2a. On the other hand, Stx2a bound to TLR4 via its A subunit is always uncleaved. For these reasons, the concentration of cleaved toxin in some patients turns out to be greater than the total concentration of toxin detected by ELISA, i.e., the latter assay could underestimate total Stx2a amount due to the lack of detection of Gb3Cer-bound cleaved toxin.

The cleaved form of the toxin is present in 2 of the 3 patients who developed HUS and in 3 out of 7 who recovered. Consequently, the presence of the cleaved form of the toxin in serum cannot be considered mandatory for the development of HUS. Bloody diarrhea, watery diarrhea, hematuria and proteinuria were found both in the patient group with the cleaved form of the toxin and in the patient group in which it was not detected.

A common feature of all patients with the cleaved form of Stx2a detected by the luminometric cell-free system and confirmed by the anti-cleaved Stx2a antibody (Vero cell assay) is the presence of the neutrophil-bound toxin (PMN+, Table 8). Patient 8 in which the positive result of the newly developed assay was not confirmed by the antibody-based assay, was negative for the binding of Stx2a to neutrophils (PMN-, Table 8). Since the binding of Stx2a to neutrophils is only possible if the toxin is not cleaved, the concomitant detection of the two forms (pts 1, 2 ,4, 10, Table 8) or only of the cleaved form of Stx2a (patients 2 and 9, Table 8) in PMN+ patients suggests two hypotheses: (i) the toxin is

released into the circulation at least in part uncleaved in order to bind to neutrophils, or (ii) it is cleaved after the binding to neutrophils.

Another hypothesis is that part of the toxin is cleaved in an earlier phase by some STEC bacterial proteases or by other bacterial proteases in the intestine (Detzner, Pohlentz, et al., 2020; Menge, 2020) and is released into the circulation already in cleaved form. In this case it can only recognize the Gb3Cer receptor expressed by circulating cells and therefore only bind to platelets and monocytes even though, given its properties, it stimulates the formation of aggregates to a lesser extent. Alternatively, since microvesicles have the same features as the cells from which they derive, those formed from monocytes and platelets can have Stx2a bound to Gb3Cer via the B chain pentamer leaving the toxin A chain exposed and available for a subsequent cleavage by host serum proteases. Finally, host serum proteases could also be responsible for the cleavage of free toxins in blood. Since the scenario is puzzling the identification of the source of protease/s inducing the toxin cleavage needs further investigations.

The observation that the cleaved form of the toxin was detected in all female patients ($n = 4$), while only in 1 out of 6 male cases ($p<0.05$), is of considerable interest. This suggests the presence of a sex-related factor responsible for the cleavage of the toxin. The cleaved form of the toxin may be able to bind to complement factor H and trigger an inflammatory cascade. Although the presence of the cleaved toxin does not appear to be a discriminating factor in patients who develop HUS, its properties could contribute to the severity of symptoms.

The new method has proved to be a useful tool for studying and obtaining more information on the contribution of the cleaved form of Stx2a in the pathogenesis of HUS and on the relationship with clinical symptoms. However, whether it actually contributes to HUS onset remains to be clarified. To better understand the role of the cleaved form of Stx2a in the pathogenesis of HUS, it will be necessary to perform targeted kinetic studies with repeated determinations over time to investigate the evolution of the clinical symptoms in STEC-infected patients and, at the same time, the appearance of cleaved Stx2a in sera.

3. NAB815 impairs the release of blood-cell derived microvesicles in human blood treated with Stx2a

The spreading and delivery of the toxin during the pathogenesis of HUS occurs in different forms: free Stx2a, Stx2a bound to circulating cells or associated to blood cell-derived microvesicles, as found in STEC-infected patients' sera before the onset of HUS.

Microvesicles, which are produced in the blood of patients by toxin-challenged circulating cells (monocytes, neutrophils, and erythrocytes), as well as platelets, are being implicated as a crucial player in the pathogenesis of HUS, according to a growing body of evidence. This toxin form is considered the main pathogenic factor responsible for the transition from bloody diarrhea to life-threatening HUS. Stx2a hits target cells through microvesicles that also contain other pathogenic factors involved in HUS development. It is therefore extremely important to identify the features and origin of the microvesicles and the subset responsible for the development of HUS.

In our experimental setting Stx2a increased the production and the release of blood-cell derived microvesicles showing by DLS a 0.5-1 μm diameter, in agreement with other studies. In addition, WES analysis of the protein extracted from the isolated microvesicles, showed the expression of Alix, as a specific marker of these extracellular vesicles.

Further evidence of the presence of microvesicles is given by gel filtration experiments. In fact, a peak corresponding to the size of the Stx2a-triggered microvesicle was detected. In addition, gel filtration of the samples revealed that the washing steps during the isolation protocol were sufficient to remove the free toxin. This result was also confirmed by the toxicity on Vero cells of the fractions corresponding to the microvesicle peak. Comparing these results with those obtained by Watanabe et al. (Watanabe-Takahashi et al., 2018) on gel filtration of exosome containing Stx2, the peak corresponding to the exosomes was eluted later as the exosomes have a lower size than microvesicles which were eluted in the void volume. However, a peak corresponding to free ^{125}I-Stx2 was also present during exosome gel filtration. This can be explained by some differences in the two methods: in the paper by Watanabe et al. HeLa S3 cells were incubated with ^{125}I-Stx2 and after washing and further incubation, the culture medium containing the exosomes produced by the cell and the released free toxin was recovered, followed by gel filtration to isolate the exosomes. We carried out the gel filtration with a sample of already isolated microvesicles instead.

The characterization of the isolated microvesicles was based on the assumption that they have the same features found in the cells from which they derive. The identification of some markers therefore allowed to determine the cell of origin of the microvesicles. Results obtained by WES analysis have shown that Stx2a stimulates the release of new microvesicles (Alix+) and that they are mainly of platelet origin (CD42a+) and also derived from leukocytes (CD45+). These results are in agreement with data obtained by flow cytometry on the subpopulation of microvesicles isolated from the blood of 13 STEC-infected pediatric patients with HUS. The majority of microvesicles identified in circulation were platelet-derived (50%), identified as CD42b+ vesicles, followed by leukocyte-derived vesicles (34%), specifically 18% were monocyte-derived (CD38+) and 16% neutrophil-derived (CD66+) (Ståhl et al., 2015). Considering the numbers of microvesicles of each cell type found in those HUS patients (Ståhl et al., 2015) and taking into account pediatric blood count ranges (1 to 4 years) of each type of circulating cells (Lanzkowsky, 1980; Miller, 1984; Nathan & Oski, 1987; Novak, Tschantz, & Krill, 1987; Saarinen & Siimes, 1978; Verma, 1981) it is easy to calculate that monocytes produce 0.4-1.3 microvesicles per cell, neutrophils 4-22 x 10^{-2} microvesicles per cell, platelets 2.7 to 3.1 x 10^{-3}. The calculation for neutrophils is probably overestimated due to the well-known neutrophilia observed in HUS patients (Tarr et al., 2005). However, for platelets, the calculation is underestimated due to thrombocytopenia, so platelets are likely to produce more microvesicles.

However, it must be taken into consideration that the mentioned results are obtained from the isolation of microvesicles from the blood of HUS+ pediatric patients, while in our case the results were obtained under experimental conditions in which the toxin was added to the blood of healthy adult donors.

When the blood of an adult donor is treated with the toxin, taken into account normal adult blood counts ranges (Royal Wolverhampton Trust Pathology Services, https://www.royalwolverhampton.nhs.uk/services/servicedirectory-a-z/pathology-services/departments/haematology/ haematology-normal-adult-reference-ranges), the ability to produce microvesicles of each cell type is very similar: monocytes, 0.3-1.1 vesicles per cell; neutrophils, 2-9 10^{-2} vesicles per cell; platelets, 1.8-5.5 x 10^{-3} vesicles per cell (Varrone et al., 2021).

Therefore, the efficiency of generation of the microvesicles from both pediatric patient and adults is similar. Moreover, the same ranking in vesicle formation among human

circulating cells was measured in unstimulated human blood analyzed by imaging flow cytometry (Headland et al., 2014) (ImageStream, Amnis Corporation, Seattle, WA). Therefore, although platelet-derived microvesicles predominate in the blood of patients during HUS, this is not due to a preferential stimulation of platelets by the toxin, but to a stimulation over the basal level while maintaining the same production efficiency per cell types.

Currently there are no effective therapies for STEC infection: most studies have shown that antibiotics should be avoided as they potentially increase the risk of developing HUS by enhancing Stx expression and their release after bacterial lysis. A recent hyperhydration protocol has appeared to reduce progression to HUS in patients with early diagnosis of STEC infection. The development of new therapies aimed at reducing the onset of HUS is therefore crucial.

We have identified the antibiotic NAB815 as an inhibitor of the binding of Stx2 to TLR4 expressed by circulating cells. This compound is a derivative of polymyxin B and is used at below than bactericidal concentrations. We have shown in previous experiments that NAB815 inhibits the binding of Stx2a to neutrophils through TLR4 and the formation of neutrophil-platelet aggregates. The results presented here are the first direct evidence of the efficacy of the antibiotic NAB815 in also significantly reducing the production of toxin-containing microvesicles, both platelet- and leukocyte-derived, by human blood challenged with the Stx2a.

By DLS NAB815 was shown to considerably reduce the formation of a specific population of microvesicles (500-1000 nm) compared to the microvesicles produced by the action of Stx2a. In addition, quantitative capillary Western Blot WES clearly showed a strong reduction of Alix, CD42a and especially of CD45 expression in the presence of the drug. Importantly, there is a significant strong reduction in the amount of toxin associated with microvesicles if the toxin treatment takes place in the presence of NAB815.

The almost total inhibition of leukocyte-derived microvesicles (CD45+) can be explained by the fact that neutrophils do not express the Gb3Cer receptor and can only bind the toxin through TLR4. Consequently, since the drug acts as an inhibitor of toxin binding to TLR4, it completely blocks neutrophil activation, aggregate formation and microvesicle release. In the case of platelets, the inhibition of microvesicle formation is minor, albeit considerable. This can be explained by the fact that platelets also express the Gb3Cer receptor. In fact, the drug, by inhibiting the binding of the toxin to TLR4 but not to Gb3Cer,

allows the toxin to bind to the latter receptor, causing a consequent activation and release of microvesicles, which is in any case significantly lower.

It is worth noting that NAB815 is able to reduce the production of extracellular vesicles containing the toxin, regardless the origin of microvesicles.

In support of these data, treatment of Vero cells for 18 h with microvesicles derived from the treatment of blood with the toxin alone induced a significant inhibition of protein synthesis that was greatly reduced in the presence of the drug NAB815. Furthermore, the results obtained from the viability assay after treatment of Vero cells for 72 h with the same microvesicles showed the same effect. The drug is therefore capable of affording protection in both assays in the short (18 h) or long term (72 h).

By comparing the IC_{50} of microvesicles on the Vero cell translation assay expressed in volume with that of the free toxin expressed in concentration, the amount of Stx2a associated to microvesicles can be traced. However, the microvesicles may also contain other pathogenic factors such as activated complement factors and tissue factor in addition to the toxin. In the cellular model (protein synthesis assay and viability assay) even if the ancillary pathogenic factors were transferred to target cells, they could not recruit other blood factors exacerbating the damage, therefore the toxicity detected as inhibition of protein synthesis or cell death is mainly related to the toxin action and not to the effect of the other factors characterizing the microvesicle pathotype. It is likely that the pathogenic microvesicles would be more toxic and NAB815 even more effective if injected into mice or baboons.

The administration of NAB815 in patients with STEC infection could be an innovative treatment for the prevention of HUS since Stx2 associated with microvesicles via TLR4 appears in the blood of patients the day before the development of HUS. These promising results lay the foundation for more targeted clinical and animal studies.

CONCLUSIONS

The research activity described in this dissertation deals with three different aspects of HUS: diagnosis, pathogenesis and therapy.

The development of an effective therapy to prevent the onset or to alleviate the symptoms of HUS is considered one of the main goals of the researchers in the field. However, this important result will be achieved only through a careful analysis of the pathogenesis in order to identify the main factors involved in the onset and evolution of HUS or those which promote more severe symptoms. Furthermore, it is worth to note that in order to reduce the likelihood of progression from bloody diarrhea to HUS, it is mandatory an early diagnosis of STEC infections.

The plasmonic biosensor described in this thesis is a new and effective diagnostic method for early detection of Stx. If further developed, it could be added to the vast array of currently used gold standard microbiological and serological diagnostic methods which, however, require very long times and specialized reference laboratories. Its use would allow to reduce the time elapsed from diagnosis and onset of the disease, and consequently to avoid any delay in the treatment of patients, a fundamental step to promote an effective therapy.

In addition, the cell-free protein synthesis method here developed to identify the presence of the cleaved form of the toxin and its detection in the blood of some patients with STEC infection will allow to better understand some steps of the pathogenesis of HUS, i.e., the role of the uncleaved and cleaved form of the toxin in the onset of HUS and their relationship with patient's gender and symptomatology. However, it remains to be clarified whether the cleaved form of toxin actually contributes to HUS.

Finally, cell cytotoxicity studies on the effects of microvesicles produced by Stx2a-triggered blood cells, the identification of their origin (platelet-derived and leukocyte-derived) has confirmed their role in the pathogenesis of the syndrome.

The observations on the pathogenesis of HUS allow to develop new therapies, such as the proposed treatment with the antibiotic NAB815 tested in this thesis and already patented. This drug acting as an inhibitor of the binding of Stx2 to TLR4 at below than bactericidal concentrations, is significantly effective in inhibiting not only the binding of the toxin to neutrophils and the formation of aggregates between leukocytes and platelets but also in impairing the formation of platelet-derived and leukocyte-derived pathogenic

microvesicles. In addition, it reduced the toxic effect of blood cell-derived microvesicles on cellular models, affording protection in the short (18 h) or long term (72 h).

Since Stx2 associated with microvesicles via TLR4 was detected in the blood of patients the day before the development of HUS, administration of NAB815 in patients with STEC infection could be an innovative treatment for the prevention of HUS. These results are promising and lay the foundation for more targeted studies to be carried out in animal models and subsequently in STEC-infected patients.

The plasmonic biosensor was developed in collaboration with a group of physicists led by Dr Lucia Petti (CNR, Pozzuoli, Naples) and the obtained results were published in ACS Appl Mater Interfaces in February 2022, *"Plasmonic Metasurfaces for Specific SERS Detection of Shiga Toxins".*

The developed method for the detection of the cleaved form of Stx2a was published in Toxins in 2021, *"Method for the Detection of the Cleaved Form of Shiga Toxin 2a Added to Normal Human Serum".*

The paper reporting the data obtained on the identification of the cleaved form of the toxin in STEC-infected patients' sera thanks to its application is under preparation.

The development and the validation of the specific monoclonal antibody against the cleaved form of the toxin, used to confirm the functional data, was carried out in collaboration with Prof. Reinhard Würzner and Prof. Dorothea Orth (Division of Hygiene and Medical Microbiology, Medical University of Innsbruck, Innsbruck, Austria) during my period abroad.

During my PhD, I focused on the topic of extracellular vesicles and a review on this subject was published *"Extracellular Vesicles and Renal Endothelial Cells: A Fatal Attraction in Hemolytic Uremic Syndrome"* in The American Journal of Pathology in 2021.

In addition, the data obtained on the characterization of the pathogenic blood cell-derived Stx2-containing microvesicles and on the efficacy of NAB815 in preventing their formation and in blocking their toxicity in cellular models *in vitro*, will be added to those already described in the patents (2019, Italian patent 102019000025414; 2021, patent extended in EU, USA, Canada, Japan and Brazil, WO2021130700 (A1)) in order to prepare the final manuscript.

Abbreviations

BSA, bovine serum albumin

CCR1, chemokine receptor 1

CER, ceramide

CFB, complement factor B

CFH, complement factor H

CFI, complement factor I

CR1, complement receptor type 1

CR3, complement receptor type 3

CXCR4, chemokine receptor 4

CXCR7, chemokine receptor 7

DLS, dynamic light scattering

DMEM, Dulbecco modificated essential medium

DTT, dithiothreitol

eEF1, eukaryotic elongation factor 1

eEF2, eukaryotic elongation factor 2

ELISA, Enzyme-Linked Immunosorbent Assay

FDA, Food and Drug Administration

Gb3Cer, globotriaosylceramide

Gb4Cer, globotetraosylceramide

Gb5Cer, globopentaosylceramide

GlcCe,r glucosylceramide

GSLs, glycosphingolipids

HMEC-1, human endothelial cell line microvascular endothelial cells

HUS, hemolytic uremic syndrome

HuSAP, human serum amyloid P component

IL-10, interleukin 10

IL-1β, interleukin 1β

IL-6, interleukin 6

IL-8, interleukin 8

LAL, Limulus amebocyte lysate

Lc2Cer, lactosylceramide

LPS, lipopolysaccharide

MAPKp38, p38 mitogen-activated protein kinases

MCP, membrane cofactor protein

MCP-1, monocyte chemoattractant peptide-1

MIP1-alpha, macrophage inflammatory protein alpha

NTA, nanoparticles tracking analysis

PAMPs, pathogen-associated molecular patterns

PBS, phosphate Buffered Saline

PCR, polymerase chain reaction

pHBMECs, primary endothelial cells of the human brain

pHRCEpiCs, primary human renal cortical epithelial cells

PI3K/Akt/mTOR, phosphatidylinositol 3-kinase/protein-kinase B/mechanistic target of rapamycin

PKC, protein-kinase C

PMN, polymorphonuclear neutrophils

PMSF, phenylmethylsulphonyl fluoride

PRI, placental RNase inhibitor

RANTES, regulated on activation normal T-cell expressed

SAPK/JNK, stress-activated protein kinases/Jun amino-terminal kinases

SDF-1, stromal derived factor-1

SERS, amplified Raman spectroscopy on surfaces

STEC, Shiga toxins-producing *Escherichia coli*

STEC-HUS, STEC-associated hemolytic uremic syndrome

Stx, Shiga toxins

Stx1, Shiga toxin 1

Stx2, Shiga toxin 2

Stx2a, Shiga toxin 2a

Stx2b, Shiga toxin 2b

Stx2c, Shiga toxin 2c

Stx2d, Shiga toxin 2d

Stx2dact, Shiga toxin 2d activatable

Stx2e, Shiga toxin 2e

Stx2f, Shiga toxin 2f

Stx2g, Shiga toxin, 2g

TEM, transmission electron microscopy

THBD, thrombomodulin

TLR4, Toll-like receptor 4

TMP-SMZ, trimethoprim-sulfamethoxazole

TNF-α, tumor necrosis factor alpha

WES, capillary quantitative Western Blot

WHO, World Health Organization

REFERENCES

Abid Hussein, M. N., Böing, A. N., Sturk, A., Hau, C. M., & Nieuwland, R. (2007). Inhibition of microparticle release triggers endothelial cell apoptosis and detachment. *Thromb Haemost, 98*(5), 1096-1107. doi:10.1160/th05-04-0231

Angelillo-Scherrer, A. (2012). Leukocyte-derived microparticles in vascular homeostasis. *Circ Res, 110*(2), 356-369. doi:10.1161/circresaha.110.233403

Ardissino, G., Salardi, S., Colombo, E., Testa, S., Borsa-Ghiringhelli, N., Paglialonga, F., Tedeschi, S. (2016). Epidemiology of haemolytic uremic syndrome in children. Data from the North Italian HUS network. *Eur J Pediatr, 175*(4), 465-473. doi:10.1007/s00431-015-2642-1

Ardissino, G., Tel, F., Possenti, I., Testa, S., Consonni, D., Paglialonga, F., Torresani, E. (2016). Early Volume Expansion and Outcomes of Hemolytic Uremic Syndrome. *Pediatrics, 137*(1). doi:10.1542/peds.2015-2153

Arfilli, V., Carnicelli, D., Rocchi, L., Ricci, F., Pagliaro, P., Tazzari, P. L., & Brigotti, M. (2010). Shiga toxin 1 and ricin A chain bind to human polymorphonuclear leucocytes through a common receptor. *Biochem J, 432*(1), 173-180. doi:10.1042/bj20100455

Armstrong, G. D., Mulvey, G. L., Marcato, P., Griener, T. P., Kahan, M. C., Tennent, G. A., Pepys, M. B. (2006). Human serum amyloid P component protects against Escherichia coli O157:H7 Shiga toxin 2 in vivo: therapeutic implications for hemolytic-uremic syndrome. *J Infect Dis, 193*(8), 1120-1124. doi:10.1086/501472

Arraud, N., Linares, R., Tan, S., Gounou, C., Pasquet, J. M., Mornet, S., & Brisson, A. R. (2014). Extracellular vesicles from blood plasma: determination of their morphology, size, phenotype and concentration. *J Thromb Haemost, 12*(5), 614-627. doi:10.1111/jth.12554

Arvidsson, I., Stahl, A. L., Hedstrom, M. M., Kristoffersson, A. C., Rylander, C., Westman, J. S., Karpman, D. (2015). Shiga toxin-induced complement-mediated hemolysis and release of complement-coated red blood cell-derived microvesicles in hemolytic uremic syndrome. *J Immunol, 194*(5), 2309-2318. doi:10.4049/jimmunol.1402470

Barbour, T., Johnson, S., Cohney, S., & Hughes, P. (2012). Thrombotic microangiopathy and associated renal disorders. *Nephrology, dialysis, transplantation, 27*(7), 2673-2685doi:https://doi.org/10.1093/ndt/gfs279

Betz, J., Dorn, I., Kouzel, I. U., Bauwens, A., Meisen, I., Kemper, B., Müthing, J. (2016). Shiga toxin of enterohaemorrhagic Escherichia coli directly injures developing human erythrocytes. *Cell Microbiol, 18*(10), 1339-1348. doi:10.1111/cmi.12592

Bevers, E. M., & Williamson, P. L. (2016). Getting to the Outer Leaflet: Physiology of Phosphatidylserine Exposure at the Plasma Membrane. *Physiol Rev, 96*(2), 605-645. doi:10.1152/physrev.00020.2015

Bielaszewska, M., Friedrich, A. W., Aldick, T., Schürk-Bulgrin, R., & Karch, H. (2006). Shiga toxin activatable by intestinal mucus in Escherichia coli isolated from humans: predictor for a severe clinical outcome. *Clin Infect Dis, 43*(9), 1160-1167. doi:10.1086/508195

Bielaszewska, M., & Karch, H. (2005). Consequences of enterohaemorrhagic Escherichia coli infection for the vascular endothelium. *Thromb Haemost, 94*(2), 312-318. doi:10.1160/th05-04-0265

Bielaszewska, M., Rüter, C., Bauwens, A., Greune, L., Jarosch, K. A., Steil, D., Karch, H. (2017). Host cell interactions of outer membrane vesicle-associated virulence factors of enterohemorrhagic Escherichia coli O157: Intracellular delivery, trafficking and mechanisms of cell injury. *PLOS Pathog, 13*(2), e1006159. doi:10.1371/journal.ppat.1006159

Biró, E., Akkerman, J. W., Hoek, F. J., Gorter, G., Pronk, L. M., Sturk, A., & Nieuwland, R. (2005). The phospholipid composition and cholesterol content of platelet-derived microparticles: a comparison with platelet membrane fractions. *J Thromb Haemost, 3*(12), 2754-2763. doi:10.1111/j.1538-7836.2005.01646.x

Bitzan, M., Richardson, S., Huang, C., Boyd, B., Petric, M., & Karmali, M. A. (1994). Evidence that verotoxins (Shiga-like toxins) from Escherichia coli bind to P blood group antigens of human erythrocytes in vitro. *Infect Immun, 62*(8), 3337-3347. doi:10.1128/iai.62.8.3337-3347.1994

Brigotti, M. (2012). The interactions of human neutrophils with shiga toxins and related plant toxins: danger or safety? *Toxins (Basel), 4*(3), 157-190. doi:10.3390/toxins4030157

Brigotti, M., Arfilli, V., Carnicelli, D., Ricci, F., Tazzari, P. L., Ardissino, G., He, X. (2018). Soluble Toll-Like Receptor 4 Impairs the Interaction of Shiga Toxin 2a with Human Serum Amyloid P Component. *Toxins (Basel), 10*(9). doi:10.3390/toxins10090379

Brigotti, M., Barbieri, L., Valbonesi, P., Stirpe, F., Montanaro, L., & Sperti, S. (1998). A rapid and sensitive method to measure the enzymatic activity of ribosome-inactivating proteins. *Nucleic Acids Res, 26*(18), 4306-4307. doi:10.1093/nar/26.18.4306

Brigotti, M., Caprioli, A., Tozzi, A. E., Tazzari, P. L., Ricci, F., Conte, R., Rizzoni, G. (2006). Shiga toxins present in the gut and in the polymorphonuclear leukocytes circulating in the blood of children with hemolytic-uremic syndrome. *Journal of clinical microbiology, 44*(2), 313-317. doi:10.1128/jcm.44.2.313-317.2006

Brigotti, M., Carnicelli, D., Arfilli, V., Porcellini, E., Galassi, E., Valerii, M. C., & Spisni, E. (2018). Human monocytes stimulated by Shiga toxin 1a via globotriaosylceramide release proinflammatory molecules associated with hemolytic uremic syndrome. *Int J Med Microbiol, 308*(7), 940-946. doi:10.1016/j.ijmm.2018.06.013

Brigotti, M., Carnicelli, D., Arfilli, V., Tamassia, N., Borsetti, F., Fabbri, E., Cassatella, M. A. (2013). Identification of TLR4 as the receptor that recognizes Shiga toxins in human neutrophils. *J Immunol, 191*(9), 4748-4758. doi:10.4049/jimmunol.1300122

Brigotti, M., Carnicelli, D., Ravanelli, E., Barbieri, S., Ricci, F., Bontadini, A., Tazzari, P. L. (2008). Interactions between Shiga toxins and human polymorphonuclear leukocytes. *J Leukoc Biol, 84*(4), 1019-1027. doi:10.1189/jlb.0308157

Brigotti, M., Orth-Holler, D., Carnicelli, D., Porcellini, E., Galassi, E., Tazzari, P. L., Wurzner, R. (2019). The structure of the Shiga toxin 2a A-subunit dictates the interactions of the toxin with blood components. *Cell Microbiol, 21*(5), e13000. doi:10.1111/cmi.13000

Brigotti, M., Tazzari, P. L., Ravanelli, E., Carnicelli, D., Barbieri, S., Rocchi, L., Caprioli, A. (2010). Endothelial damage induced by Shiga toxins delivered by neutrophils during transmigration. *J Leukoc Biol, 88*(1), 201-210. doi:10.1189/jlb.0709475

Brigotti, M., Tazzari, P. L., Ravanelli, E., Carnicelli, D., Rocchi, L., Arfilli, V., Caprioli, A. (2011). Clinical relevance of shiga toxin concentrations in the blood of patients with hemolytic uremic syndrome. *Pediatr Infect Dis J, 30*(6), 486-490. doi:10.1097/INF.0b013e3182074d22

Brigotti M., X. H., Carnicelli, D., Arfilli, V., Porcellini, E., Galassi, E., Tazzari, PL., Ricci, F., Patfield, S., Testa, S., Paglialonga, F., Picicco, D., Caprioli, A., Scavia, G., Morabito, S., Ardissino, G.,. (2020). Particulate Shiga Toxin 2 in Blood is Associated to the Development of Hemolytic Uremic Syndrome in Children. *Blood Cells, Inflammation and Infection thromb Haemost, 120*(1), 107-120. doi:10.1055/s-0039-3400301

Brooks, J. T., Sowers, E. G., Wells, J. G., Greene, K. D., Griffin, P. M., Hoekstra, R. M., & Strockbine, N. A. (2005). Non-O157 Shiga toxin-producing Escherichia coli infections in the United States, 1983-2002. *J Infect Dis, 192*(8), 1422-1429. doi:10.1086/466536

Bunger, J. C., Melton-Celsa, A. R., & O'Brien, A. D. (2013). Shiga toxin type 2dact displays increased binding to globotriaosylceramide in vitro and increased lethality in mice after activation by elastase. *Toxins (Basel), 5*(11), 2074-2092. doi:10.3390/toxins5112074

Buteau, C., Proulx, F., Chaibou, M., Raymond, D., Clermont, M. J., Mariscalco, M. M., Seidman, E. (2000). Leukocytosis in children with Escherichia coli O157:H7 enteritis developing the hemolytic-uremic syndrome. *Pediatr Infect Dis J, 19*(7), 642-647. doi:10.1097/00006454-200007000-00012

Camussi, G., Deregibus, M. C., Bruno, S., Cantaluppi, V., & Biancone, L. (2010). Exosomes/microvesicles as a mechanism of cell-to-cell communication. *Kidney Int, 78*(9), 838-848. doi:10.1038/ki.2010.278

Canpolat, N. (2015). Hemolytic uremic syndrome. *Turk Pediatri Ars, 50*(2), 73-82. doi:10.5152/tpa.2015.2297

Carnicelli, D., Arfilli, V., Ricci, F., Velati, C., Tazzari, P. L., & Brigotti, M. (2016). The Antibiotic Polymyxin B Impairs the Interactions between Shiga Toxins and Human Neutrophils. *J Immunol, 196*(3), 1177-1185. doi:10.4049/jimmunol.1500671

Chaisri, U., Nagata, M., Kurazono, H., Horie, H., Tongtawe, P., Hayashi, H., . . . Chaicumpa, W. (2001). Localization of Shiga toxins of enterohaemorrhagic Escherichia coli in kidneys of paediatric and geriatric patients with fatal haemolytic uraemic syndrome. *Microb Pathog, 31*(2), 59-67. doi:10.1006/mpat.2001.0447

Chart, H., Perry, N. T., Cheasty, T., & Wright, P. A. (2002). The kinetics of antibody production to antigens of Escherichia coli O157 in a pregnant woman with haemolytic uraemic syndrome. *J Med Microbiol, 51*(6), 522-525. doi:10.1099/0022-1317-51-6-522

Cheng, L. W., Henderson, T. D., Patfield, S., Stanker, L. H., & He, X. (2013). Mouse in vivo neutralization of Escherichia coli Shiga toxin 2 with monoclonal antibodies. *Toxins (Basel), 5*(10), 1845-1858. doi:10.3390/toxins5101845

Cheung, V., & Trachtman, H. . (2014). Hemolytic uremic syndrome: toxins, vessels, and inflammation. *Frontiers in medicine, 1*(42). doi: https://doi.org/10.3389/fmed.2014.00042

Chui, L., Lee, M. C., Allen, R., Bryks, A., Haines, L., & Boras, V. (2013). Comparison between ImmunoCard STAT!(®) and real-time PCR as screening tools for both O157:H7 and non-O157 Shiga toxin-producing Escherichia coli in Southern Alberta, Canada. *Diagn Microbiol Infect Dis, 77*(1), 8-13. doi:10.1016/j.diagmicrobio.2013.05.015

Colic, E., Dieperink, H., Titlestad, K., & Tepel, M. (2011). Management of an acute outbreak of diarrhoea-associated haemolytic uraemic syndrome with early plasma exchange in adults from southern Denmark: an observational study. *Lancet, 378*(9796), 1089-1093. doi:10.1016/s0140-6736(11)61145-8

Colombo, M., Raposo, G., & Théry, C. (2014). Biogenesis, secretion, and intercellular interactions of exosomes and other extracellular vesicles. *Annu Rev Cell Dev Biol, 30*, 255-289. doi:10.1146/annurev-cellbio-101512-122326

Corogeanu, D., Willmes, R., Wolke, M., Plum, G., Utermöhlen, O., & Krönke, M. (2012). Therapeutic concentrations of antibiotics inhibit Shiga toxin release from enterohemorrhagic E. coli O104:H4 from the 2011 German outbreak. *BMC Microbiol, 12*, 160. doi:10.1186/1471-2180-12-160

DeGrandis, S., Law, H., Brunton, J., Gyles, C., & Lingwood, C. A. (1989). Globotetraosylceramide is recognized by the pig edema disease toxin. *J Biol Chem, 264*(21), 12520-12525.

Del Conde, I., Shrimpton, C. N., Thiagarajan, P., & López, J. A. (2005). Tissue-factor-bearing microvesicles arise from lipid rafts and fuse with activated platelets to initiate coagulation. *Blood, 106*(5), 1604-1611. doi:10.1182/blood-2004-03-1095

Detzner, J., Krojnewski, E., Pohlentz, G., Steil, D., Humpf, H. U., Mellmann, A., Müthing, J. (2021). Shiga Toxin (Stx)-Binding Glycosphingolipids of Primary Human Renal Cortical Epithelial Cells (pHRCEpiCs) and Stx-Mediated Cytotoxicity. *Toxins (Basel), 13*(2). doi:10.3390/toxins13020139

Detzner, J., Pohlentz, G., & Müthing, J. (2020). Valid Presumption of Shiga Toxin-Mediated Damage of Developing Erythrocytes in EHEC-Associated Hemolytic Uremic Syndrome. *Toxins (Basel), 12*(6). doi:10.3390/toxins12060373

Detzner, J., Pohlentz, G., & Müthing, J. (2022). Enterohemorrhagic Escherichia coli and a Fresh View on Shiga Toxin-Binding Glycosphingolipids of Primary Human Kidney and Colon Epithelial Cells and Their Toxin Susceptibility. *Int J Mol Sci, 23*(13). doi:10.3390/ijms23136884

Detzner, J., Steil, D., Pohlentz, G., Legros, N., Humpf, H. U., Mellmann, A., Müthing, J. (2020). Real-time interaction analysis of Shiga toxins and membrane microdomains of primary human brain microvascular endothelial cells. *Glycobiology, 30*(3), 174-185. doi:10.1093/glycob/cwz091

Dragovic, R. A., Gardiner, C., Brooks, A. S., Tannetta, D. S., Ferguson, D. J. P., Hole, P., Sargent, I. L. (2011). Sizing and phenotyping of cellular vesicles using Nanoparticle Tracking Analysis. *Nanomedicine: Nanotechnology, Biology and Medicine, 7*(6), 780-788. doi:https://doi.org/10.1016/j.nano.2011.04.003

Ehrlenbach, S., Rosales, A., Posch, W., Wilflingseder, D., Hermann, M., Brockmeyer, J., Orth-Höller, D. (2013). Shiga toxin 2 reduces complement inhibitor CD59 expression on human renal tubular epithelial and glomerular endothelial cells. *Infect Immun, 81*(8), 2678-2685. doi:10.1128/iai.01079-12

Erickson, H. P. (2009). Size and shape of protein molecules at the nanometer level determined by sedimentation, gel filtration, and electron microscopy. *Biol Proced Online, 11*, 32-51. doi:10.1007/s12575-009-9008-x

Espinosa, L., Gray, A., Duffy, G., Fanning, S., & McMahon, B. J. (2018). A scoping review on the prevalence of Shiga-toxigenic Escherichia coli in wild animal species. *Zoonoses Public Health, 65*(8), 911-920. doi:10.1111/zph.12508

Falguières, T., Mallard, F., Baron, C., Hanau, D., Lingwood, C., Goud, B., Johannes, L. (2001). Targeting of Shiga toxin B-subunit to retrograde transport route in association with detergent-resistant membranes. *Mol Biol Cell, 12*(8), 2453-2468. doi:10.1091/mbc.12.8.2453

FAO/WHO. (2019). *Attributing illness caused by Shiga toxin-producing Escherichia coli (STEC) to specific foods. Microbiological Risk Assessment Series. No 32. Rome. 74 pp. Licence: CC BY-NC-SA 3.0 IGO.*

Feng, J., Xu, K., Shi, X., Xu, L., Liu, L., Wang, F., Zhan, S. (2022). Incidence and cost of haemolytic uraemic syndrome in urban China: a national population-based analysis. *BMC Nephrol, 23*(1), 122. doi:10.1186/s12882-022-02746-2

Flaumenhaft, R., Dilks, J. R., Richardson, J., Alden, E., Patel-Hett, S. R., Battinelli, E., Italiano, J. E., Jr. (2009). Megakaryocyte-derived microparticles: direct visualization and distinction from platelet-derived microparticles. *Blood, 113*(5), 1112-1121. doi:10.1182/blood-2008-06-163832

Frank, C., Werber, D., Cramer, J. P., Askar, M., Faber, M., an der Heiden, M., Krause, G. (2011). Epidemic profile of Shiga-toxin-producing Escherichia coli O104:H4 outbreak in Germany. *N Engl J Med, 365*(19), 1771-1780. doi:10.1056/NEJMoa1106483

Friedrich, A. W., Bielaszewska, M., Zhang, W. L., Pulz, M., Kuczius, T., Ammon, A., & Karch, H. (2002). Escherichia coli harboring Shiga toxin 2 gene variants: frequency and association with clinical symptoms. *J Infect Dis, 185*(1), 74-84. doi:10.1086/338115

Fukushima, H., Hashizume, T., Morita, Y., Tanaka, J., Azuma, K., Mizumoto, Y., Kitani, T. (1999). Clinical experiences in Sakai City Hospital during the massive outbreak of enterohemorrhagic Escherichia coli O157 infections in Sakai City, 1996. *Pediatr Int, 41*(2), 213-217. doi:10.1046/j.1442-200x.1999.4121041.x

Fürst, S., Scheef, J., Bielaszewska, M., Rüssmann, H., Schmidt, H., & Karch, H. (2000). Identification and characterisation of Escherichia coli strains of O157 and non-O157 serogroups containing three distinct Shiga toxin genes. *J Med Microbiol, 49*(4), 383-386. doi:10.1099/0022-1317-49-4-383

García, A., Marini, R. P., Catalfamo, J. L., Knox, K. A., Schauer, D. B., Rogers, A. B., & Fox, J. G. (2008). Intravenous Shiga toxin 2 promotes enteritis and renal injury characterized by polymorphonuclear leukocyte infiltration and thrombosis in Dutch Belted rabbits. *Microbes Infect, 10*(6), 650-656. doi:10.1016/j.micinf.2008.03.004

Geelen, J. M., van der Velden, T. J., van den Heuvel, L. P., & Monnens, L. A. (2007). Interactions of Shiga-like toxin with human peripheral blood monocytes. *Pediatr Nephrol, 22*(8), 1181-1187. doi:10.1007/s00467-007-0512-4

Gentry, M. K., & Dalrymple, J. M. (1980). Quantitative microtiter cytotoxicity assay for Shigella toxin. *Journal of clinical microbiology, 12*(3), 361-366. doi:10.1128/jcm.12.3.361-366.1980

Gianviti, A., Perna, A., Caringella, A., Edefonti, A., Penza, R., Remuzzi, G., & Rizzoni, G. (1993). Plasma exchange in children with hemolytic-uremic syndrome at risk of poor outcome. *Am J Kidney Dis, 22*(2), 264-266. doi:10.1016/s0272-6386(12)70316-5

Goldstein, J., Nuñez-Goluboay, K., & Pinto, A. (2021). Therapeutic Strategies to Protect the Central Nervous System against Shiga Toxin from Enterohemorrhagic Escherichia coli. *Curr Neuropharmacol, 19*(1), 24-44. doi:10.2174/1570159x18666200220143001

Gould, L. H., Bopp, C., Strockbine, N., Atkinson, R., Baselski, V., Body, B., Gerner-Smidt, P. (2009). Recommendations for diagnosis of shiga toxin--producing Escherichia coli infections by clinical laboratories. *MMWR Recomm Rep, 58*(Rr-12), 1-14.

Griener, T. P., Mulvey, G. L., Marcato, P., & Armstrong, G. D. (2007). Differential binding of Shiga toxin 2 to human and murine neutrophils. *J Med Microbiol, 56*(Pt 11), 1423-1430. doi:10.1099/jmm.0.47282-0

Grif, K., Dierich, M. P., Karch, H., & Allerberger, F. (1998). Strain-specific differences in the amount of Shiga toxin released from enterohemorrhagic Escherichia coli O157 following exposure to subinhibitory concentrations of antimicrobial agents. *Eur J Clin Microbiol Infect Dis, 17*(11), 761-766. doi:10.1007/s100960050181

György, B., Szabó, T. G., Pásztói, M., Pál, Z., Misják, P., Aradi, B., Buzás, E. I. (2011). Membrane vesicles, current state-of-the-art: emerging role of extracellular vesicles. *Cell Mol Life Sci, 68*(16), 2667-2688. doi:10.1007/s00018-011-0689-3

Harel, Y., Silva, M., Giroir, B., Weinberg, A., Cleary, T. B., & Beutler, B. (1993). A reporter transgene indicates renal-specific induction of tumor necrosis factor (TNF) by shiga-like toxin. Possible involvement of TNF in hemolytic uremic syndrome. *J Clin Invest, 92*(5), 2110-2116. doi:10.1172/jci116811

He, X., Ardissino, G., Patfield, S., Cheng, L. W., Silva, C. J., & Brigotti, M. (2018). An Improved Method for the Sensitive Detection of Shiga Toxin 2 in Human Serum. *Toxins (Basel), 10*(2). doi:10.3390/toxins10020059

He, X., Quiñones, B., Loo, M. T., Loos, S., Scavia, G., Brigotti, M., Monnens, L. (2015). Serum Shiga toxin 2 values in patients during acute phase of diarrhoea-associated haemolytic uraemic syndrome. *Acta Paediatr, 104*(12), e564-568. doi:10.1111/apa.13211

Headland, S. E., Jones, H. R., D'Sa, A. S. V., Perretti, M., & Norling, L. V. (2014). Cutting-Edge Analysis of Extracellular Microparticles using ImageStreamX Imaging Flow Cytometry. *Sci Rep, 4*(1), 5237. doi:10.1038/srep05237

Heuvelink, A. E., Van de Kar, N. C., Van Der Velden, T. J., Chart, H., & Monnens, L. A. (1999). Verocytotoxin-producing Escherichia coli infection in household members of children with hemolytic-uremic syndrome in The Netherlands. *Pediatr Infect Dis J, 18*(8), 709-714. doi:10.1097/00006454-199908000-00011

Ikeda, K., Ida, O., Kimoto, K., Takatorige, T., Nakanishi, N., & Tatara, K. (1999). Effect of early fosfomycin treatment on prevention of hemolytic uremic syndrome accompanying Escherichia coli O157:H7 infection. *Clin Nephrol, 52*(6), 357-362.

Inward, C. D., Howie, A. J., Fitzpatrick, M. M., Rafaat, F., Milford, D. V., & Taylor, C. M. (1997). Renal histopathology in fatal cases of diarrhoea-associated haemolytic uraemic syndrome. British Association for Paediatric Nephrology. *Pediatr Nephrol, 11*(5), 556-559. doi:10.1007/s004670050337

Iwami, K.-i., Matsuguchi, T., Masuda, A., Kikuchi, T., Musikacharoen, T., & Yoshikai, Y. (2000). Cutting Edge: Naturally Occurring Soluble Form of Mouse Toll-Like Receptor 4 Inhibits Lipopolysaccharide Signaling1. *The Journal of Immunology, 165*, 6682 - 6686.

Jacewicz, M. S., Mobassaleh, M., Gross, S. K., Balasubramanian, K. A., Daniel, P. F., Raghavan, S., Keusch, G. T. (1994). Pathogenesis of Shigella diarrhea: XVII. A mammalian cell membrane glycolipid, Gb3, is required but not sufficient to confer sensitivity to Shiga toxin. *J Infect Dis, 169*(3), 538-546. doi:10.1093/infdis/169.3.538

Jandhyala, D. M., Thorpe, C. M., & Magun, B. . (2012). Ricin and Shiga toxins: effects on host cell signal transduction. . *Current topics in microbiology and immunology,, 357*, 41-65. doi:https://doi.org/10.1007/82_2011_181

Jaresová, I., Rozková, D., Spísek, R., Janda, A., Brázová, J., & Sedivá, A. (2007). Kinetics of Toll-like receptor-4 splice variants expression in lipopolysaccharide-stimulated antigen presenting cells of healthy donors and patients with cystic fibrosis. *Microbes Infect, 9*(11), 1359-1367. doi:10.1016/j.micinf.2007.06.009

Johnson, S., & Taylor, C. M. (2008). What's new in haemolytic uraemic syndrome? *Eur J Pediatr, 167*(9), 965-971. doi:10.1007/s00431-008-0745-7

Kakoullis, L., Papachristodoulou, E., Chra, P., & Panos, G. (2019). Shiga toxin-induced haemolytic uraemic syndrome and the role of antibiotics: a global overview. *J Infect, 79*(2), 75-94. doi:10.1016/j.jinf.2019.05.018

Kamitsuji, H., Nonami, K., Murakami, T., Ishikawa, N., Nakayama, A., & Umeki, Y. (2000). Elevated tissue factor circulating levels in children with hemolytic uremic syndrome caused by verotoxin-producing E. coli. *Clin Nephrol, 53*(5), 319-324.

Kanazawa, K., Sato, Y., Ohki, K., Okimura, K., Uchida, Y., Shindo, M., & Sakura, N. (2009). Contribution of each amino acid residue in polymyxin B(3) to antimicrobial and lipopolysaccharide binding activity. *Chem Pharm Bull (Tokyo), 57*(3), 240-244. doi:10.1248/cpb.57.240

Kang, G., Pulimood, A. B., Koshi, R., Hull, A., Acheson, D., Rajan, P., Mathan, M. M. (2001). A monkey model for enterohemorrhagic Escherichia coli infection. *J Infect Dis, 184*(2), 206-210. doi:10.1086/322011

Karmali, M. A. (2009). Host and pathogen determinants of verocytotoxin-producing Escherichia coli-associated hemolytic uremic syndrome. *Kidney Int Suppl*(112), S4-7. doi:10.1038/ki.2008.608

Karpman, D., Loos, S., Tati, R., & Arvidsson, I. (2017). Haemolytic uraemic syndrome. *J Intern Med, 281*(2), 123-148. doi:10.1111/joim.12546

Karpman, D., Papadopoulou, D., Nilsson, K., Sjögren, A. C., Mikaelsson, C., & Lethagen, S. (2001). Platelet activation by Shiga toxin and circulatory factors as a pathogenetic mechanism in the hemolytic uremic syndrome. *Blood, 97*(10), 3100-3108. doi:10.1182/blood.v97.10.3100

Karpman, D., & Ståhl, A. L. (2014). Enterohemorrhagic Escherichia coli Pathogenesis and the Host Response. *Microbiol Spectr, 2*(5). doi:10.1128/microbiolspec.EHEC-0009-2013

Keepers, T. R., Gross, L. K., & Obrig, T. G. (2007). Monocyte chemoattractant protein 1, macrophage inflammatory protein 1 alpha, and RANTES recruit macrophages to the kidney in a mouse model of hemolytic-uremic syndrome. *Infect Immun, 75*(3), 1229-1236. doi:10.1128/iai.01663-06

Keepers, T. R., Psotka, M. A., Gross, L. K., & Obrig, T. G. (2006). A murine model of HUS: Shiga toxin with lipopolysaccharide mimics the renal damage and physiologic response of human disease. *J Am Soc Nephrol, 17*(12), 3404-3414. doi:10.1681/asn.2006050419

Khalid, M., & Andreoli, S. (2019). Extrarenal manifestations of the hemolytic uremic syndrome associated with Shiga toxin-producing Escherichia coli (STEC HUS). *Pediatr Nephrol, 34*(12), 2495-2507. doi:10.1007/s00467-018-4105-1

Kim, J. S., Lee, M. S., & Kim, J. H. (2020). Recent Updates on Outbreaks of Shiga Toxin-Producing Escherichia coli and Its Potential Reservoirs. *Front Cell Infect Microbiol, 10*, 273. doi:10.3389/fcimb.2020.00273

Kimmitt, P. T., Harwood, C. R., & Barer, M. R. (2000). Toxin gene expression by shiga toxin-producing Escherichia coli: the role of antibiotics and the bacterial SOS response. *Emerg Infect Dis, 6*(5), 458-465. doi:10.3201/eid0605.000503

Kimura, T., Tani, S., Matsumoto Yi, Y., & Takeda, T. (2001). Serum amyloid P component is the Shiga toxin 2-neutralizing factor in human blood. *J Biol Chem, 276*(45), 41576-41579. doi:10.1074/jbc.M107819200

Koster, F. T., Boonpucknavig, V., Sujaho, S., Gilman, R. H., & Rahaman, M. M. (1984). Renal histopathology in the hemolytic-uremic syndrome following shigellosis. *Clin Nephrol, 21*(2), 126-133.

Lai, R. C., Tan, S. S., Yeo, R. W., Choo, A. B., Reiner, A. T., Su, Y., Lim, S. K. (2016). MSC secretes at least 3 EV types each with a unique permutation of membrane lipid, protein and RNA. *J Extracell Vesicles, 5*, 29828. doi:10.3402/jev.v5.29828

Lanzkowsky. (1980). *Manual of pediatric hematology and oncology a Treatise for the Clinician.* . New York: McGraw-Hill

Lapeyraque, A. L., Malina, M., Fremeaux-Bacchi, V., Boppel, T., Kirschfink, M., Oualha, M., Schaefer, F. (2011). Eculizumab in severe Shiga-toxin-associated HUS. *N Engl J Med, 364*(26), 2561-2563. doi:10.1056/NEJMc1100859

Law, D. (1994). Adhesion and its role in the virulence of enteropathogenic Escherichia coli. *Clin Microbiol Rev, 7*(2), 152-173. doi:10.1128/cmr.7.2.152

Lee, M. S., & Tesh, V. L. (2019). Roles of Shiga Toxins in Immunopathology. *Toxins (Basel), 11*(4). doi:10.3390/toxins11040212

Legros, N., Pohlentz, G., Steil, D., & Müthing, J. (2018). Shiga toxin-glycosphingolipid interaction: Status quo of research with focus on primary human brain and kidney endothelial cells. *Int J Med Microbiol, 308*(8), 1073-1084. doi:10.1016/j.ijmm.2018.09.003

Lindberg, A. A., Brown, J. E., Strömberg, N., Westling-Ryd, M., Schultz, J. E., & Karlsson, K. A. (1987). Identification of the carbohydrate receptor for Shiga toxin produced by Shigella dysenteriae type 1. *J Biol Chem, 262*(4), 1779-1785.

Lindgren, S. W., Samuel, J. E., Schmitt, C. K., & O'Brien, A. D. (1994). The specific activities of Shiga-like toxin type II (SLT-II) and SLT-II-related toxins of enterohemorrhagic Escherichia coli differ when measured by Vero cell cytotoxicity but not by mouse lethality. *Infect Immun, 62*(2), 623-631. doi:10.1128/iai.62.2.623-631.1994

Litalien, C., Proulx, F., Mariscalco, M. M., Robitaille, P., Turgeon, J. P., Orrbine, E., Seidman, E. (1999). Circulating inflammatory cytokine levels in hemolytic uremic syndrome. *Pediatr Nephrol, 13*(9), 840-845. doi:10.1007/s004670050712

Locatelli, M., Buelli, S., Pezzotta, A., Corna, D., Perico, L., Tomasoni, S., Morigi, M. (2014). Shiga toxin promotes podocyte injury in experimental hemolytic uremic syndrome via activation of the alternative pathway of complement. *J Am Soc Nephrol, 25*(8), 1786-1798. doi:10.1681/asn.2013050450

Loos, S., Aulbert, W., Hoppe, B., Ahlenstiel-Grunow, T., Kranz, B., Wahl, C., Kemper, M. J. (2017). Intermediate Follow-up of Pediatric Patients With Hemolytic Uremic Syndrome During the 2011 Outbreak Caused by E. coli O104:H4. *Clin Infect Dis, 64*(12), 1637-1643. doi:10.1093/cid/cix218

Lösche, W., Scholz, T., Temmler, U., Oberle, V., & Claus, R. A. (2004). Platelet-derived microvesicles transfer tissue factor to monocytes but not to neutrophils. *Platelets, 15*(2), 109-115. doi:10.1080/09537100310001649885

Ludwig, K., Bitzan, M., Bobrowski, C., & Müller-Wiefel, D. E. (2002). Escherichia coli O157 fails to induce a long-lasting lipopolysaccharide-specific, measurable humoral immune response in children with hemolytic-uremic syndrome. *J Infect Dis, 186*(4), 566-569. doi:10.1086/341781

Ludwig, K., Sarkim, V., Bitzan, M., Karmali, M. A., Bobrowski, C., Ruder, H., Müller-Wiefel, D. E. (2002). Shiga toxin-producing Escherichia coli infection and antibodies against Stx2 and Stx1 in household contacts of children with enteropathic hemolytic-uremic syndrome. *Journal of clinical microbiology, 40*(5), 1773-1782. doi:10.1128/jcm.40.5.1773-1782.2002

Luna-Gierke, R. E., Griffin, P. M., Gould, L. H., Herman, K., Bopp, C. A., Strockbine, N., & Mody, R. K. (2014). Outbreaks of non-O157 Shiga toxin-producing Escherichia coli infection: USA. *Epidemiol Infect, 142*(11), 2270-2280. doi:10.1017/s0950268813003233

Lynn, R. M., O'Brien, S. J., Taylor, C. M., Adak, G. K., Chart, H., Cheasty, T., Coia, J. E., Gillespie, I. A., Locking, M. E., Reilly, W. J., Smith, H. R., Waters, A., & Willshaw, G. A. . Childhood hemolytic uremic syndrome, United Kingdom and Ireland. *Emerging infectious diseases, 11*(4), 590-596. doi:https://doi.org/10.3201/eid1104.040833

Macher, B. A., & Klock, J. C. (1980). Isolation and chemical characterization of neutral glycosphingolipids of human neutrophils. *J Biol Chem, 255*(5), 2092-2096.

Mahat, U., Matar, R. B., & Rotz, S. J. (2019). Use of complement monoclonal antibody eculizumab in Shiga toxin producing Escherichia coli associated hemolytic uremic syndrome: A review of current evidence. *Pediatr Blood Cancer, 66*(11), e27913. doi:10.1002/pbc.27913

Majowicz, S. E., Scallan, E., Jones-Bitton, A., Sargeant, J. M., Stapleton, J., Angulo, F. J., Kirk, M. D. (2014). Global incidence of human Shiga toxin-producing Escherichia coli infections and deaths: a systematic review and knowledge synthesis. *Foodborne Pathog Dis, 11*(6), 447-455. doi:10.1089/fpd.2013.1704

Maloney, M., & Lingwood, C. (2003). Synergistic effect of verotoxin and interferon-alpha on erythropoiesis. *Cell Mol Biol (Noisy-le-grand), 49*(8), 1363-1369.

Marcato, P., Vander Helm, K., Mulvey, G. L., & Armstrong, G. D. (2003). Serum amyloid P component binding to Shiga toxin 2 requires both a subunit and B pentamer. *Infect Immun, 71*(10), 6075-6078. doi:10.1128/iai.71.10.6075-6078.2003

Markiewski, M. M., & Lambris, J. D. (2007). The role of complement in inflammatory diseases from behind the scenes into the spotlight. *Am J Pathol, 171*(3), 715-727. doi:10.2353/ajpath.2007.070166

Matussek, A., Lauber, J., Bergau, A., Hansen, W., Rohde, M., Dittmar, K. E., Gunzer, F. (2003). Molecular and functional analysis of Shiga toxin-induced response patterns in human vascular endothelial cells. *Blood, 102*(4), 1323-1332. doi:10.1182/blood-2002-10-3301

Matussek, A., Lauber, J., Bergau, A., Hansen, W., Rohde, M., Dittmar, K. E. J., Gunzer, F. (2003). Molecular and functional analysis of Shiga toxin-induced response patterns in human vascular endothelial cells. *Blood, 102*(4), 1323-1332. doi:10.1182/blood-2002-10-3301

McKee, R. S., Schnadower, D., Tarr, P. I., Xie, J., Finkelstein, Y., Desai, N., Freedman, S. B. (2020). Predicting Hemolytic Uremic Syndrome and Renal Replacement Therapy in Shiga Toxin-producing Escherichia coli-infected Children. *Clin Infect Dis, 70*(8), 1643-1651. doi:10.1093/cid/ciz432

Melton-Celsa, A. R. (2014). Shiga Toxin (Stx) Classification, Structure, and Function. *Microbiol Spectr, 2*(4), Ehec-0024-2013. doi:10.1128/microbiolspec.EHEC-0024-2013

Melton-Celsa, A. R., Darnell, S. C., & O'Brien, A. D. (1996). Activation of Shiga-like toxins by mouse and human intestinal mucus correlates with virulence of enterohemorrhagic Escherichia coli O91:H21 isolates in orally infected, streptomycin-treated mice. *Infect Immun, 64*(5), 1569-1576. doi:10.1128/iai.64.5.1569-1576.1996

Melton-Celsa, A. R., Kokai-Kun, J. F., & O'Brien, A. D. (2002). Activation of Shiga toxin type 2d (Stx2d) by elastase involves cleavage of the C-terminal two amino acids of the A2 peptide in the context of the appropriate B pentamer. *Mol Microbiol, 43*(1), 207-215. doi:10.1046/j.1365-2958.2002.02733.x

Melton-Celsa, A. R., O'Brien, A. D., & Feng, P. C. (2015). Virulence Potential of Activatable Shiga Toxin 2d-Producing Escherichia coli Isolates from Fresh Produce. *J Food Prot, 78*(11), 2085-2088. doi:10.4315/0362-028x.jfp-15-180

Menge, C. (2020). Molecular Biology of Escherichia Coli Shiga Toxins' Effects on Mammalian Cells. *Toxins (Basel), 12*(5). doi:10.3390/toxins12050345

Menne, J., Nitschke, M., Stingele, R., Abu-Tair, M., Beneke, J., Bramstedt, J., Kuehbacher, T. (2012). Validation of treatment strategies for enterohaemorrhagic Escherichia coli O104:H4 induced haemolytic uraemic syndrome: case-control study. *Bmj, 345*, e4565. doi:10.1136/bmj.e4565

Miller (1984). *Blood Diseases of Infancy and childhood*. St. Louis, MO: Mosby.
Ministerio de Salud y Desarrollo Social de la Nación, Boletín Integrado de Vigilancia 463 SE 34/219. (2019).

Morigi, M., Galbusera, M., Gastoldi, S., Locatelli, M., Buelli, S., Pezzotta, A., Zoja, C. (2011). Alternative pathway activation of complement by Shiga toxin promotes exuberant C3a formation that triggers microvascular thrombosis. *J Immunol, 187*(1), 172-180. doi:10.4049/jimmunol.1100491

Morrison, D. C., & Jacobs, D. M. (1976). Binding of polymyxin B to the lipid A portion of bacterial lipopolysaccharides. *Immunochemistry, 13*(10), 813-818. doi:10.1016/0019-2791(76)90181-6

Mühlen, S., & Dersch, P. (2020). Treatment Strategies for Infections With Shiga Toxin-Producing Escherichia coli. *Front Cell Infect Microbiol, 10*, 169. doi:10.3389/fcimb.2020.00169

Mulcahy, L. A., Pink, R. C., & Carter, D. R. (2014). Routes and mechanisms of extracellular vesicle uptake. *J Extracell Vesicles, 3*. doi:10.3402/jev.v3.24641

Müthing, J., Schweppe, C. H., Karch, H., & Friedrich, A. W. (2009). Shiga toxins, glycosphingolipid diversity, and endothelial cell injury. *Thromb Haemost, 101*(2), 252-264.

Nathan, D. G., & Oski, F. A. (1987). *Hematology of Infancy and childhood*. Philadelphia, PA: Saunders.

Noris, M., & Remuzzi, G. (2005). Hemolytic uremic syndrome. *J Am Soc Nephrol, 16*(4), 1035-1050. doi:10.1681/asn.2004100861

Noris, M., & Remuzzi, G. (2009). Atypical Hemolytic–Uremic Syndrome. *New England Journal of Medicine, 361*(17), 1676-1687. doi:10.1056/NEJMra0902814

Novak, R. W., Tschantz, J. A., & Krill, C. E., Jr. (1987). Normal Platelet and Mean Platelet Volumes in Pediatric Patients. *Laboratory Medicine, 18*(9), 613-614. doi:10.1093/labmed/18.9.613

Obata, F., Tohyama, K., Bonev, A. D., Kolling, G. L., Keepers, T. R., Gross, L. K., Nelson, M. T., Sato, S., & Obrig, T. G. (2008). Shiga toxin 2 affects the central nervous system through receptor globotriaosylceramide localized to neurons. *The Journal of infectious diseases,, 198*(9), 1398-1406. doi:https://doi.org/10.1086/591911

Okuda, T., Tokuda, N., Numata, S., Ito, M., Ohta, M., Kawamura, K., Furukawa, K. (2006). Targeted disruption of Gb3/CD77 synthase gene resulted in the complete deletion of globo-series glycosphingolipids and loss of sensitivity to verotoxins. *J Biol Chem, 281*(15), 10230-10235. doi:10.1074/jbc.M600057200

Orth, D., Grif, K., Zimmerhackl, L. B., & Würzner, R. (2008). Prevention and treatment of enterohemorrhagic Escherichia coli infections in humans. *Expert Rev Anti Infect Ther, 6*(1), 101-108. doi:10.1586/14787210.6.1.101

Orth, D., Khan, A. B., Naim, A., Grif, K., Brockmeyer, J., Karch, H., Würzner, R. (2009). Shiga Toxin Activates Complement and Binds Factor H: Evidence for an Active Role of Complement in Hemolytic Uremic Syndrome. *The Journal of Immunology, 182*(10), 6394-6400. doi:10.4049/jimmunol.0900151

Penzo, M., Carnicelli, D., Montanaro, L., & Brigotti, M. (2016). A reconstituted cell-free assay for the evaluation of the intrinsic activity of purified human ribosomes. *Nature Protocols, 11*, 1309-1325.

Petruzziello-Pellegrini, T. N., Yuen, D. A., Page, A. V., Patel, S., Soltyk, A. M., Matouk, C. C., Marsden, P. A. (2012). The CXCR4/CXCR7/SDF-1 pathway contributes to the pathogenesis of Shiga toxin-associated hemolytic uremic syndrome in humans and mice. *J Clin Invest, 122*(2), 759-776. doi:10.1172/jci57313

Podbilewicz, B. (2014). Virus and cell fusion mechanisms. *Annu Rev Cell Dev Biol, 30*, 111-139. doi:10.1146/annurev-cellbio-101512-122422

Proulx, F., Seidman, E. G., & Karpman, D. (2001). Pathogenesis of Shiga toxin-associated hemolytic uremic syndrome. *Pediatr Res, 50*(2), 163-171. doi:10.1203/00006450-200108000-00002

Proulx, F., Toledano, B., Phan, V., Clermont, M. J., Mariscalco, M. M., & Seidman, E. G. (2002). Circulating granulocyte colony-stimulating factor, C-X-C, and C-C chemokines in children with Escherichia coli O157:H7 associated hemolytic uremic syndrome. *Pediatr Res, 52*(6), 928-934. doi:10.1203/00006450-200212000-00019

Proulx, F., Turgeon, J. P., Delage, G., Lafleur, L., & Chicoine, L. (1992). Randomized, controlled trial of antibiotic therapy for Escherichia coli O157:H7 enteritis. *J Pediatr, 121*(2), 299-303. doi:10.1016/s0022-3476(05)81209-0

Public Health Agency of Canada: National Enteric Surveillance Program (NESP), Annual summary 2017 (2019).

Qin, X., Klein, E. J., Galanakis, E., Thomas, A. A., Stapp, J. R., Rich, S., Tarr, P. I. (2015). Real-Time PCR Assay for Detection and Differentiation of Shiga Toxin-Producing Escherichia coli from Clinical Samples. *Journal of clinical microbiology, 53*(7), 2148-2153. doi:10.1128/jcm.00115-15

Ramos MV, F. G., Patey N, Schierloh P, Exeni R, Grimoldi I. (2007). Involvement of the fractalkine pathway in the pathogenesis of childhood hemolytic uremic syndrome. *Blood, 109* 2438-2445. doi:doi:10.1182/blood2006-06-026997

Raposo, G., & Stoorvogel, W. (2013). Extracellular vesicles: exosomes, microvesicles, and friends. *J Cell Biol, 200*(4), 373-383. doi:10.1083/jcb.201211138

Ratajczak, J., Wysoczynski, M., Hayek, F., Janowska-Wieczorek, A., & Ratajczak, M. Z. (2006). Membrane-derived microvesicles: important and underappreciated mediators of cell-to-cell communication. *Leukemia, 20*(9), 1487-1495. doi:10.1038/sj.leu.2404296

Rawish, E., Sauter, M., Sauter, R., Nording, H., & Langer, H. F. (2021). Complement, inflammation and thrombosis. *Br J Pharmacol, 178*(14), 2892-2904. doi:10.1111/bph.15476

Richardson, S. E., Karmali, M. A., Becker, L. E., & Smith, C. R. (1988). The histopathology of the hemolytic uremic syndrome associated with verocytotoxin-producing Escherichia coli infections. *Hum Pathol, 19*(9), 1102-1108. doi:10.1016/s0046-8177(88)80093-5

Rippa, M., Sagnelli, D., Vestri, A., Marchesano, V., Munari, B., Carnicelli, D., Petti, L. (2022). Plasmonic Metasurfaces for Specific SERS Detection of Shiga Toxins. *ACS Appl Mater Interfaces, 14*(4), 4969-4979. doi:10.1021/acsami.1c21553

Rivas, M., Chinen, I., Miliwebsky, E., & Masana, M. (2014). Risk Factors for Shiga Toxin-Producing Escherichia coli-Associated Human Diseases. *Microbiol Spectr, 2*(5). doi:10.1128/microbiolspec.EHEC-0002-2013

Rizzoni, G., Claris-Appiani, A., Edefonti, A., Facchin, P., Franchini, F., Gusmano, R., Remuzzi, G. (1988). Plasma infusion for hemolytic-uremic syndrome in children: results of a multicenter controlled trial. *J Pediatr, 112*(2), 284-290. doi:10.1016/s0022-3476(88)80071-4

Robson, W. L., Fick, G. H., & Wilson, P. C. (1988). Prognostic factors in typical postdiarrhea hemolytic-uremic syndrome. *Child Nephrol Urol, 9*(4), 203-207.

Rocchetti, L., Munari, B., Varrone, E., Porcellini, E., Orth-Höller, D., Würzner, R., Brigotti, M. (2021). Method for the Detection of the Cleaved Form of Shiga Toxin 2a Added to Normal Human Serum. *Toxins (Basel), 13*(2). doi:10.3390/toxins13020094

Rosales, A., Hofer, J., Zimmerhackl, L. B., Jungraithmayr, T. C., Riedl, M., Giner, T., Karch, H. (2012). Need for long-term follow-up in enterohemorrhagic Escherichia coli-associated hemolytic uremic syndrome due to late-emerging sequelae. *Clin Infect Dis, 54*(10), 1413-1421. doi:10.1093/cid/cis196

Rubin, O., Canellini, G., Delobel, J., Lion, N., & Tissot, J.-D. (2012). Red blood cell microparticles: clinical relevance. *Transfusion medicine and hemotherapy : offizielles Organ der Deutschen Gesellschaft fur Transfusionsmedizin und Immunhamatologie, 39*(5), 342-347. doi:10.1159/000342228

Rubin, O., Delobel, J., Prudent, M., Lion, N., Kohl, K., Tucker, E. I., . . . Angelillo-Scherrer, A. (2013). Red blood cell-derived microparticles isolated from blood units initiate and propagate thrombin generation. *Transfusion, 53*(8), 1744-1754. doi:10.1111/trf.12008

Russo, L. M., Melton-Celsa, A. R., Smith, M. J., & O'Brien, A. D. (2014). Comparisons of native Shiga toxins (Stxs) type 1 and 2 with chimeric toxins indicate that the source of the binding subunit dictates degree of toxicity. *PLoS One, 9*(3), e93463. doi:10.1371/journal.pone.0093463

Saarinen, U. M., & Siimes, M. A. (1978). Developmental changes in red blood cell counts and indices of infants after exclusion of iron deficiency by laboratory criteria and continuous iron supplementation. *J Pediatr, 92*(3), 412-416. doi:10.1016/s0022-3476(78)80429-6

Safdar, N., Said, A., Gangnon, R. E., & Maki, D. G. (2002). Risk of hemolytic uremic syndrome after antibiotic treatment of Escherichia coli O157:H7 enteritis: a meta-analysis. *JAMA, 288*(8), 996-1001. doi:10.1001/jama.288.8.996

Sapet, C., Simoncini, S., Loriod, B., Puthier, D., Sampol, J., Nguyen, C., . . . Anfosso, F. (2006). Thrombin-induced endothelial microparticle generation: identification of a novel pathway involving ROCK-II activation by caspase-2. *Blood, 108*(6), 1868-1876. doi:10.1182/blood-2006-04-014175

Scallan, E., Hoekstra, R. M., Angulo, F. J., Tauxe, R. V., Widdowson, M. A., Roy, S. L., Griffin, P. M. (2011). Foodborne illness acquired in the United States--major pathogens. *Emerg Infect Dis, 17*(1), 7-15. doi:10.3201/eid1701.p11101

Scheiring, J., Rosales, A., & Zimmerhackl, L. B. (2010). Clinical practice. Today's understanding of the haemolytic uraemic syndrome. *Eur J Pediatr, 169*(1), 7-13. doi:10.1007/s00431-009-1039-4

Schüller, S., Frankel, G., & Phillips, A. D. (2004). Interaction of Shiga toxin from Escherichia coli with human intestinal epithelial cell lines and explants: Stx2 induces epithelial damage in organ culture. *Cell Microbiol, 6*(3), 289-301. doi:10.1046/j.1462-5822.2004.00370.x

Shaikh, N., & Tarr, P. I. (2003). Escherichia coli O157:H7 Shiga toxin-encoding bacteriophages: integrations, excisions, truncations, and evolutionary implications. *J Bacteriol, 185*(12), 3596-3605. doi:10.1128/jb.185.12.3596-3605.2003

Shiraishi, M., Ichiyama, T., Matsushige, T., Iwaki, T., Iyoda, K., Fukuda, K., Furukawa, S. (2008). Soluble tumor necrosis factor receptor 1 and tissue inhibitor of metalloproteinase-1 in hemolytic uremic syndrome with encephalopathy. *J Neuroimmunol, 196*(1-2), 147-152. doi:10.1016/j.jneuroim.2008.02.012

Skotland, T., Sandvig, K., & Llorente, A. (2017). Lipids in exosomes: Current knowledge and the way forward. *Prog Lipid Res, 66*, 30-41. doi:10.1016/j.plipres.2017.03.001

Smirnova, I., Poltorak, A., Chan, E. K., McBride, C., & Beutler, B. (2000). Phylogenetic variation and polymorphism at the toll-like receptor 4 locus (TLR4). *Genome Biol, 1*(1), Research002. doi:10.1186/gb-2000-1-1-research002

Smith, K. E., Wilker, P. R., Reiter, P. L., Hedican, E. B., Bender, J. B., & Hedberg, C. W. (2012). Antibiotic treatment of Escherichia coli O157 infection and the risk of hemolytic uremic syndrome, Minnesota. *Pediatr Infect Dis J, 31*(1), 37-41. doi:10.1097/INF.0b013e31823096a8

Srimal, S., Surolia, N., Balasubramanian, S., & Surolia, A. (1996). Titration calorimetric studies to elucidate the specificity of the interactions of polymyxin B with lipopolysaccharides and lipid A. *Biochem J, 315 (Pt 2)*(Pt 2), 679-686. doi:10.1042/bj3150679

Ståhl, A. L., Arvidsson, I., Johansson, K. E., Chromek, M., Rebetz, J., Loos, S., . . . Karpman, D. (2015). A novel mechanism of bacterial toxin transfer within host blood cell-derived microvesicles. *PLOS Pathog, 11*(2), e1004619. doi:10.1371/journal.ppat.1004619

Ståhl, A. L., Johansson, K., Mossberg, M., Kahn, R., & Karpman, D. (2019). Exosomes and microvesicles in normal physiology, pathophysiology, and renal diseases. *Pediatr Nephrol, 34*(1), 11-30. doi:10.1007/s00467-017-3816-z

Stahl, A. L., Sartz, L., & Karpman, D. (2011). Complement activation on platelet-leukocyte complexes and microparticles in enterohemorrhagic Escherichia coli-induced hemolytic uremic syndrome. *Blood, 117*(20), 5503-5513. doi:10.1182/blood-2010-09-309161

Stahl, A. L., Sartz, L., Nelsson, A., Bekassy, Z. D., & Karpman, D. (2009). Shiga toxin and lipopolysaccharide induce platelet-leukocyte aggregates and tissue factor release, a thrombotic mechanism in hemolytic uremic syndrome. *PLoS One, 4*(9), e6990. doi:10.1371/journal.pone.0006990

Stearns-Kurosawa, D. J., Collins, V., Freeman, S., Tesh, V. L., & Kurosawa, S. (2010). Distinct physiologic and inflammatory responses elicited in baboons after challenge with Shiga toxin type 1 or 2 from enterohemorrhagic Escherichia coli. *Infect Immun, 78*(6), 2497-2504. doi:10.1128/iai.01435-09

Stearns-Kurosawa, D. J., Oh, S. Y., Cherla, R. P., Lee, M. S., Tesh, V. L., Papin, J., Kurosawa, S. (2013). Distinct renal pathology and a chemotactic phenotype after enterohemorrhagic Escherichia coli shiga toxins in non-human primate models of hemolytic uremic syndrome. *Am J Pathol, 182*(4), 1227-1238. doi:10.1016/j.ajpath.2012.12.026

Stevens, M. P., & Frankel, G. M. (2014). The Locus of Enterocyte Effacement and Associated Virulence Factors of Enterohemorrhagic Escherichia coli. *Microbiol Spectr, 2*(4), Ehec-0007-2013. doi:10.1128/microbiolspec.EHEC-0007-2013

Tarr, P. I., & Freedman, S. B. (2022). Why antibiotics should not be used to treat Shiga toxin-producing Escherichia coli infections. *Curr Opin Gastroenterol, 38*(1), 30-38. doi:10.1097/mog.0000000000000798

Tarr, P. I., Gordon, C. A., & Chandler, W. L. (2005). Shiga-toxin-producing Escherichia coli and haemolytic uraemic syndrome. *Lancet, 365*(9464), 1073-1086. doi:S0140-6736(05)71144-2 [pii] 10.1016/S0140-6736(05)71144-2

Tarr, P. I., Neill, M. A., Clausen, C. R., Watkins, S. L., Christie, D. L., & Hickman, R. O. (1990). Escherichia coli O157:H7 and the hemolytic uremic syndrome: importance of early cultures in establishing the etiology. *J Infect Dis, 162*(2), 553-556. doi:10.1093/infdis/162.2.553

Taylor, F. B., Jr., Tesh, V. L., DeBault, L., Li, A., Chang, A. C., Kosanke, S. D., Siegler, R. L. (1999). Characterization of the baboon responses to Shiga-like toxin: descriptive study of a new primate model of toxic responses to Stx-1. *Am J Pathol, 154*(4), 1285-1299. doi:10.1016/s0002-9440(10)65380-1

Tazzari, P. L., Ricci, F., Carnicelli, D., Caprioli, A., Tozzi, A. E., Rizzoni, G., Brigotti, M. (2004). Flow cytometry detection of Shiga toxins in the blood from children with hemolytic uremic syndrome. *Cytometry B Clin Cytom, 61*(1), 40-44. doi:10.1002/cyto.b.20022

te Loo, D. M., Monnens, L. A., van Der Velden, T. J., Vermeer, M. A., Preyers, F., Demacker, P. N., van Hinsbergh, V. W. (2000). Binding and transfer of verocytotoxin by polymorphonuclear leukocytes in hemolytic uremic syndrome. *Blood, 95*(11), 3396-3402.

Terajima, J., Iyoda, S., Ohnishi, M., & Watanabe, H. (2014). Shiga Toxin (Verotoxin)-Producing Escherichia coli in Japan. *Microbiol Spectr, 2*(5). doi:10.1128/microbiolspec.EHEC-0011-2013

Tesh, V. L. (2012). The induction of apoptosis by Shiga toxins and ricin. *Curr Top Microbiol Immunol, 357*, 137-178. doi:10.1007/82_2011_155

Thurman, J. M., Marians, R., Emlen, W., Wood, S., Smith, C., Akana, H., Trachtman, H. (2009). Alternative pathway of complement in children with diarrhea-associated hemolytic uremic syndrome. *Clin J Am Soc Nephrol, 4*(12), 1920-1924. doi:10.2215/cjn.02730409

Torgersen, M. L., Engedal, N., Pedersen, A. M., Husebye, H., Espevik, T., & Sandvig, K. (2011). Toll-like receptor 4 facilitates binding of Shiga toxin to colon carcinoma and primary umbilical vein endothelial cells. *FEMS Immunol Med Microbiol, 61*(1), 63-75. doi:10.1111/j.1574-695X.2010.00749.x

Torres, A. G., Amaral, M. M., Bentancor, L., Galli, L., Goldstein, J., Kruger, A., & Rojas-Lopez, M. (2018). Recent Advances in Shiga Toxin-Producing Escherichia coli Research in Latin America. *Microorganisms, 6*(4). doi:10.3390/microorganisms6040100

Trachtman, H., Austin, C., Lewinski, M., & Stahl, R. A. (2012). Renal and neurological involvement in typical Shiga toxin-associated HUS. *Nat Rev Nephrol, 8*(11), 658-669. doi:10.1038/nrneph.2012.196

Trachtman, H., Cnaan, A., Christen, E., Gibbs, K., Zhao, S., Acheson, D. W., Hirschman, G. H. (2003). Effect of an oral Shiga toxin-binding agent on diarrhea-associated hemolytic uremic syndrome in children: a randomized controlled trial. *JAMA, 290*(10), 1337-1344. doi:10.1001/jama.290.10.1337

Tsuji, B. T., Pogue, J. M., Zavascki, A. P., Paul, M., Daikos, G. L., Forrest, A., Kaye, K. S. (2019). International Consensus Guidelines for the Optimal Use of the Polymyxins: Endorsed by the American College of Clinical Pharmacy (ACCP), European Society of Clinical Microbiology and Infectious Diseases (ESCMID), Infectious Diseases Society of America (IDSA), International Society for Anti-infective Pharmacology (ISAP), Society of Critical Care Medicine (SCCM), and Society of Infectious Diseases Pharmacists (SIDP). *Pharmacotherapy, 39*(1), 10-39. doi:10.1002/phar.2209

Turco, A. E., Lam, W., Rule, A. D., Denic, A., Lieske, J. C., Miller, V. M., Jayachandran, M. (2016). Specific renal parenchymal-derived urinary extracellular vesicles identify age-associated structural changes in living donor kidneys. *J Extracell Vesicles, 5*, 29642. doi:10.3402/jev.v5.29642

Tzipori, S., Sheoran, A., Akiyoshi, D., Donohue-Rolfe, A., & Trachtman, H. (2004). Antibody therapy in the management of shiga toxin-induced hemolytic uremic syndrome. *Clin Microbiol Rev, 17*(4), 926-941, table of contents. doi:10.1128/cmr.17.4.926-941.2004

Vaara, M. (2010). Polymyxins and their novel derivatives. *Curr Opin Microbiol, 13*(5), 574-581. doi:10.1016/j.mib.2010.09.002

Vaara, M. (2013). Novel derivatives of polymyxins. *Journal of Antimicrobial Chemotherapy, 68*(6), 1213-1219. doi:10.1093/jac/dkt039

Vaara, M., Vaara, T., Kuka, J., Sevostjanovs, E., Grinberga, S., Dambrova, M., & Liepinsh, E. (2020). Excretion of the Polymyxin Derivative NAB739 in Murine Urine. *Antibiotics (Basel), 9*(4). doi:10.3390/antibiotics9040143

Vaara, M., Vaara, T., & Tyrrell, J. M. (2017). Structure-activity studies on polymyxin derivatives carrying three positive charges only reveal a new class of compounds with strong antibacterial activity. *Peptides, 91*, 8-12. doi:10.1016/j.peptides.2017.03.002

Vaara, M., Vaara, T., & Vingsbo Lundberg, C. (2018). Polymyxin derivatives NAB739 and NAB815 are more effective than polymyxin B in murine Escherichia coli pyelonephritis. *J Antimicrob Chemother, 73*(2), 452-455. doi:10.1093/jac/dkx394

Van de Kar, N. C., Monnens, L. A., Karmali, M. A., & van Hinsbergh, V. W. (1992). Tumor necrosis factor and interleukin-1 induce expression of the verocytotoxin receptor globotriaosylceramide on human endothelial cells: implications for the pathogenesis of the hemolytic uremic syndrome. *Blood, 80*(11), 2755-2764.

Van de Kar, N. C., Monnens, L. A., & Van Hinsbergh, V. W. (1993). Tumor necrosis factor and interleukin 1 induce expression of the glycolipid verotoxin receptor in human endothelial cells. Implications for the pathogenesis of the haemolytic uraemic syndrome. *Behring Inst Mitt*(92), 202-209.

van Setten, P. A., Monnens, L. A., Verstraten, R. G., van den Heuvel, L. P., & van Hinsbergh, V. W. (1996). Effects of verocytotoxin-1 on nonadherent human monocytes: binding characteristics, protein synthesis, and induction of cytokine release. *Blood, 88*(1), 174-183.

van Setten, P. A., van Hinsbergh, V. W., van den Heuvel, L. P., Preyers, F., Dijkman, H. B., Assmann, K. J., Monnens, L. A. (1998). Monocyte chemoattractant protein-1 and interleukin-8 levels in urine and serum of patents with hemolytic uremic syndrome. *Pediatr Res, 43*(6), 759-767. doi:10.1203/00006450-199806000-00008

Varrone, E., Carnicelli, D., & Brigotti, M. (2021). Extracellular Vesicles and Renal Endothelial Cells: A Fatal Attraction in Hemolytic Uremic Syndrome. *Am J Pathol, 191*(5), 795-804. doi:10.1016/j.ajpath.2021.02.011

Verma, I. C. (1981). Pediatrics, Edited by Abraham M. Rudolph. *The Indian Journal of Pediatrics, 48*(2), 178-178. doi:10.1007/BF02816997

Villysson, A., Tontanahal, A., & Karpman, D. (2017). Microvesicle Involvement in Shiga Toxin-Associated Infection. *Toxins, 9*(11), 376. doi:10.3390/toxins9110376

Waddell, T., Head, S., Petric, M., Cohen, A., & Lingwood, C. (1988). Globotriosyl ceramide is specifically recognized by the Escherichia coli verocytotoxin 2. *Biochem Biophys Res Commun, 152*(2), 674-679. doi:10.1016/s0006-291x(88)80091-3

Walsh, P. R., & Johnson, S. (2019). Eculizumab in the treatment of Shiga toxin haemolytic uraemic syndrome. *Pediatr Nephrol, 34*(9), 1485-1492. doi:10.1007/s00467-018-4025-0

Walterspiel, J. N., Ashkenazi, S., Morrow, A. L., & Cleary, T. G. (1992). Effect of subinhibitory concentrations of antibiotics on extracellular Shiga-like toxin I. *Infection, 20*(1), 25-29. doi:10.1007/bf01704889

Watanabe-Takahashi, M., Yamasaki, S., Murata, M., Kano, F., Motoyama, J., Yamate, J., Nishikawa, K. (2018). Exosome-associated Shiga toxin 2 is released from cells and causes severe toxicity in mice. *Sci Rep, 8*(1), 10776-10776. doi:10.1038/s41598-018-29128-9

Wijnsma, K. L., van Bommel, S. A., van der Velden, T., Volokhina, E., Schreuder, M. F., van den Heuvel, L. P., & van de Kar, N. C. (2016). Fecal diagnostics in combination with serology: best test to establish STEC-HUS. *Pediatr Nephrol, 31*(11), 2163-2170. doi:10.1007/s00467-016-3420-7

Willysson, A., Ståhl, A. L., Gillet, D., Barbier, J., Cintrat, J. C., Chambon, V., Karpman, D. (2020). Shiga Toxin Uptake and Sequestration in Extracellular Vesicles Is Mediated by Its B-Subunit. *Toxins (Basel), 12*(7). doi:10.3390/toxins12070449

Wong, C. S., Jelacic, S., Habeeb, R. L., Watkins, S. L., & Tarr, P. I. (2000). The risk of the hemolytic-uremic syndrome after antibiotic treatment of Escherichia coli O157:H7 infections. *N Engl J Med, 342*(26), 1930-1936. doi:10.1056/nejm200006293422601

Würzner, R., Riedl, M., Rosales, A., & Orth-Höller, D. (2014). Treatment of enterohemorrhagic Escherichia coli-induced hemolytic uremic syndrome (eHUS). *Semin Thromb Hemost, 40*(4), 508-516. doi:10.1055/s-0034-1375298

Yokoyama, K., Horii, T., Yamashino, T., Hashikawa, S., Barua, S., Hasegawa, T., Ohta, M. (2000). Production of shiga toxin by Escherichia coli measured with reference to the membrane vesicle-associated toxins. *FEMS Microbiol Lett, 192*(1), 139-144. doi:10.1111/j.1574-6968.2000.tb09372.x

Yu, Z., Qin, W., Lin, J., Fang, S., & Qiu, J. (2015). Antibacterial mechanisms of polymyxin and bacterial resistance. *Biomed Res Int, 2015*, 679109. doi:10.1155/2015/679109

Zangari, T., Melton-Celsa, A. R., Panda, A., Smith, M. A., Tatarov, I., De Tolla, L., & O'Brien, A. D. (2014). Enhanced virulence of the Escherichia coli O157:H7 spinach-associated outbreak strain in two animal models is associated with higher levels of Stx2 production after induction with ciprofloxacin. *Infect Immun, 82*(12), 4968-4977. doi:10.1128/iai.02361-14

Zhang, X., McDaniel, A. D., Wolf, L. E., Keusch, G. T., Waldor, M. K., & Acheson, D. W. (2000). Quinolone antibiotics induce Shiga toxin-encoding bacteriophages, toxin production, and death in mice. *J Infect Dis, 181*(2), 664-670. doi:10.1086/315239

Zoja, C., Angioletti, S., Donadelli, R., Zanchi, C., Tomasoni, S., Binda, E., Morigi, M. (2002). Shiga toxin-2 triggers endothelial leukocyte adhesion and transmigration via NF-κB dependent up-regulation of IL-8 and MCP-11: 1See Editorial by Siegler and Pysher, p. 1088. *Kidney Int, 62*(3), 846-856. doi:https://doi.org/10.1046/j.1523-1755.2002.00503.x

Zoja, C., Buelli, S., & Morigi, M. (2010). Shiga toxin-associated hemolytic uremic syndrome: pathophysiology of endothelial dysfunction. *Pediatr Nephrol, 25*(11), 2231-2240. doi:10.1007/s00467-010-1522-1